Weierstraß-Institut

für Angewandte Analysis und Stochastik

Leibniz-Institut im Forschungsverbund Berlin e. V.

Preprint ISSN 2198-5855

Theory and structure of the metal/electrolyte interface incorporating adsorption and solvation effects

Wolfgang Dreyer, Clemens Guhlke, Manuel Landstorfer

submitted: December 18, 2014

Weierstrass-Institute
Mohrenstr. 39
10117 Berlin
Germany
E-Mail: Wolfgang.Dreyer@wias-berlin.de
Clemens.Guhlke@wias-berlin.de
Manuel.Landstorfer@wias-berlin.de

No. 2058

Berlin 2014

2010 *Mathematics Subject Classification.* 78A57, 35Q35, 34B15.

2010 *Physics and Astronomy Classification Scheme.* 82.45.Gj, 68.43.-h, 68.35.Md.

Key words and phrases. Double Layer, Adsorption, Solvation, Surface Mixture Theory, Gouy-Chapman-Stern Model, Electrode/Electrolyte Interface.

Edited by
Weierstraß-Institut für Angewandte Analysis und Stochastik (WIAS)
Leibniz-Institut im Forschungsverbund Berlin e. V.
Mohrenstraße 39
10117 Berlin
Germany

Fax: +49 30 20372-303
E-Mail: preprint@wias-berlin.de
World Wide Web: http://www.wias-berlin.de/

Abstract

In this work we present a continuum theory for the metal/electrolyte interface which explicitly takes into account adsorption and partial solvation on the metal surface. It is based on a general theory of coupled thermo-electrodynamics for volumes and surfaces, utilized here in equilibrium and a 1D approximation. We provide explicit free energy models for the metal and electrolyte phases and derive a surface free energy for the species present on the metal surface. This surface mixture theory explicitly takes into account the very different amount of sites an adsorbate requires, originating from solvation effects on the surface. Additionally we account for electron transfer reactions on the surface and the associated stripping of the solvation shell. Based on our surface free energy we thus provide explicit expressions of the surface chemical potentials of all constituents. The equilibrium representations of the coverages and the electric charge are briefly summarized. Our model is then applied to three representative examples and compared to experimental data. The Ag(110)|$\mathrm{KPF_6}$ example serves to discuss some general aspects of our model and validate our theory when no specific adsorption of ionic species occurs. Next, the Ag|$\mathrm{NaClO_4}$ interface for (110), (100), and (111) metal surfaces, compares our theory to multiple experimental data and shows its validity within the experimental error. Finally we discuss the structure of the Ag(110)|NaF interface in a wide potential range. It turns out that various layers self-consistently form within the overall space charge region, which are compared to historic and recent pictures of the double layer. Based on this we present new interpretations of what is known as inner and outer Helmholtz-planes and finally provide a thermodynamic consistent picture of the metal/electrolyte interface structure.

1 Introduction

One of the main questions of modern electrochemistry is certainly *how* the structure of the metal/electrolyte interface actually looks like for externally applied potentials. This question has a long history in physical chemistry, and many conceptional suggestions of the double layer structure have been proposed. The most common view *a priori* sketches the formation of several layers in front of the metal surface, namely the inner Helmholtz-plane, which covers specifically adsorbed ions, the outer Helmholtz-plane, covering *non-specifically adsorbed* ions and the diffuse double layer (c.f. Figure 1).

This conception of the double layer structure was *transferred* to theoretical models, in order to understand various phenomena occurring at electrochemical interfaces. The groundbreaking observations by Lippmann[44] and Gouy[28] of the electrocapillarity lead to the development of the double layer theory by Helmholtz, Chapman[14], Stern[58] and others at the beginning of the 20$^{\text{th}}$ century. The theory was developed further by numerous researches[24, 26, 8] and found its preliminary completion in 1947 with the seminal paper of D. Grahame [29]. The theory used by Grahame relies on Gibbsian thermodynamics for the surface, the theory of O. Stern for non-specifically adsorbed ions, and statistical mechanics (Boltzmann distribution or Gouy–Chapman theory) in order to determine the diffuse part of the double layer.

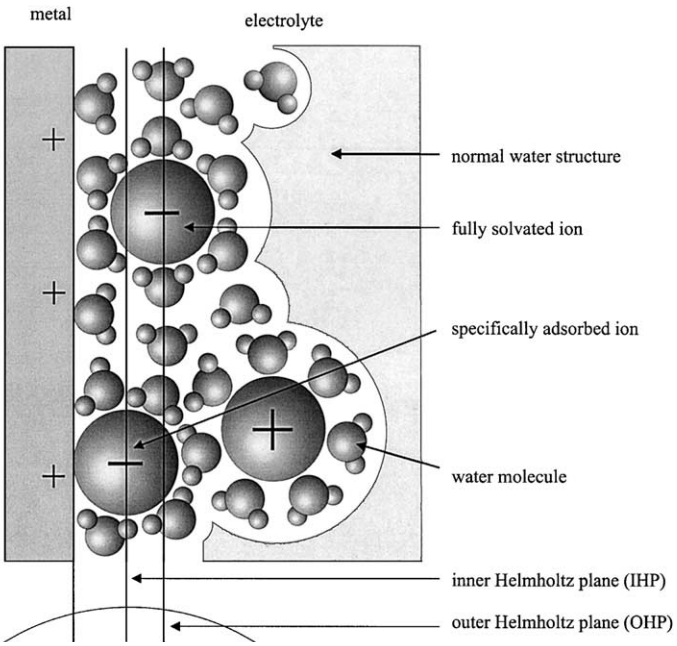

Figure 1: Sketch of the metal/electrolyte interface structure according to D. Kolb (Fig. 1.a from [39], reprinted with permission from Elsevier)

Common to all of these modeling approaches is the translation of an *a priori perception* of the double layer to a mathematical model. Based on these models the crucial quantity characterizing the metal/electrolyte interface was computed: the differential capacitance. Although the theory of Grahame describes qualitatively several aspects of the measured capacity, its agreement is restricted to a rather narrow potential range, i.e. ± 0.1V, as well as small salt concentrations. Especially the diffuse layer part, i.e. the Gouy–Chapman theory, is restricted to several mV around the potential of zero charge and marked as "brilliant failure"[11] by Bockris. Hence, the whole *perception* of the double layer structure is restricted to this narrow potential range since there is no satisfactory validation for ± 0.5V around the potential of zero charge.

The question is, if the approach of an *a priori perception*, and its translation to a mathematical model, is at all constructive. It seems rather *impossible* to extend Grahame's treatment systematically to curved surfaces, various metals, higher concentrations, mixtures of electrolytes, different solvents and so on. And even worse, its consistent embedding in non-equilibrium thermodynamics is outstanding and may even be impossible. However, this step is crucial for many disciplines adjacent to fundamental electrochemistry, i.e. corrosion and colloidal science, battery and fuel cell research, porous material science, etc. From the perspective of a general theory this is the actual drawback of the theory presented by Grahame.

With this work we provide a conceptionally different strategy. We do not prescribe at all any structure of the metal/electrolyte interface, but rather compute it based on coupled continuum thermo-electrodynamics for volumes[47, 16] and surfaces[4, 30]. Even though we employ thermodynamic equilibrium throughout this work, it is crucial to mention that our theory is derived completely within the framework of non-equilibrium thermodynamics.

The continuum approach ignores the atomistic structure of the material at hand, but covers

many aspects of its microscopic structure in the central quantity of continuum thermodynamics: the free energy density. Rational thermodynamics states some general, material independent conditions and reduces the whole *material modeling* to the derivation of an explicit free energy function. This strict separation between general conditions, which hold for every material, and material specific free energy densities allows for a systematic modeling of the metal, its surface, and the electrolyte phase within one general theory.

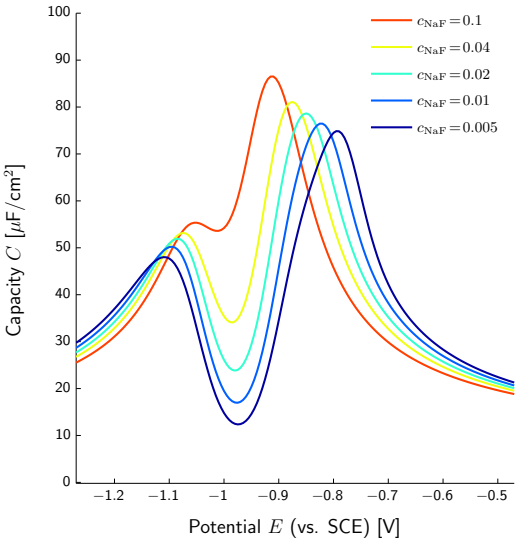

(a) Computed capacity

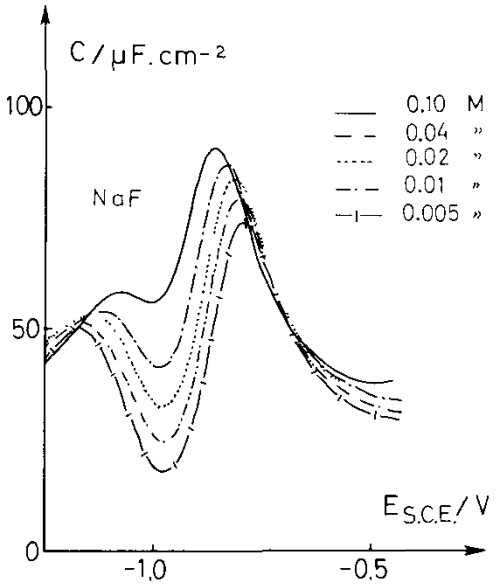

(b) Measured capacity (Fig 2.a from [61], reprinted with permission from Elsevier)

Figure 2: Comparison of the computed capacity (a) and the measured capacity (b) of the Ag(110)|NaF interface for concentrations of $(0.005 - 0.1)$M. Below a sketch of our reinterpretation.

The metal is described by metal ions and free electrons in the conduction band, whereas the electrolyte consists of neutral solvent, several ionic as well as undissociated species. Particularly we consider all species additionally on the surface in terms of a surface mixture theory. We provide explicit functions of the free energy for all phases, which account for solvation effects in the volume and on the surface, incompressibility, entropic contributions and reference states. The electrostatic potential arises naturally within the theory due to the consistent derivation based on non-equilibrium thermo-electrodynamics. We emphasize that an *a priori* distinction between Galvani or Volta potentials is not necessary. We are then able to deduce representations of the double layer charge Q and the capacity C based on our model. The remaining set of parameter are well defined equilibrium properties and discussed within this work.

Figure 2 displays a comparison between computed and measured capacity curves for aqueous NaF solutions in contact to Ag(110). We obtain a broad qualitative **and** quantitative agreement to the experimental data and emphasize that all parameters are kept fixed, except the bulk salt concentration. This remarkable accordance is achieved by a consistent incorporation of

the material pressure p within the electrolyte in our derivation, which is completely neglected in Grahame's theory. However, the pressure term actually accounts for the very different sizes (partial molar volumes) of solvent and **solvated** ions and is thus the main contribution which encodes the solvation effect. Particularly within the boundary layer the pressure p adopts very high values, which are counter balanced by the Maxwell stress, and thus cannot be ignored. It turns out that the free charge density n^{F} is not a function of the electric potential φ alone, which is common to all continuum double layer theories, but subject to the coupled problem

$$\nabla p = -n^{\mathrm{F}}(\varphi, p)\nabla\varphi, \qquad -\varepsilon\Delta\varphi = n^{\mathrm{F}}(\varphi, p). \tag{1}$$

A similar relationship is also found on the surface which couples the surface charge density to the surface tension.

The comparison in Figure 2 validates our theory in the potential range of $E = [-1.3, -0.5]$V. We are thus able to **compute** of the corresponding double layer structure based on the equation system (1). Figure 3 displays exemplarily the computed structure for $E = -0.6$V, which corresponds to a metal surface/electrolyte potential drop of $\underset{s}{\varphi} - \varphi^{\mathrm{E}} = 0.37$V. The space dependent mole densities of solvent, cations and anions are the solid lines wheres the respective coverages on the metal surface are encoded in the bar chart. The electrostatic potential is shown as black dashed line.

We find indeed the formation of several layers in front of the metal surface. Based on the classical perception, we reinterpret our findings in the terminology of inner- and outer Helmholtz plane, Stern layer, diffuse layer, and provide **sharp** definitions of their actual position. However, very significant differences are found to some classical assumptions, e.g. that of a constant Stern layer width or a *fixed* layer of adsorbates forming the inner Helmholtz plane. We discuss this more in detail in Section 11.

This work should be understood as general thermodynamic framework for arbitrary metal/ electrolyte interfaces. Some selected examples serve to show its validity. However, we derive the whole equation system universal enough to account for mixtures of salts, weak acids, different solvents, electron transfer reactions, metal surface orientations and other effects. It allows further for a systematic extension to non-equilibrium situations, however, ensuring that in equilibrium accordance to measured data is obtained. This is especially of interest for the widely used Poisson–Nernst–Planck models [48, 51, 53, 2, 3, 55, 27, 41], which actually lead in equilibrium to the Gouy–Chapman theory and are thus only valid in a very narrow potential range. The free energy functions we employ in this work are rather simplistic, although providing already a good agreement to experimental data. However, applying more sophisticated free energy models within our theory is straight forward, e.g. (surface) phase separation, enthalpy contributions, virial expansions, temperature effects.

Organization of this paper. In Chapter 2 we present basic assumptions, quantities, properties and restrictions of the general constitutive theory. The general equilibrium conditions are derived in Chapter 3.

The special constitutive theory of the electrochemical system at hand is the main focus of Chapter 4. Here we summarize the free energy models for the metal, the electrolyte and the surface.

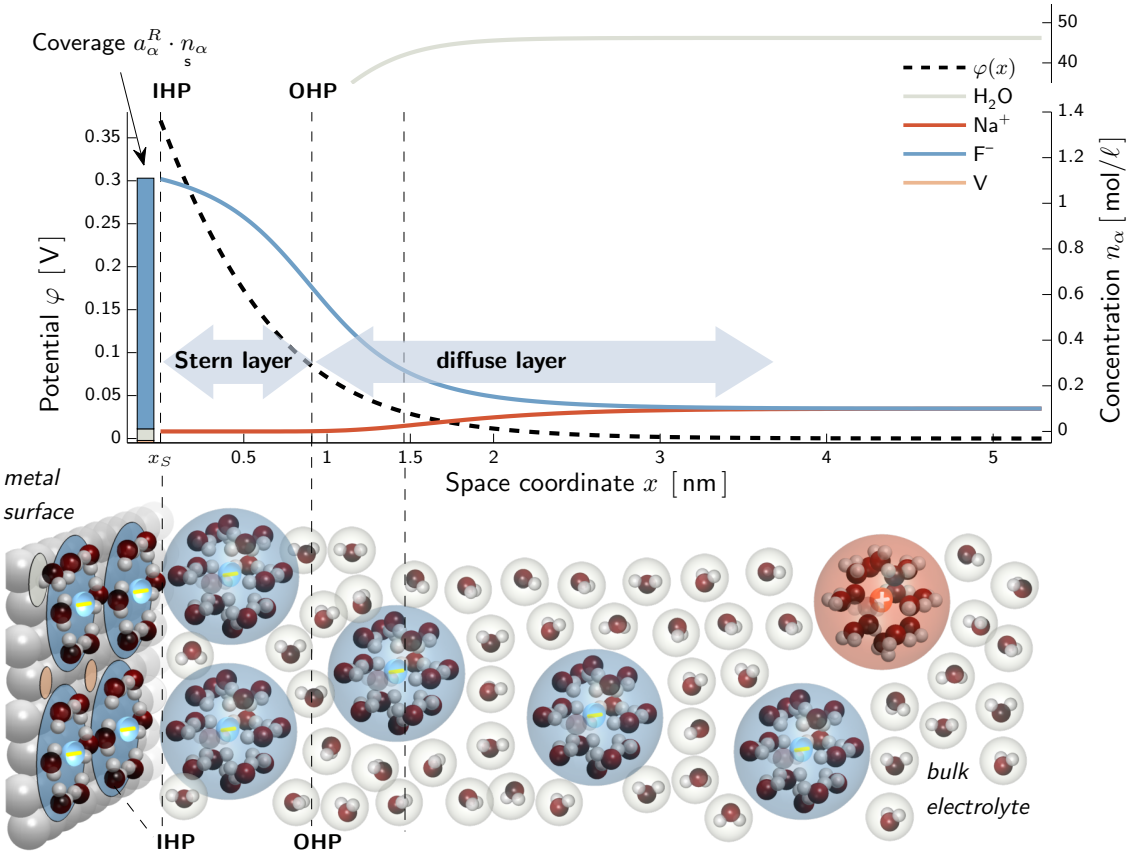

Figure 3: Compute structure of the metal surface/electrolyte interface for $E = -0.6$ (which corresponds to $\varphi|_{x_S} - \varphi|_{x_E} = 0.37$V).

Chapter 5 specifies the considered adsorption and surface reactions and provides the derivation of the relevant equations that are needed to describe the combined electrochemical system. This derivation is based on the equilibrium conditions from Chapter 3 and the constitutive model developed in Chapter 4. A careful discussion of the complete metal-interface-electrolyte model concludes Chapter 5.

Chapter 6 discusses the parameter arising in our model. These include the solvation number, partial molar volumes and areas, adsorption and reaction energies and others.

In Chapter 7 we define the measurable cell potential E, the double layer charge Q and the capacity C. Based on a derivation of the current-charge relation we are able to obtain explicit representations of Q and C based on the equations of Chapter 5. We provide definitions of the reference potential as well as the potential of zero charge and establish the link between our model and experimental quantities.

The new capabilities of our model are illustrated in Chapter 8-11 by a discussion of several examples. General discussions of our model are provided on the example of Ag(110)|$\mathrm{KPF_6}$ (Chapter 9). A comparison to different experimental data as well as different metal surfaces is given in Chapter 10. Finally we investigate the structure of the Ag(110)|NaF interface in Chapter 11, which provides also our new definitions of inner- and outer Helmholtz plane and discusses

the comparison to the classical perception.

A conclusion and some final remarks are given in Chapter 12.

2 Metal/electrolyte interface in the context of thermodynamics

Our theory is based on the framework of non-equilibrium continuum thermodynamics [46, 47, 16, 13, 4, 30], which consistently couples electrodynamics and thermodynamics. It describes mass, momentum and energy as well as electromagnetic field as continuous variables of space and time. The theory relies on universal balance equations which must be supplement by constitutive equations to describe the material at hand. Since we explicitly take into account the metal/electrolyte interface, we include thermodynamics of singular surfaces [47, 4, 30]. The notion singular surface is used because here certain quantities suffer discontinuities, for example the mass density.

In this study we are exclusively interested in thermodynamic equilibrium and we only consider planar interfaces. For the general non-equilibrium case we refer to [20].

2.1 Basic assumptions

Before we derive the model for the metal/electrode interface we make some preliminary assumptions on both the geometry and the equilibrium case.

Assumptions on the domain geometry. We consider a liquid electrolyte $\Omega_{\mathtt{E}} \subset \mathbb{R}^3$ in contact with some metal $\Omega_{\mathtt{M}} \subset \mathbb{R}^3$. The domains $\Omega_{\mathtt{E}}$ and $\Omega_{\mathtt{M}}$ share a common interface S with $S = \partial\Omega_{\mathtt{M}} \cap \partial\Omega_{\mathtt{E}}$. We simplify the geometric properties of the interface by assuming that S is plane and lies parallel to the coordinate plane (y, z) whose normal vector $\boldsymbol{\nu}$ is oriented in x direction and points into the electrolyte domain $\Omega_{\mathtt{E}}$.

Due to the one-dimensional setting of the interface we assume that also every quantity defined in the electrolyte and the metal, respectively, is likewise a function of the space coordinate x. Thus we consider the one dimensional approximation of a metal/electrolyte interface and its surrounding. In the one-dimensional setting the interface is located at the position $x_{\mathtt{S}}$ and the domains for the metal and electrolyte are represented by

$$\Omega_{\mathtt{M}} = [x_{\mathtt{M}}, x_{\mathtt{S}}] \qquad \text{and} \qquad \Omega_{\mathtt{E}} = [x_{\mathtt{S}}, x_{\mathtt{E}}] \,. \tag{2}$$

Temperature and barycentric velocity. Recall that we are only interested in thermodynamic equilibrium, which yields some simplifications concerning the temperature T and the barycentric velocity $\boldsymbol{v}$. In fact, in equilibrium temperature and velocity must be uniform in the bulk domains and they are continuous at singular interfaces [47, 16]. In this case the velocity can be set to zero and the temperature appears only as a constant parameter.

2.2 Constituents and chemical reactions

The three domains $\Omega_{\mathtt{E}}, \Omega_{\mathtt{M}}$ and S are represented by mixtures consisting of different constituents which are described in the following.

The liquid electrolyte consists of $N_{\mathtt{E}} + 1$ constituents, namely the solvent A_0 and solvated ions $A_\alpha, \alpha = 1, \ldots, N_{\mathtt{E}}$.

The metal consists of two constituents, namely the metal ions A_M and the free electrons A_e.

Furthermore, we explicitly account for the interface S in terms of surface constituents $\underset{s}{A}_\alpha, \alpha = 0, \ldots, N_s$. We assume that each constituent of the metal and the electrolyte may also be present on the interface S. However, due to interfacial chemical reactions further constituents may arise as reaction products.

The electrolyte species one the surface are denoted by $\underset{s}{A}_0, \ldots, \underset{s}{A}_{N_{\mathtt{E}}}$ and the surface metal ions are numbered as $\underset{s}{A}_{N_s-1} = \underset{s}{A}_M$ and $\underset{s}{A}_{N_s} = \underset{s}{A}_e$.

The constituents have (molar) masses $m_\alpha \,[\,\mathrm{kg/mol}\,]$ and may be carrier of electric charges $z_\alpha e_0 \,[\,\mathrm{C/mol}\,]$. The positive constant e_0 is the elementary charge per mol and the integers z_α are the charge numbers. Moreover the constituents of the electrolyte are equipped with a solvation number κ_α, characterizing the number of solvent molecules in the solvation shell.

In the electrolyte we consider M general chemical reactions

$$\nu'_{0,i}\, A_0 + \cdots + \nu'_{N_{\mathtt{E}},i}\, \underset{s}{A}_{N_{\mathtt{E}}} \rightleftharpoons \nu''_{0,i}\, \underset{s}{A}_0 + \cdots + \nu''_{N_{\mathtt{E}},i}\, \underset{s}{A}_{N_{\mathtt{E}}} \qquad i = 1, \ldots, M \tag{3}$$

which later on describe self-ionization or dissociation. The quantities $\nu'_{\alpha,i}$, $\nu''_{\alpha,i}$ are positive integers and $\nu_{\alpha,i} = \nu''_{\alpha,i} - \nu'_{\alpha,i}$ denote the stoichiometric coefficients of reaction.

On the surface M_s chemical reactions may occur, which are of the general type

$$\underset{s}{\nu'_{0,i}}\, \underset{s}{A}_0 + \cdots + \underset{s}{\nu'_{N_{\mathtt{E}},i}}\, \underset{s}{A}_{N_s} \rightleftharpoons \underset{s}{\nu''_{0,i}}\, \underset{s}{A}_0 + \cdots + \underset{s}{\nu''_{N_s,i}}\, \underset{s}{A}_{N_s} \qquad i = 1, \ldots, M_s\,. \tag{4}$$

Similar to the volume, $\underset{s}{\nu'_{\alpha,i}}$, $\underset{s}{\nu''_{\alpha,i}}$ are positive integers and $\underset{s}{\nu_{\alpha,i}} = \underset{s}{\nu''_{\alpha,i}} - \underset{s}{\nu'_{\alpha,i}}$ the stoichiometric coefficients of the surface reaction.

Mass and charge are conserved in every chemical reaction, i.e.

$$\sum_{\alpha=0}^{N_{\mathtt{E}}} \nu_{\alpha,i} m_\alpha = 0 \qquad \text{and} \qquad \sum_{\alpha=0}^{N_{\mathtt{E}}} \nu_{\alpha,i} z_\alpha = 0 \qquad \text{for} \qquad i = 1, \ldots, M \tag{5}$$

for the electrolyte phase, whereas similar conditions also hold for the surface reactions.

2.3 Basic quantities

In equilibrium the thermodynamic state of the domains $\Omega_{\mathtt{M}}$, $\Omega_{\mathtt{E}}$ is described by the mole densities n_α and the electric field $\boldsymbol{E}$. On the interface S the thermodynamic states is described by the interfacial mole densities $\underset{s}{n}_\alpha$.

Note that n_α are volume densities (with units mol/m^3) functions of space $x \in \Omega_{\mathtt{M/E}}$ while $\underset{s}{n_\alpha}$ are surface densities (with units mol/m^2) and constants with respect to space due to the one-dimensional setting.

Multiplication of the mole densities by the atomic masses m_α give the partial mass densities in the bulk and on the surface,

$$\rho_\alpha = m_\alpha n_\alpha \qquad \text{and} \qquad \underset{s}{\rho_\alpha} = m_\alpha \underset{s}{n_\alpha} \, . \tag{6}$$

The total mass densities in the bulk and on the surface are defined as

$$\rho = \sum_{\alpha=0}^{N} \rho_\alpha \qquad \text{and} \qquad \underset{s}{\rho} = \sum_{\alpha=0}^{N_s} \underset{s}{\rho_\alpha} \, . \tag{7}$$

Similar, multiplication of the mole densities by the electric charges $z_\alpha e_0$ and summation gives the total free charge densities in the bulk and on the surface,

$$n^{\mathrm{F}} = \sum_{\alpha=0}^{N} z_\alpha e_0 n_\alpha \qquad \text{and} \qquad \underset{s}{n^{\mathrm{F}}} = \sum_{\alpha=0}^{N_s} z_\alpha e_0 \underset{s}{n_\alpha} \, . \tag{8}$$

According to Maxwells theory the total electric charge densities $n^{\mathrm{e}}/\underset{s}{n^{\mathrm{e}}}$ consist of two contributions, viz. the free charge densities $n^{\mathrm{F}}/\underset{s}{n^{\mathrm{F}}}$, as defined above, and the polarization charges $n^{\mathrm{P}}/\underset{s}{n^{\mathrm{P}}}$ due to polarization of the matter, i.e.

$$n^{\mathrm{e}} = n^{\mathrm{F}} + n^{\mathrm{P}} \qquad \text{and} \qquad \underset{s}{n^{\mathrm{e}}} = \underset{s}{n^{\mathrm{F}}} + \underset{s}{n^{\mathrm{P}}} \, . \tag{9}$$

2.4 General constitutive model: Free energies, chemical potentials, polarization, stress, pressure and surface tension.

The constitutive behavior of the metal/interface/electrolyte system is determined by the free energy densities for the metal, the electrolyte and the interface.

We describe the metal as well as the electrolyte as a polarizable mixture and assume that the free energy densities have the general representations

$$\rho\psi_{\mathtt{M}} = \rho\hat{\psi}_{\mathtt{M}}(T, n_M, n_e) - \tfrac{1}{2}\chi_{\mathtt{M}}\varepsilon_0|\boldsymbol{E}|^2 \quad \text{and} \quad \rho\psi_{\mathtt{E}} = \rho\hat{\psi}_{\mathtt{E}}(T, n_0, n_1, ..., n_{N_{\mathtt{E}}}) - \tfrac{1}{2}\chi_{\mathtt{E}}\varepsilon_0|\boldsymbol{E}|^2 \, . \tag{10}$$

The constants $\chi_{\mathtt{M/E}}$ are the electric susceptibilities of the metal and the electrolyte at hand. On the interface S we assume a free energy density of the general form

$$\underset{s}{\psi} = \underset{s}{\hat{\psi}}(T, \underset{s}{n_0}, \underset{s}{n_1}, \ldots, \underset{s}{n_{N_s}}) \, . \tag{11}$$

Note that the energy functions (10) of the electrolyte and the metal have the same general structure. Thus, if no confusion arises we usually drop the subscripts $_{\mathtt{E}}$ and $_{\mathtt{M}}$.

All further constitutive functions are derived from the three free energy functions. Details of the following representations, particularly their status as definitions and conclusions, are given in [20, 30].

The chemical potentials in the bulk and on the surface are defined as

$$\mu_\alpha = \frac{\partial \rho\psi}{\partial n_\alpha} \qquad \text{and} \qquad \underset{s}{\mu_\alpha} = \frac{\partial \underset{s}{\psi}}{\partial \underset{s}{n_\alpha}} \,. \tag{12}$$

The constancy of the susceptibilities χ implies that the chemical potentials are independent of the electric field $\boldsymbol{E}$. The polarization vector is given by the relation

$$\boldsymbol{P} = -\frac{\partial \rho\psi}{\partial \boldsymbol{E}} = \chi\varepsilon_0 \boldsymbol{E} \,. \tag{13}$$

The total stress tensor $\boldsymbol{\Sigma}$ includes the stress due to matter and the Maxwell stress so that the equilibrium momentum balance is written as $\mathrm{div}\boldsymbol{\Sigma} = 0$. The representation of $\boldsymbol{\Sigma}$ reads

$$\boldsymbol{\Sigma} = \Big(\rho\psi - \sum_{\alpha=0}^{N} n_\alpha\mu_\alpha\Big)\mathbf{1} - \tfrac{1}{2}\varepsilon_0|\boldsymbol{E}|^2\mathbf{1} + \boldsymbol{E}\otimes\big(\varepsilon_0\boldsymbol{E} + \boldsymbol{P}\big) \,. \tag{14}$$

The definition of the pressure p depends likewise on the form of the momentum balance. We define p so that the equilibrium momentum balance assumes the form $\nabla p = n^F\boldsymbol{E}$. Then the pressure is given by

$$p = -\rho\hat{\psi} + \sum_{\alpha=0}^{N} n_\alpha\mu_\alpha \,, \tag{15}$$

and, due to the constancy of the susceptibility, p is independent of the electric field. For this reason p is called material pressure. The constitutive relation (15) is known as the Gibbs-Duhem equation.

The interface S is equipped with a surface tension, γ, which is calculated by the interfacial Gibbs-Duhem equation

$$\gamma = \underset{s}{\psi} - \sum_{\alpha=0}^{N_s} \underset{s}{n_\alpha}\underset{s}{\mu_\alpha} \,. \tag{16}$$

3 Equilibrium conditions

The considered system exhibits five different kinds of equilibria: 1. electrical equilibrium, 2. mechanical equilibrium, 3. diffusion equilibrium in $\Omega_{\mathtt{M,E}}$, 4. adsorption equilibrium at S, 5. chemical equilibrium on S and in $\Omega_{\mathtt{E}}$. Next we specify and discuss the equations that describe the equilibria in the metal and electrolyte as well as on the interface.

To formulate the interface equations, it is necessary to introduce the boundary values and the jump of a generic function $u(x)$ in $\Omega_{\mathtt{M/E}}$ across the interface. We define

$$u|_S^{\mathtt{M}} = \lim_{x\in\Omega_{\mathtt{M}}\to S} u(x) \,, \qquad u|_S^{\mathtt{E}} = \lim_{x\in\Omega_{\mathtt{E}}\to S} u(x) \,, \qquad [\![u]\!] = u|_S^{\mathtt{E}} - u|_S^{\mathtt{M}} \,. \tag{17}$$

Electrical equilibrium is determined by the Poisson equation resulting from both Maxwell's equation $\varepsilon_0 \mathrm{div}(\boldsymbol{E}) = n^{\mathrm{e}}$ with $\boldsymbol{E} = -\nabla\varphi$ and the equation for polarization $\mathrm{div}\boldsymbol{P} = -n^{\mathrm{P}}$. Inserting the electric potential and the charge density as well as the polarization leads in the considered one dimensional case to

$$-\varepsilon_0(1+\chi)\partial_{xx}\varphi = n^{\mathrm{F}} \qquad \text{in} \quad \Omega_{\mathtt{M/E}} \,. \tag{18}$$

Across the interface S the jump conditions for the electric field, $\varepsilon_0[\![\boldsymbol{E}\cdot\boldsymbol{\nu}]\!] = \underset{s}{n^{\mathrm{e}}}$, and for the polarization vector, $[\![\boldsymbol{P}\cdot\boldsymbol{\nu}]\!] = -\underset{s}{n^{\mathrm{P}}}$, lead to

$$-\varepsilon_0[\![(1+\chi)\partial_x\varphi]\!] = \underset{s}{n^{\mathrm{F}}} \qquad \text{on} \quad S \,. \tag{19}$$

The electrostatic potential φ is continuous at the interface, i.e.

$$\varphi|_S^{\mathtt{M}} = \varphi|_S^{\mathtt{E}} = \underset{s}{\varphi} \qquad \text{on} \quad S \,. \tag{20}$$

The quantity $\underset{s}{\varphi}$ is called the surface electric potential.

Mechanical equilibrium is determined by the quasi-static momentum balance $\mathrm{div}(\boldsymbol{\Sigma}) = 0$. Inserting the electric potential and the stress tensor leads in the considered one dimensional case to

$$\partial_x\Sigma = 0 \qquad \text{with} \quad \Sigma = -p + \tfrac{1}{2}\varepsilon_0(1+\chi)(\partial_x\varphi)^2 \qquad \text{in} \quad \Omega_{\mathtt{M,E}} \,. \tag{21}$$

The surface balance equation for momentum yields the continuity of the total stress tensor

$$[\![\Sigma]\!] = 0 \qquad \text{on} \quad S \,. \tag{22}$$

There is an useful representation of (21) that can be easily derived. It reads

$$\partial_x p = -n^{\mathrm{F}}\partial_x\varphi \qquad \text{in} \quad \Omega_{\mathtt{M,E}} \,. \tag{23}$$

Chemical equilibrium in the electrolyte is characterized by the law of mass action for each reaction:

$$\sum_{\alpha=0}^{N_{\mathtt{E}}} \nu_{\alpha,i}\mu_\alpha = 0 \qquad \text{in} \quad \Omega_{\mathtt{E}} \,., \qquad i = 1,2,...,M \,. \tag{24}$$

Diffusional equilibrium is defined by zero diffusion fluxes. For a general mixture this is ensured by the conditions [16, 20]

$$\partial_x\Big(\big(\mu_\alpha - \tfrac{m_0}{m_\alpha}\mu_0\big) + e_0\big(z_\alpha - \tfrac{m_0}{m_\alpha}z_0e_0\big)\varphi\Big) = 0 \,, \qquad \alpha = 1,\dots,N \qquad \text{in } \Omega \,. \tag{25}$$

However, these conditions can be simplified: At first note that the gradient of the Gibbs–Duhem equation $(15)_2$ implies

$$\partial_x p = \sum_{\alpha=0}^{N} n_\alpha\partial_x\mu_\alpha \qquad \text{in } \Omega \,. \tag{26}$$

Elimination of $\partial_x p$ by the mechanical equilibrium condition (23) yields

$$\sum_{\alpha=0}^{N} n_\alpha(\partial_x \mu_\alpha + e_0 z_\alpha \partial_x \varphi) = 0 \qquad \text{in } \Omega\ . \tag{27}$$

This equation is combined with (25) so that we obtain for the electrolyte

$$\partial_x(\mu_\alpha + e_0 z_\alpha \varphi) = 0\ , \qquad \alpha = 0, 1, \ldots, N \qquad \text{in } \Omega_{\mathtt{E}}\ . \tag{28}$$

and for the metal

$$\partial_x(\mu_\alpha + e_0 z_\alpha \varphi) = 0\ , \qquad \alpha = e, M \qquad \text{in } \Omega_{\mathtt{M}}\ . \tag{29}$$

Adsorption equilibrium concerns diffusion from the bulk to the interface. The conditions for adsorption equilibrium concern only those constituents which are defined in the bulk domains. The adsorption conditions read

$$\mu_\alpha|_S^{\mathtt{M}} = \underset{s}{\mu_\alpha}, \quad \alpha = M, e \qquad \text{and} \qquad \mu_\alpha|_S^{\mathtt{E}} = \underset{s}{\mu_\alpha}, \quad \alpha = 0, 1, \ldots N_{\mathtt{E}}\ . \tag{30}$$

Surface chemical equilibrium on the interface is characterized by the law of mass action for each reaction:

$$\sum_{\alpha=0}^{N_s} \underset{s}{\nu_{\alpha,i}} \underset{s}{\mu_\alpha} = 0\ , \qquad i = 1, 2, ..., M_s\ . \tag{31}$$

Summary and boundary conditions. The equilibrium of a metal/electrolyte interface is described by the equations (18)–(20) and (28)–(31). The equation system serves to determine the unknowns

$$\begin{aligned}
(\underset{s}{\varphi}, \varphi) &- \text{electric potentials} \\
(n_M, n_e) &- \text{metal species densities} \\
(n_0, n_1, \ldots, n_{N_{\mathtt{E}}}) &- \text{electrolyte species densities} \\
(\underset{s}{n_0}, \ldots, \underset{s}{n_{N_s}}) &- \text{surface species densities}\ .
\end{aligned} \tag{32}$$

To solve the equilibrium equations we need further conditions at the external boundaries of $\Omega_{\mathtt{M}} \cup \Omega_{\mathtt{E}}$. We assume at the metal boundary $x_{\mathtt{M}}$ and the electrolyte boundary $x_{\mathtt{E}}$, respectively, the following conditions:

$$\varphi|_{x=x_{\mathtt{M}}} = \varphi^{\mathtt{M}}\ , \qquad \varphi|_{x=x_{\mathtt{E}}} = \varphi^{\mathtt{E}}\ , \tag{33}$$

$$n_\alpha|_{x=x_{\mathtt{M}}} = n_\alpha^{\mathtt{M}}\ , \qquad n_\alpha|_{x=x_{\mathtt{E}}} = n_\alpha^{\mathtt{E}}\ , \tag{34}$$

$$\Sigma|_{x=x_{\mathtt{M}}} = -p^{\mathtt{M}}\ , \qquad \Sigma|_{x=x_{\mathtt{E}}} = -p^{\mathtt{E}}\ . \tag{35}$$

Thus in the bulk metal and bulk electrolyte far away from the interface we prescribe the electric potential, the number densities and the stress.

Furthermore we assume that the bulk densities $n_\alpha^{\mathtt{M},\mathtt{E}}$ satisfy the electroneutrality conditions

$$z_M n_M^{\mathtt{M}} + z_e n_e^{\mathtt{M}} = 0 \qquad \text{and} \qquad \sum_{\alpha=1}^{N_{\mathtt{E}}} z_\alpha n_\alpha^{\mathtt{E}} = 0 \,. \tag{36}$$

The mechanical equilibrium conditions (21) and (22) require that the stresses at $x_{\mathtt{M}}$ and $x_{\mathtt{E}}$ are equal, which implies

$$p^{\mathtt{M}} = p^{\mathtt{E}} \,. \tag{37}$$

4 Free energy models

The equilibrium conditions of the last section become explicit equations for the unknowns (24) if the free energy densities for the metal, the electrolyte and the interface were known. In this section we will specify the three constitutive functions of the free energy. The motivation and derivation of the free energy densities are described in detail in the Appendix A.

4.1 Electrolyte

We consider the electrolyte as an elastic liquid mixture consisting of a solvent and solvated ions [18]. The free energy density $\rho\hat{\psi}_{\mathtt{E}}$ of the electrolyte will be decomposed into three additive contributions of different origins. We write

$$\rho\hat{\psi}_{\mathtt{E}}(T, n_0, n_1, ..., n_{N_{\mathtt{E}}}) = \rho\psi^{\text{ref}} + \rho\psi^{\text{mech}} + \rho\psi^{\text{mix}}. \tag{38}$$

The quantity ψ^{ref} describes a suitable chosen reference state. $\rho\psi^{\text{mech}}$ encodes mechanical free energy contributions due to the elastic behavior of the liquid and $\rho\psi^{\text{mix}}$ represents the entropic contribution to the free energy due to mixing of particles of different kind.

For the representation of the entropic and mechanical contribution to the free energy we introduce the total mole density of particles n and the mole fractions y_α by

$$n = \sum_{\alpha=0}^{N_{\mathtt{E}}} n_\alpha \qquad \text{and} \qquad y_\alpha = \frac{n_\alpha}{n} \quad \text{with} \quad \sum_{\alpha=0}^{N_{\mathtt{E}}} y_\alpha = 1 \,. \tag{39}$$

The entropic contribution to the free energy is given by

$$\rho\psi^{\text{mix}} = k_B T n \sum_{\alpha=0}^{N_{\mathtt{E}}} y_\alpha \ln(y_\alpha) \,, \tag{40}$$

where k_B denotes the Boltzmann constant. The mechanical contribution to the free energy density is chosen as

$$\rho\psi^{\text{mech}} = (p^R - K)(n\,H - 1) + K_E n\,H \ln(nH) \qquad \text{with} \qquad H = \sum_{\alpha=0}^{N_{\mathtt{E}}} v_\alpha^R y_\alpha \,. \tag{41}$$

Herein p^R is the pressure in the reference state and K_E denotes the bulk modulus of the liquid. The v_α^R is the partial molar volume of the constituent A_α in the reference state. The function H accounts for volume changes due a local variation of the mixtures composition.

Finally, the reference contribution to the free energy is assumed to be

$$\rho\psi^{\text{ref}} = \sum_{\alpha=0}^{N_{\mathtt{E}}} n_\alpha \psi_\alpha^R, \tag{42}$$

where ψ_α^R denotes the reference free energy of each individual constituent.

Pressure. The free energy contributions (38)–(42) yields for the pressure p via its definition (15) the representation

$$p = p^R + K_E(nH - 1) \qquad \text{with} \qquad H = \sum_{\alpha=0}^{N_{\mathtt{E}}} v_\alpha^R y_\alpha \ . \tag{43}$$

Particularly the choice (41) has been made so that we obtain this simple law for the pressure.

Chemical potentials. The definition (12) is now used to calculate the chemical potentials μ_α from the free energy contributions (38)–(42),

$$\mu_\alpha = \psi_\alpha^R + v_\alpha^R\Big(p^R + K_E\ \ln\Big(1 + \frac{p - p^R}{K_E}\Big)\Big) + k_B T \ln y_\alpha \qquad \text{for} \quad \alpha = 0, 1, \ldots, N_{\mathtt{E}}. \tag{44}$$

Incompressibility. In the incompressible limit, i.e. $K_E \to \infty$, the constitutive equation (43) for the pressure p implies the constraint

$$n \sum_{\alpha=0}^{N_{\mathtt{E}}} v_\alpha^R y_\alpha = 1 \ . \tag{45}$$

Thus in the incompressible limit the total mole density of the mixture is already determined by the mole fractions. However, in this limit the constitutive equation (43) cannot be used anymore to determine the pressure p. For this reason the pressure must be included in the list of unknowns.

Further the limit $K_E \to \infty$ reduce the constitutive function (44) of the chemical potentials to

$$\mu_\alpha = g_\alpha^R + v_\alpha^R\,(p - p^R) + k_B T \ln(y_\alpha) \ , \qquad \alpha = 0, 1, \ldots, N_{\mathtt{E}} \ . \tag{46}$$

with reference Gibbs free energy $g_\alpha^R = \psi_\alpha^R + v_\alpha^R\, p^R$. Note that the chemical potentials become linear functions of the pressure p in the incompressible limit.

4.2 Metal

The basic constitutive properties of the metal electrode rely on Sommerfeld's model where the metal consists of an ionic lattice and free electrons [57]. The free energy density $\rho\hat{\psi}_{\mathtt{M}}$ of the metal is additively decomposed into the free energy densities of the metal ions and the electrons,

$$\rho\hat{\psi}_{\mathtt{M}}(T, n_e, n_M) = n_e\psi_e(T, n_e) + n_M\psi_M(T, n_M) \ . \tag{47}$$

Here the partial specific free energy of constituent $\alpha \in \{e, M\}$ depends only on the mole density of constituent α.

The decomposition (47) implies a corresponding decomposition of the pressure p into its partial pressures

$$p(T, n_e, n_M) = p_M(T, n_M) + p_e(T, n_e) \ . \tag{48}$$

The partial free energy density of the electrons is determined on Sommerfeld's model of a metal [57],

$$n_e\psi_e = \frac{3}{5}\left(\frac{3}{8\pi}\right)^{2/3}\frac{h^2}{2m_e}n_e^{5/3} \ , \tag{49}$$

where h is Planck's constant. The free energy density contribution of the metal ions is given by

$$n_M\psi_M = n_M\psi_M^R + (p_M^R - K_M)(v_M^R\, n_M - 1) + K_M v_M^R\, n_M \ln(v_M^R\, n_M) \ . \tag{50}$$

Here K_M is the bulk modulus of the metal, v_M^R is the partial molar volume of the metal ions in the lattice and p_M^R is a reference pressure. The choice (50) has been made to obtain a simple linear relation between the partial pressure p_M and the lattice deformation characterized by the mole density n_M.

Pressure. In an analogous manner to the electrolyte we use (15) to calculate the total pressure of the metal from the constitutive model (47)–(50). Hereafter we identify the partial pressures p_e and p_M for which we obtain

$$p_e = \frac{2}{5}\left(\frac{3}{8\pi}\right)^{2/3}\frac{h^2}{2m_e}n_e^{5/3} \qquad \text{and} \qquad p_M = p_M^R + K_M(v_M^R\, n_M - 1) \ . \tag{51}$$

Chemical potentials. The constitutive model (47)–(50) leads to chemical potentials μ_e and μ_M of the electrons and metal ions, respectively, that are represented by

$$\mu_e = \left(\frac{3}{8\pi}\right)^{2/3}\frac{h^2}{2m_e}n_e^{2/3} \qquad \text{and} \qquad \mu_M = \psi_M^R + v_\alpha^R\Big(p_M^R + K_M\, \ln\Big(1 + \frac{p - p_M^R}{K_M}\Big)\Big). \tag{52}$$

Incompressibility. As in the electrolyte we consider for the metal also the incompressible limit $K_M \to \infty$. The consequences are similar as before: (i) the mole density n_M is calculated from the constraint

$$n_M v_M^R = 1 \tag{53}$$

and reduces here to a constant. (ii) Instead of n_M the partial pressure p_M is the unknown variable in the incompressible limit, and (iii) the chemical potential μ_M becomes a linear function of p_M, viz.

$$\mu_M = \psi_M^R + v_M^R p_M \ . \tag{54}$$

According to the relation $p = p_e + p_M$ we can use the total pressure p instead of p_M as the new unknown, which is more convenient.

4.3 Interface

It is assumed that there is no energy exchange due to thermal motion between the interfacial electrons and the ensemble of remaining constituents. Thus the total surface free energy density $\underset{s}{\psi}$ additively splits in a contribution of the electrons, $\underset{s}{\psi_e}$, and of the remaining surface constituents, $\underset{s}{\psi_r}$, i.e.

$$\underset{s}{\psi} = \underset{s}{\psi_e}(T, \underset{s}{n_e}) + \underset{s}{\psi_r}(T, \underset{s}{n_0}, \underset{s}{n_1}, \ldots, \underset{s}{n_{N_s-1}}) \ . \tag{55}$$

The free energy density $\underset{s}{\psi_e}$ only depends on the electron density $\underset{s}{n_e}$ whereas the free energy density $\underset{s}{\psi_r}$ is independent of $\underset{s}{n_e}$.

The surface tension γ thus decomposes into a corresponding contribution of the electrons and an elastic contribution of the remaining constituents, i.e.

$$\gamma = \gamma_e + \gamma_r \qquad \text{with} \qquad \gamma_e = \underset{s}{\psi_e} - \underset{s}{n_e}\underset{s}{\mu_e} \quad \text{and} \quad \gamma_r = \underset{s}{\psi_r} - \sum_{\alpha=0}^{N_s-1} \underset{s}{n_\alpha}\underset{s}{\mu_\alpha} \ . \tag{56}$$

Due to the decomposition (55) we can separately discuss the modeling procedure of $\underset{s}{\psi_e}$ and $\underset{s}{\psi_r}$, starting with the surface free energy of the adsorbates and the metal species.

We assume that $\underset{s}{\psi_r}$ consists of some reference state contribution $\underset{s}{\psi_r^{\text{ref}}}$, a mechanical contribution $\underset{s}{\psi_r^{\text{mech}}}$, which covers the elastic behavior of the lattice, and an entropic contribution $\underset{s}{\psi_r^{\text{mix}}}$ due to entropic mixing, i.e.

$$\underset{s}{\psi_r} = \underset{s}{\psi_r^{\text{ref}}} + \underset{s}{\psi_r^{\text{mix}}} + \underset{s}{\psi_r^{\text{mech}}}. \tag{57}$$

Of course, further contributions to $\underset{s}{\psi_r}$ can be considered, e.g. enthalpy of mixing [35].

The interfacial free energy of mixing is different from the corresponding contribution in the electrolyte because there are lattice sites on S which are absent in the liquid electrolyte. Each metal ion on S allocates ω_M adsorption sites. The surface density of adsorption sites is thus $\omega_M \underset{s}{n_M}$. Each particle of constituent $\alpha \in 1, 2, \ldots, N_s - 2$ requires ω_α sites. Therefore the surface density of vacancies, i.e. of empty sites, is given by

$$\underset{s}{n_V} = \omega_M \underset{s}{n_M} - \sum_{\alpha=0}^{N_s-2} \omega_\alpha \underset{s}{n_\alpha} \ . \tag{58}$$

We denote the partial molar area of the surface metal ions with a_M^R which define the corresponding molar areas of vacancies and adsorbates,

$$a_V^R = \frac{1}{\omega_M} a_M^R \qquad \text{and} \qquad a_\alpha^R = \frac{\omega_\alpha}{\omega_M} a_M^R \; . \tag{59}$$

For the formulation of the free energy contributions it is useful to introduce total mole densities $\underset{s}{n}$ (of mixing particles) and surface fractions $\underset{s}{y_\alpha}$ of adsorbates and vacancies, respectively,

$$\underset{s}{n} = \sum_{\alpha=0}^{N_s-2} \underset{s}{n_\alpha} + \underset{s}{n_V} \qquad \text{and} \qquad \underset{s}{y_\alpha} = \frac{\underset{s}{n_\alpha}}{\underset{s}{n}} \qquad \text{with} \qquad \sum_{\alpha=0}^{N_s-2} \underset{s}{y_\alpha} + \underset{s}{y_V} = 1 \; . \tag{60}$$

The mixing of the adsorbates with the vacancies in a liquid like manner leads to the free energy contribution

$$\underset{s}{\psi_r^{\text{mix}}} = k_B T \left(\sum_{\alpha=0}^{N_s-2} \underset{s}{n_\alpha} \ln(\underset{s}{y_\alpha}) + \underset{s}{n_V} \ln(\underset{s}{y_V}) \right) \; . \tag{61}$$

The mechanical part of the surface free energy is determined in a similar manner as in the bulk metal,

$$\underset{s}{\psi_r^{\text{mech}}} = \underset{s}{\psi_M^R} - (\gamma^R - \underset{s}{K})(a_M^R \underset{s}{n_M} - 1) - \underset{s}{K}\, a_M^R \underset{s}{n_M} \ln(a_M^R \underset{s}{n_M}) \; , \tag{62}$$

where a_M^R is the partial molar area of the metal at the surface, $\underset{s}{K}$ the surface compressibility of the lattice and γ^R denotes a reference surface tension for an clean surface, i.e. $\underset{s}{y_V} = 1$.

The interfacial free energy contribution of the reference state is

$$\underset{s}{\psi_r^{\text{ref}}} = \sum_{\alpha=0}^{N_s-2} \underset{s}{n_\alpha} \underset{s}{\psi_\alpha^R} \tag{63}$$

where $\underset{s}{\psi_\alpha^R}$ denotes the reference surface free energy of the adsorbates.

To our knowledge there seems to be no accepted model for the interfacial free energy density of the electrons, [37]. Therefore we do not specify the free energy density of the electrons in this study. It is sufficient to assume that the interfacial free energy of the electrons, $\underset{s}{\psi_e}$, exclusively depends on the mole density $\underset{s}{n_e}$, i.e.

$$\underset{s}{\psi_e} = \underset{s}{\hat{\psi}_e}(\underset{s}{n_e}). \tag{64}$$

Since we have not specified an explicit function $\underset{s}{\psi_e}$ yet, we have no explicit representation of the surface electron chemical potentials $\underset{s}{\mu_e}$. We can only conclude that $\underset{s}{\mu_e}$ depends exclusively on the surface electron density $\underset{s}{n_e}$, i.e.

$$\underset{s}{\mu_e} = \underset{s}{\hat{\mu}_e}(\underset{s}{n_e}) \; . \tag{65}$$

However, we can expand $\underset{s}{\mu_e}$ in a Taylor series around some prescribed reference density $\underset{s}{n_e^R}$. In this study we are only interested in the first term of the series, with which we have a constant chemical potential,

$$\underset{s}{\mu_e} \approx \underset{s}{\hat{\mu}_e}(\underset{s}{n_e^R}) = \text{const.} \tag{66}$$

Further we assume that the free energie density is a linear function of $\underset{s}{n_e}$, i.e.

$$\underset{s}{\psi_e} = \underset{s}{\psi_e^R} + \underset{s}{\mu_e}\underset{s}{n_e} \, . \tag{67}$$

Surface tension. According to (56) our constitutive model of the free energy implies

$$\gamma = \gamma^R + \underset{s}{K}\left(a_M^R \underset{s}{n_M} - 1\right) \, . \tag{68}$$

We observe that the surface tension only depends on the metal ion density $\underset{s}{n_M}$.

Chemical potentials. For the adsorbates we obtain the chemical potentials

$$\underset{s}{\mu_\alpha} = \underset{s}{\psi_\alpha^R} + k_B T \ln(\underset{s}{y_\alpha}) - \omega_\alpha k_B T \ln(\underset{s}{y_V}) \, , \qquad \alpha = 0, 1, \ldots, (N_s - 2) \, . \tag{69}$$

The chemical potential for the surface metal ions is given by

$$\underset{s}{\mu_M} = \underset{s}{\psi_M^R} + \omega_M k_B T \ln(\underset{s}{y_V}) - a_M^R \left(\gamma^R + \underset{s}{K} \ln\left(\frac{\gamma - \gamma^R}{\underset{s}{K}} + 1\right)\right) \, . \tag{70}$$

Incompressibility. As in the bulk, we perform the limit $\underset{s}{K} \to \infty$. In this case we conclude from the constitutive relation (68) that the surface density $\underset{s}{n_M}$ of the metal ions is a constant and given by

$$a_M^R \underset{s}{n_M} = 1 \, , \tag{71}$$

while, as before, instead of $\underset{s}{n_M}$ the surface tension γ_r becomes a new independent unknown of the system. Moreover the chemical potential of the metal ions reduces to

$$\underset{s}{\mu_M} = \underset{s}{\psi_M^R} + \omega_M k_B T \ln \underset{s}{y_V} - a_M^R \gamma \, . \tag{72}$$

The surface incompressibility constraint (71) and the condition (58) determines the total number density $\underset{s}{n}$ in terms of the surface fractions $\underset{s}{y_\alpha}$. We insert the constraint (71) into the equation (58) and obtain after some rearrangements

$$\frac{1}{\underset{s}{n}} = a_V^R \underset{s}{y_V} + \sum_{\alpha=0}^{N_s-2} a_\alpha^R \underset{s}{y_\alpha} \, . \tag{73}$$

Finally we suggest $\underset{s}{n_e^R} = z_M \underset{s}{n_M}$ as the reference density for the Taylor expansion of $\underset{s}{\mu_e}$. The actual value of the (constant) chemical potential $\underset{s}{\mu_e}$ thus depends (parametrically) on the molar area a_M^R of the metal surface lattice. We define the abbreviation

$$\underset{s}{\mu_e^{\mathtt{M}}} = \underset{s}{\hat{\mu}_e}(\tfrac{z_M}{a_M^R}). \tag{74}$$

Note that the parameter a_M^R covers the actual structure of the metal surface, e.g. (110) or (100) surface. Hence the constant $\underset{s}{\mu_e^{\mathtt{M}}}$ is (parametrically) dependent on the surface orientation.

5 The metal/electrolyte/interface model

In this section we exploit the metal/electrolyte/interface model from Sections 3 and 4 for some explicit reactions in the electrolyte phase and on the metal surface. Particularly we derive the representations of the bulk and interfacial mole densities as functions of the electrostatic potentials $\varphi/\underset{s}{\varphi}$, the pressure p and the surface tension γ. Finally we discuss the remaining set of equations that determine φ,$\underset{s}{\varphi}$, p and γ.

5.1 Considered chemical reactions

Here we specify the chemical reactions (3) and (4) for the metal/electrolyte/interface model. The considered reactions are general enough to describe a wide range of electrolytic solutions, however, specific enough to obtain some explicit results.

5.1.1 Electrolyte reactions

In the electrolyte phase we consider exclusively dissociation reactions, which account for the self ionization of the solvent, the dissociation of acids as well as the dissolution of salts.

The explicit representation of these chemical reactions requires a consecutive indexing, where A_α denotes the solvent, acid, or salt constituent, and $A_{\alpha+1}$, $A_{\alpha+2}$ the reaction products. Since the reaction products are ionic species, solvation occurs has to be considered in the dissociation reaction. Hence the general scheme of dissociation reactions is

$$A_\alpha + (\kappa_{\alpha+1} + \kappa_{\alpha+2})A_0 \rightleftharpoons A_{\alpha+1} + A_{\alpha+2}, \quad \alpha = 0, 3, \ldots, N_{\mathtt{E}} - 2. \tag{75}$$

5.1.2 Surface reactions

On the interface we describe four different phenomena which occur on the electrolytic side. There is adsorption of all electrolytic constituents which is followed by a reaction where the adsorbates loose a part of their solvation shell. Moreover the adsorbates are involved in electron transfer reactions which are also accompanied by a further reduction of the remaining solvation shell. Finally dissociation of adsorbates on the surface may occur.

The explicit representation of these chemical reactions requires the introduction of a double index (α, β) for numbering the adsorbates. The first index indicates the corresponding ion in the electrolyte of the interfacial constituent, while the second index counts the number of involved electron transfer reactions.

In detail the following reactions occur:

- **Adsorption** corresponds to the diffusion process from a point $x \to x_S$ onto the surface S. We follow the convention in chemistry and write adsorption as some kind of chemical reaction,

$$A_\alpha \rightleftharpoons \underset{s}{A}_\alpha \,, \qquad \alpha = 0, \ldots, N_{\mathtt{E}}. \tag{76}$$

  The charge number z_α, mass m_α and solvation number κ_α are equal for A_α and $\underset{s}{A}_\alpha$.

- **Solvation shell stripping** corresponds to the restructuring and release of solvent molecules of an adsorbed, solvated ion. We denote by $(\underset{s}{A}_{1,0}, \ldots, \underset{s}{A}_{N_{\mathtt{E}},0})$ the reaction products of this process and write the solvation shell stripping reactions as

$$\underset{s}{A}_\alpha \rightleftharpoons \underset{s}{A}_{\alpha,0} + (\kappa_\alpha - \kappa_{\alpha,0})\, \underset{s}{A}_0 \,, \qquad \alpha = 0, 1, \ldots, N_{\mathtt{E}}. \tag{77}$$

  Hence, the species $\underset{s}{A}_{\alpha,0}$ are partially solvated ions with solvation number $\kappa_{\alpha,0}$ and charge number $z_{\alpha,0} = z_\alpha$. Note that a shrinking of the solvation shell releases solvent molecules $\underset{s}{A}_0$ on the surface.

- **Electron transfer** is further considered in elementary steps. The first electron is transferred from (or to) a partially solvated ion $\underset{s}{A}_{\alpha,0}$, producing a species $\underset{s}{A}_{\alpha,1}$ with charge number $z_{\alpha,1} = z_\alpha - \,\mathrm{sgn}(z_\alpha)\, 1$ and solvation number $\kappa_{\alpha,1}$. This species $\underset{s}{A}_{\alpha,1}$ could further react with an electron to produce a constituent $\underset{s}{A}_{\alpha,2}$, and so forth. The general scheme for $\alpha = 1, \ldots, N_{\mathtt{E}}$ is thus

$$\underset{s}{A}_{\alpha,\beta-1} + \,\mathrm{sgn}(z_\alpha) \underset{s}{A}_e \rightleftharpoons \underset{s}{A}_{\alpha,\beta} + (\kappa_{\alpha,\beta-1} - \kappa_{\alpha,\beta}) \underset{s}{A}_0 \,, \qquad \beta = 1, \ldots, |z_\alpha|. \tag{78}$$

  where the species $\underset{s}{A}_{\alpha,\beta}$ has charge number $z_{\alpha,\beta} = z_\alpha - \,\mathrm{sgn}(z_\alpha)\, \beta$ and solvation number $\kappa_{\alpha,\beta}$.

- **Dissociation** is finally considered as elementary surface reaction. Similar to the volume we introduce a consecutive indexing where $\underset{s}{A}_\alpha$ dissociates to the ionic species $\underset{s}{A}_{\alpha+1,\beta}$ and $\underset{s}{A}_{\alpha+2,\beta}$. We assume that there is for each bulk dissociation reaction a corresponding dissociation reaction on the surface. The surface dissociation also accounts for the (surface) solvation effect,

$$\underset{s}{A}_\alpha + (\kappa_{\alpha+1,\beta} + \kappa_{\alpha+2,\beta}) \underset{s}{A}_0 \rightleftharpoons \underset{s}{A}_{\alpha+1,\beta} + A_{\alpha+2,\beta} \tag{79}$$

  for $\beta = 0, 1, \ldots, |z_\alpha|,\ \alpha = 0, 3, \ldots, N_{\mathtt{E}} - 2$.

5.2 Equilibrium representations

Next we derive the equilibrium representations of the mole densities in each phase as well as on the interface.

5.2.1 Electrolyte

The thermodynamic state of the electrolyte is described by the space dependent quantities: electrostatic potential φ, mole fractions y_α, total mole density n and pressure p. The total mole density n is determined already by the incompressibility constraint (46),

$$n \sum_{\alpha=0}^{N_{\mathrm{E}}} v_\alpha^R y_\alpha = 1 \,. \tag{80}$$

At first we integrate the equations (28) of diffusional equilibrium. Using the representations (46) and the boundary conditions (33)–(35) to express the mole fractions y_α in terms of φ and p we obtain

$$\hat{y}_\alpha(\varphi{-}\varphi^{\mathrm{E}}, p{-}p^{\mathrm{E}}) = y_\alpha^{\mathrm{E}} \exp\Big(-\frac{z_\alpha e_0}{k_B T}(\varphi{-}\varphi^{\mathrm{E}}){-}\frac{v_\alpha^R}{k_B T}(p{-}p^{\mathrm{E}})\Big) \qquad \alpha = 0, 1, \ldots, N_{\mathrm{E}} \,. \tag{81}$$

The quantities y_α^{E}, φ^{E} and p^{E} are given values of mole fractions, electrostatic potential and pressure far away from the interface at x_{E}.

The free charge density $n^{\mathrm{F}} = \sum_{\alpha=0}^{N_{\mathrm{E}}} z_\alpha e_0 n_\alpha$ follows from the incompressibility constraint (80) and the representation (81),

$$\hat{n}^{\mathrm{F}}(\varphi - \varphi^{\mathrm{E}}, p - p^{\mathrm{E}}) = \frac{\sum_{\alpha=0}^{N_{\mathrm{E}}} z_\alpha e_0 \, y_\alpha^{\mathrm{E}} \exp\big(-z_\alpha \frac{e_0}{k_B T}(\varphi - \varphi^{\mathrm{E}}) - \frac{v_\alpha^R}{k_B T}(p - p^{\mathrm{E}})\big)}{\sum_{\alpha=0}^{N_{\mathrm{E}}} v_\alpha^R \, y_\alpha^{\mathrm{E}} \, \exp\big(-z_\alpha \frac{e_0}{k_B T}(\varphi - \varphi^{\mathrm{E}}) - \frac{v_\alpha^R}{k_B T}(p - p^{\mathrm{E}})\big)} \,. \tag{82}$$

Note that the free charge density of the electrolyte depends on both the electrostatic potential φ and the pressure p. Therefore the Poisson equation (18) and the momentum balance equation (23) form a coupled system to determine φ and p:

$$\varepsilon_0(1 + \chi_{\mathrm{E}})\partial_{xx}\varphi = -\hat{n}^{\mathrm{F}}(\varphi - \varphi^{\mathrm{E}}, p - p^{\mathrm{E}}) \,, \tag{83}$$

$$\partial_x p = -\hat{n}^{\mathrm{F}}(\varphi - \varphi^{\mathrm{E}}, p - p^{\mathrm{E}})\partial_x\varphi \,. \tag{84}$$

The associated boundary conditions at x_{E} and x_{S} are given by (20) and (33)–(35), respectively.

5.2.2 Metal

The thermodynamic state of the metal is described by three space dependent quantities, viz. the electrostatic potential φ, the electron density n_e and the partial pressure p. The number density n_M of the ions is a constant in this model and is determined by the incompressibility constraint (53),

$$n_M = \frac{1}{v_M^R} . \tag{85}$$

From the diffusional equilibrium (29) of the electrons we obtain a representation of the electron density n_e as a function of the electrostatic potential φ,

$$\hat{n}_e(\varphi - \varphi^{\mathtt{M}}) = n_e^{\mathtt{M}}\Big(1 + \frac{e_0}{\mu_e^{\mathtt{M}}}\big(\varphi - \varphi^{\mathtt{M}}\big)\Big)^{\frac{3}{2}} . \tag{86}$$

Herein $n_e^{\mathtt{M}}$, $\mu_e^{\mathtt{M}}$ and $\varphi^{\mathtt{M}}$ denote the values of electron density, chemical potential and electric potential in the bulk metal at $x_{\mathtt{M}}$, which are determined from the boundary conditions (33)–(35). Due to the bulk electroneutrality (36) one has $n_e^{\mathtt{M}} = z_M n_M^{\mathtt{M}}$.

Thus the electron density n_e only depends on the electrostatic potential while the metal ion density n_M is a constant. Accordingly the free charge density $n^{\mathrm{F}} = z_e e_0 n_e + z_e e_0 n_M$ is a function of φ only, i.e.

$$\hat{n}^{\mathrm{F}}(\varphi - \varphi^{\mathtt{M}}) = \frac{z_M}{v_M^R}\Big(1 - \Big(1 + \frac{e_0}{\mu_e^{\mathtt{M}}}\big(\varphi - \varphi^{\mathtt{M}}\big)\Big)^{\frac{3}{2}}\Big) \tag{87}$$

The electrostatic potential in the metal is thus determined by the Poisson equation (18) with (87), i.e.

$$-\varepsilon_0(1 + \chi_{\mathtt{M}})\partial_{xx}\varphi = \hat{n}^{\mathrm{F}}(\varphi - \varphi^{\mathtt{M}}) . \tag{88}$$

The boundary conditions for the Poisson equations at $x_{\mathtt{M}}$ and $x_{\mathtt{S}}$ are given by (20) and (33), respectively.

In contrast to the electrolyte the free charge density n^{F} does not depend on the pressure p. Hence, the Poisson equation (88) is sufficient to determine φ. After that the momentum balance equation (23) is used to determine the pressure p as a function of the electrostatic potential φ.

5.2.3 Interface

The thermodynamic state of the interface is described by the quantities $\underset{s}{\varphi}, \underset{s}{y_\alpha}, \underset{s}{n_M}, \underset{s}{n_e}$ and γ. Note that these quantities have no space dependence which results from our simplified geometry. However, due to the intricate surface reactions (76)–(79) the determination of the interfacial thermodynamic state is much more involved as the thermodynamic state of the two bulk regions.

Next we derive some useful representations that relate the unknown quantities of the interface to the variables of the adjacent bulk domains.

Surface potential. In this study our constitutive model for the interface, see (66), implies a constant interfacial chemical potential $\underset{s}{\mu_e^{\mathtt{M}}}$ of the electrons. Consequently the potential difference $\varphi^{\mathtt{M}} - \underset{s}{\varphi}$, which is determined by $\underset{s}{\mu_e}$ and $\underset{s}{\mu_e^{\mathtt{M}}}$, is constant as well. This proposition follows (i) from the equations of diffusional and adsorption equilibrium, viz. (28) and (30),respectively, and (ii) from the continuity (20) of the electric potential at S. We obtain

$$\varphi^{\mathtt{M}} - \underset{s}{\varphi} = \tfrac{1}{z_e e_0}\big(\underset{s}{\mu_e^{\mathtt{M}}} - \mu_e^{\mathtt{M}}\big) . \tag{89}$$

Note that the value of the right hand side of (89) depends on the crystal structure of the metal as well as its surface orientation.

Surface fractions – Vacancies. The representation of the surface mole fraction of vacancies relies on (i) the continuity of the electrostatic potential at S, (20), (ii) the equation (30) that describes the adsorption equilibrium (30) for the metal ions, (iii) the equation (28) relating the the chemical potential μ_M at S by the corresponding chemical potential at $x_{\mathtt{M}}$ and (iv) by the constitutive equation (72). The intermediate result reads

$$a_M^R\gamma - \omega_M k_B T \ln \underset{s}{y_V} = \underset{s}{\psi_M^R} - \mu_M^{\mathtt{M}} - z_M e_0(\varphi^{\mathtt{M}} - \underset{s}{\varphi}) \,. \tag{90}$$

Due to the condition (89) the potential drop $\varphi^{\mathtt{M}} - \underset{s}{\varphi}$ is constant. Thus the right hand side of (90) is constant as well. This enables us to define the reference surface tension γ^R of a clean surface, i.e. for $\underset{s}{y_V} = 1$. Then (90) gives

$$\gamma^R = \tfrac{1}{a_M^R}\big(\underset{s}{\psi_M^R} - \mu_M^{\mathtt{M}} - z_M e_0(\varphi_{\mathtt{M}} - \underset{s}{\varphi})\big) \,, \tag{91}$$

which is now used to simplify (90) for the general case $\underset{s}{y_V} < 1$. Since (90) also holds if adsorbates are present. Thus we finally obtain a useful relationship between the surface tension and the surface fraction of the vacancies,

$$\underset{s}{\hat{y}_V} = \exp\Big(\frac{a_M^R}{\omega_M k_B T}\big(\gamma - \gamma^R\big)\Big) \,. \tag{92}$$

Surface fractions – Adsorption. Next, we seek explicit expressions of the surface fractions $\underset{s}{y_\alpha}$ for the adsorbed electrolyte species. To this end we use (i) the equations (28) of diffusional equilibrium, (ii) the equations (30) describing adsorption equilibrium and (iii) the continuity of the electrostatic potential at S, (20). These conditions give

$$\mu_\alpha^{\mathtt{E}} + z_\alpha e_0 \varphi^{\mathtt{E}} = \underset{s}{\mu_\alpha} + z_\alpha e_0 \underset{s}{\varphi} \,, \qquad \alpha = 0, 1, \ldots, N_{\mathtt{E}}. \tag{93}$$

Finally we insert in (93) the representations (46) and (69) for the chemical potentials and obtain

$$\underset{s}{y_\alpha} = y_\alpha^{\mathtt{E}} (\underset{s}{y_V})^{\omega_\alpha} \exp\Big(-\frac{\Delta g_\alpha^A}{k_B T} - \frac{z_\alpha e_0}{k_B T}(\underset{s}{\varphi} - \varphi^{\mathtt{E}})\Big) \,, \qquad \alpha = 0, 1, \ldots, N_{\mathtt{E}}. \tag{94}$$

The Gibbs free energies of the adsorption processes are defined here by $\Delta g_\alpha^A := \underset{s}{\psi_\alpha^R} - g_\alpha^R$. We observe, if the reference free energy $\underset{s}{\psi_\alpha^R}$ of the adsorbate $\underset{s}{A_\alpha}$ is lower than the Gibbs free energy g_α^R of the corresponding bulk constituent A_α, i.e. $\Delta g_\alpha^A < 0$, then it is favorable for the electrolyte constituent A_α to adsorb at the surface.

Due to equation (92) the mole fraction of vacancies, $\underset{s}{y_V}$, can be written in terms of γ,

$$\underset{s}{\hat{y}_\alpha} = y_\alpha^{\mathtt{E}} \exp\Big(-\frac{\Delta g_\alpha^A}{k_B T} - \frac{z_\alpha e_0}{k_B T}(\underset{s}{\varphi} - \varphi^{\mathtt{E}}) + \frac{a_\alpha^R}{k_B T}\big(\gamma - \gamma^R\big)\Big) \,, \qquad \alpha = 0, 1, \ldots, N_{\mathtt{E}}. \tag{95}$$

We conclude that the surface fractions $\underset{s}{\hat{y}_\alpha}$ of the adsorbates is a function of the potential difference $\underset{s}{\varphi} - \varphi^{\mathtt{E}}$ and of the surface tension difference $\gamma - \gamma^R$.

Surface fractions – Solvation shell stripping. The surface mole fractions of surface constituents that are produced by solvation shell stripping reactions (77) are calculated from the corresponding chemical equilibrium equations (31), which are given by

$$\underset{s}{\mu}_{\alpha} = \underset{s}{\mu}_{\alpha,0} + (\kappa_\alpha - \kappa_{\alpha,0})\underset{s}{\mu}_0 \,, \qquad \alpha = 1, \ldots, N_{\mathtt{E}} \,. \tag{96}$$

Inserting here the constitutive equations (69) yields as representations of the surface mole fractions

$$\underset{s}{y}_{\alpha,0} = \frac{\underset{s}{y}_{\alpha}(\underset{s}{y}_V)^{\omega_{\alpha,0}-\omega_\alpha+\omega_0(\kappa_\alpha-\kappa_{\alpha,0})}}{(\underset{s}{y}_0)^{\kappa_\alpha-\kappa_{\alpha,0}}} \exp\Big(-\frac{\Delta g^S_{\alpha,0}}{k_BT}\Big) \,, \qquad \alpha = 1, \ldots, N_{\mathtt{E}} \,. \tag{97}$$

The newly introduced Gibbs free energy differences $\Delta g^S_{\alpha,0} = \underset{s}{\psi}^R_{\alpha,0} + (\kappa_\alpha - \kappa_{\alpha,0})\underset{s}{\psi}^R_0 - \underset{s}{\psi}^R_\alpha$ describe loss (or gain) due to the solvation shell stripping reactions. If it is thermodynamically favorable for an ionic species to strip off parts of its solvation shell, we have $\Delta g^S_{\alpha,0} < 0$.

Finally we replace the surface fractions $\underset{s}{y}_V$ and $\underset{s}{y}_\alpha$ by the representations (92) and (95) to obtain

$$\underset{s}{\hat{y}}_{\alpha,0} = y^{\mathtt{E}}_\alpha (y^{\mathtt{E}}_0)^{(\kappa_{\alpha,0}-\kappa_\alpha)} \exp\Big(-\frac{\Delta g^A_{\alpha,0}}{k_BT} - \frac{z_\alpha e_0}{k_BT}(\underset{s}{\varphi} - \varphi^{\mathtt{E}}) + \frac{a^R_{\alpha,0}}{k_BT}\big(\gamma - \gamma^R\big)\Big). \tag{98}$$

We call the abbreviation $\Delta g^A_{\alpha,0} = \underset{s}{\psi}^R_{\alpha,0} - g^R_\alpha - (\kappa_\alpha - \kappa_{\alpha,0})g^R_0$ *adsorption energy* of $\underset{s}{A}_{\alpha,0}$.

As before the surface mole fractions of the partially solvated ionic species are functions of the potential difference $\underset{s}{\varphi} - \varphi^{\mathtt{E}}$ and of the surface tension $\gamma - \gamma^R$.

Surface fractions – Electron transfer reactions. The representations of the surface mole fractions $\underset{s}{y}_{\alpha,\beta}$ of constituents that are produced by the electron transfer reactions (78) rely on the corresponding equilibrium conditions (31) and read

$$\underset{s}{\mu}_{\alpha,\beta-1} + \mathsf{sgn}(z_\alpha)\underset{s}{\mu}_e = \underset{s}{\mu}_{\alpha,\beta} + (\kappa_{\alpha,\beta-1} - \kappa_{\alpha,\beta})\underset{s}{\mu}_0 \,, \quad \beta = 1, \ldots, |z_\alpha| \,; \alpha = 1, \ldots, N_{\mathtt{E}} \,. \tag{99}$$

Insertion of the constitutive equations (69) into (99) leads to

$$\underset{s}{y}_{\alpha,\beta} = \underset{s}{y}_{\alpha,\beta-1}(\underset{s}{y}_V)^{\omega_{\alpha,\beta}-\omega_{\alpha,\beta-1}+(\kappa_{\alpha,\beta-1}-\kappa_{\alpha,\beta})\omega_0}(\underset{s}{y}_0)^{\kappa_{\alpha,\beta}-\kappa_{\alpha,\beta-1}} \exp\Big(\frac{-\Delta g^E_{\alpha,\beta}}{k_BT}\Big). \tag{100}$$

The sign of $\Delta g^E_{\alpha,\beta} = \underset{s}{\psi}^R_{\alpha,\beta} - \underset{s}{\psi}^R_{\alpha,\beta-1} + (\kappa_{\alpha,\beta-1} - \kappa_{\alpha,\beta})\underset{s}{\psi}^R_0 - \frac{\mathsf{sgn}(z_\alpha)}{k_BT}\underset{s}{\mu}_e$ determines if it is favorable for an electron to transfer, $\Delta g^E_{\alpha,\beta} < 0$, or to remain on the metal surface, $\Delta g^E_{\alpha,\beta} > 0$.

We replace the surface mole fractions fractions by their representations (92),(94), (98) and obtain

$$\underset{s}{\hat{y}}_{\alpha,\beta} = y^{\mathtt{E}}_\alpha (y^{\mathtt{E}}_0)^{(\kappa_{\alpha,\beta}-\kappa_\alpha)} \exp\Big(-\frac{\Delta g^A_{\alpha,0}}{k_BT} - \frac{z_\alpha e_0}{k_BT}(\underset{s}{\varphi} - \varphi^{\mathtt{E}}) + \frac{a_{\alpha,\beta}}{k_BT}\big(\gamma - \gamma^R\big)\Big). \tag{101}$$

As in the previous cases the Gibbs free energy difference $\Delta g^A_{\alpha,\beta} = \underset{s}{\psi}{}^R_{\alpha,0} - g^R_\alpha - (\kappa_\alpha - \kappa_{\alpha,\beta}) g^R_0 - \beta\,\mathrm{sgn}(z_\alpha)\underset{s}{\mu}_e$ is termed *adsorption energy* of constituent $\underset{s}{A}_{\alpha,\beta}$.

In an analogous manner (95) and (98), the representation (101) of the electron transfer reaction products $A_{\alpha,\beta}$ are functions of the potential difference $\underset{s}{\varphi} - \varphi^{\mathrm{E}}$ and of the surface tension $\gamma - \gamma^R$.

Surface tension. In the previous paragraphs we have determined all surface mole fractions as functions of two variables: the electrostatic potential $\underset{s}{\varphi}$ and the surface tension γ. The electrostatic potential is already determined by the equation (89). In order to obtain a full set of equation we thus finally need an equation for the surface tension. That equation relies on the constraint $(60)_3$,

$$\underset{s}{y_V} + \sum_{\alpha=0}^{N_{\mathrm{E}}} \underset{s}{y_\alpha} + \sum_{\alpha=0}^{N_{\mathrm{E}}} \sum_{\beta=0}^{|z_\alpha|} \underset{s}{y_{\alpha,\beta}} = 1\,. \tag{102}$$

Introducing here the surface mole fraction $\underset{s}{\hat{y}_\alpha}(\underset{s}{\varphi} - \varphi_{\mathrm{E}}, \gamma - \gamma^R)$ of the previous paragraphs leads to an algebraic equation that relates the surface tension γ to the electrostatic potential $\underset{s}{\varphi}$, i.e. $\gamma = \underset{s}{\hat{\gamma}}(\underset{s}{\varphi} - \varphi_{\mathrm{E}})$. Note, however, that this relation is only implicitly given.

Surface electron density. Recall that the surface chemical potential of the electrons is a constant in the current model. Thus the adsorption condition (30) cannot be used to determine the surface electron density $\underset{s}{n_e}$. However, Maxwell's equation (19) serves to determine $\underset{s}{n_e}$, i.e.

$$-\varepsilon_0 [\![(1+\chi)\partial_x \varphi]\!] = z_M e_0 \underset{s}{n_M} + z_e e_0 \underset{s}{n_e} + \sum_{\alpha=0}^{N_{\mathrm{E}}} z_\alpha e_0 \underset{s}{n_\alpha} + \sum_{\alpha=1}^{N_{\mathrm{E}}} \sum_{\beta=0}^{|z_\alpha|} z_{\alpha,\beta} e_0 n_{\alpha,\beta}\,. \tag{103}$$

Inserting the surface mole fractions of the previous paragraphs yields the surface density of electrons in terms of the electrostatic potential difference $\underset{s}{\varphi} - \varphi^{\mathrm{E}}$ and its derivative.

5.3 Discussion on the new metal/electrolyte/interface model

We now discuss the main results of Section 5.2 and add some remarks for illustration.

I. Most importantly is the observation that besides the electrostatic potentials $\varphi/\underset{s}{\varphi}$ the pressure p and and the surface tension γ are central quantities of the model. While the electron density in the metal, n_e, is only dependent on the electrostatic potential φ, the mole fractions in the electrolyte, y_α, are represented by functions of φ and the material pressure p. Analogously the surface electron density $\underset{s}{n_e}$ and the surface mole fractions $\underset{s}{y_\alpha}$ are given as functions of the surface electrostatic potential $\underset{s}{\varphi}$ and of the surface tension γ. The potential φ and the pressure p are determined by the coupled system of Poisson equation (83) and momentum balance (84).

The surface potential $\underset{s}{\varphi}$ and the surface tension γ are determined by the relation (89) and the non-linear constraint (102).

II. The calculational effort to determine φ of the metal/electrolyte/interface model is significantly reduced because the chemical potential of the surface electrons, $\underset{s}{\mu_e}$, is a constant material parameter. Eq. (89) determines the surface potential as

$$\underset{s}{\varphi} = \varphi^{\mathtt{M}} + \tfrac{1}{e_0}\big(\underset{s}{\mu_e^{\mathtt{M}}} - \mu_e^{\mathtt{M}}\big) \tag{104}$$

which serves as explicit boundary condition for the metal and the electrolyte domain. It turns out that the thermodynamic state in the bulk electrolyte and bulk metal can be calculated independently of each other.

III. Apart from the momentum balance equation (84) which relates the gradients of the electrostatic potential φ and the pressure p, there is an useful alternative relation between pressure p and potential φ that is based on the constraint $\sum_{\alpha=0}^{N_{\mathtt{E}}} y_\alpha = 1$. Inserting here the representations (81) leads to

$$1 = \sum_{\alpha=0}^{N_{\mathtt{E}}} y_\alpha^{\mathtt{E}} \exp\Big(-\frac{z_\alpha e_0}{k_B T}(\varphi - \varphi^{\mathtt{E}}) - \frac{v_\alpha}{k_B T}(p - p^{\mathtt{E}})\Big) \,. \tag{105}$$

The momentum equation (84) was already used to derive the representations (81) for the mole fraction y_α by means of the equilibrium conditions (28). Therefore the equation (105) can be used instead of the momentum balance equation (84) to determine p.

IV. We conclude from equation (105) that the pressure p is implicitly given by the potential difference $\varphi - \varphi^{\mathtt{E}}$ of the electrolyte, i.e. $p = \hat{p}(\varphi - \varphi^{\mathtt{E}})$. Particularly, (105) yields

$$\frac{d\hat{p}}{d(\varphi - \varphi^{\mathtt{E}})} = -\frac{\sum_{\alpha=0}^{N_{\mathtt{E}}} z_\alpha e_0 y_\alpha^{\mathtt{E}} \exp\Big(-\frac{z_\alpha e_0}{k_B T}(\varphi - \varphi^{\mathtt{E}}) - \frac{v_\alpha}{k_B T}(p - p^{\mathtt{E}})\Big)}{\sum_{\alpha=0}^{N_{\mathtt{E}}} v_\alpha^R y_\alpha^{\mathtt{E}} \exp\Big(-\frac{z_\alpha e_0}{k_B T}(\varphi - \varphi^{\mathtt{E}}) - \frac{v_\alpha}{k_B T}(p - p^{\mathtt{E}})\Big)} \,. \tag{106}$$

A comparison with the representation (82) of the free charge density n^{F} identifies

$$\frac{d\hat{p}}{d(\varphi - \varphi^{\mathtt{E}})} = -\hat{n}^{\mathrm{F}}(\varphi - \varphi^{\mathtt{E}}, p - p^{\mathtt{E}}) \,. \tag{107}$$

At first glance this relation is not what one would expect. Equation (107) of the new model predicts a far-reaching elementary relation between pressure, electrostatic potential and electric charge in the electrolyte.

V. A similar relation is found on the surface. The constraint (102) yields an implicit relation between the surface tension γ and potential difference $\underset{s}{\varphi} - \varphi^E$, i.e. $\gamma = \hat{\gamma}(\underset{s}{\varphi} - \varphi^E)$. Differentiation

of (102) with respect to $\underset{s}{\varphi} - \varphi^E$ yields at first

$$\frac{d\hat{\gamma}}{d(\underset{s}{\varphi} - \varphi^{\mathrm{E}})} = \frac{\sum_{\alpha=0}^{N_{\mathrm{E}}} z_\alpha e_0 \underset{s}{y_\alpha} + \sum_{\alpha=1}^{N_{\mathrm{E}}} \sum_{\beta=0}^{|z_\alpha|} z_\alpha e_0 \underset{s}{y_{\alpha,\beta}}}{a_V^R \underset{s}{y_V} + \sum_{\alpha=0}^{N_{\mathrm{E}}} a_\alpha^R \underset{s}{y_\alpha} + \sum_{\alpha=1}^{N_{\mathrm{E}}} \sum_{\beta=0}^{|z_\alpha|} a_{\alpha,\beta}^R \underset{s}{y_{\alpha,\beta}}} \,. \tag{108}$$

By means of (73) this can be written as

$$\frac{d\hat{\gamma}}{d(\underset{s}{\varphi} - \varphi^{\mathrm{E}})} = \sum_{\alpha=0}^{N_{\mathrm{E}}} z_\alpha e_0 \underset{s}{n_\alpha} + \sum_{\alpha=1}^{N_{\mathrm{E}}} \sum_{\beta=0}^{|z_\alpha|} z_\alpha e_0 \underset{s}{n_{\alpha,\beta}} \,. \tag{109}$$

The equation (109) is the surface analogy to the equation (107). Hence surface tension, surface potential and charge are intimately related to each other.

VI. A further useful identity for the electrolyte can be derived. It relates the pressure and the electric field $-\partial_x\varphi$. Integration of the momentum balance(84) yields

$$-\partial_x\varphi = \operatorname{sgn}(\varphi - \varphi^{\mathrm{E}}) \sqrt{\frac{2}{\varepsilon_0(1+\chi_{\mathrm{E}})}\big(p - p^{\mathrm{E}}\big) + (\partial_x\varphi)^2|_{x_{\mathrm{E}}}}. \tag{110}$$

The sign in relation (110) relies on the known monotonicity of the electrostatic potential between x_{S} and x_{E}, i.e. $\varphi - \varphi^{\mathrm{E}} > 0$ implies $\partial_x\varphi < 0$.

In equilibrium the electric field $-\partial_x\varphi$ exponentially tends to zero in the electrolyte, see [19]. Thus at a distance sufficiently far away from the surface we may assume

$$(\partial_x\varphi)|_{x_{\mathrm{E}}} = 0 \,. \tag{111}$$

Then (110) reduces to

$$\partial_x\varphi = -\operatorname{sgn}(\varphi - \varphi^{\mathrm{E}}) \sqrt{\frac{2}{\varepsilon_0(1+\chi_{\mathrm{E}})}\big(p - p^{\mathrm{E}}\big)}. \tag{112}$$

The equations (112) and (105) imply that the electric field $\partial_x\varphi$ is a function of both pressure p and potential φ.

VII. There is a further interesting similarity between bulk and the surface equations. In the representations (81) the term $v_\alpha^R\,(p - p^{\mathrm{E}})$ accounts for volumetric size effects of the electrolytic constituents. In a similar manner the term $a_\alpha^R\,(\gamma - \gamma^R)$ in (95), (98) and (101) represents corresponding size effects on the surface.

VIII. Notice further an important consequence of the solvation phenomenon that relies on the representation (82) of the charge density. If all constituents were to have the same partial molar

volume v_α^R, the pressure term cancels in (82). Only in this case the charge density exclusively depends on the electrostatic potential,

$$v_\alpha^R = v^R, \alpha = 0, 1, \ldots, N_{\mathtt{E}} \qquad \Rightarrow \quad \hat{n}^{\mathtt{F}} = \frac{1}{v^R} \frac{\sum_{\alpha=1}^{N} z_\alpha \, y_\alpha^{\mathtt{E}} \, \exp(-z_\alpha \frac{e_0}{k_B T}(\varphi - \varphi^{\mathtt{E}}))}{\sum_{\alpha=0}^{N_{\mathtt{E}}} y_\alpha^{\mathtt{E}} \, \exp(-z_\alpha \frac{e_0}{k_B T}(\varphi - \varphi^{\mathtt{E}}))}. \tag{113}$$

Then the Poisson equation and the momentum balance decouples. However, the solvation effect certainly implies $v_\alpha^R > v_0^R$ and this is the origin of the inherent coupling between the Poisson equation (83) and the momentum balance (84).

IX. The dissociation reactions in the electrolyte (75) are not required to deduce the equilibrium representations of the mole fractions (81). Instead they provide some constraint between the material parameter.

The dissociation reaction (75) in equilibrium, evaluated in the bulk $x = x_{\mathtt{E}}$, leads to (24)

$$\frac{y_{\alpha+1}^{\mathtt{E}} \, y_{\alpha+2}^{\mathtt{E}}}{y_\alpha^{\mathtt{E}} \, (y_0^{\mathtt{E}})^{(\kappa_{\alpha+1}+\kappa_{\alpha+2})}} = \exp\Big(- \frac{\Delta g_\alpha^D}{k_B T} \Big) \qquad \alpha = 0, 3, \ldots, N_{\mathtt{E}} - 2, \tag{114}$$

with $\Delta g_\alpha^D = g_{\alpha+1}^R + g_{\alpha+2}^R - g_\alpha^R - (\kappa_{\alpha+1} + \kappa_{\alpha+2}) g_0^R$. Since the bulk mole fractions $y_\alpha^{\mathtt{E}}$ are already fixed by boundary condition (34). Thus the relation (114) actually determines the reaction free energy Δg_α^D. However, for weak acids, which do not dissociate completely, it is more practicable to prescribe Δg_α^D and determine the actual bulk concentrations $y_\alpha^{\mathtt{E}}$ from the condition (114).

X. A similar circumstance also holds for the surface dissociation reactions (79) which are not required to deduce the equilibrium representations of the surface mole fractions (92), (95),(98) and (101). They provide also some constraint between the material parameter.

In equilibrium, the surface dissociation writes

$$\frac{\underset{s}{y}_{\alpha+1,\beta} \, \underset{s}{y}_{\alpha+2,\beta}}{\underset{s}{y}_{\alpha} \, (\underset{s}{y}_0)^{(\kappa_{\alpha+1,\beta}+\kappa_{\alpha+2,\beta})}} = \exp\Big(- \frac{\underset{s}{\Delta} g_{\alpha,\beta}^D}{k_B T} \Big) \exp\Big(- \Delta\omega_\alpha \frac{a_M^R}{\omega_M k_B T} \big(\gamma - \gamma^R\big) \Big) \tag{115}$$

with $\underset{s}{\Delta} g_{\alpha,\beta}^D = \underset{s}{\psi}_{\alpha+1,\beta} + \underset{s}{\psi}_{\alpha+2,\beta} - \underset{s}{\psi}_{\alpha} - (\kappa_{\alpha+1,\beta} + \kappa_{\alpha+2,\beta}) \underset{s}{\psi}_0$ and $\Delta\omega_\alpha = \omega_{\alpha+1,\beta}^R + \omega_{\alpha+2,\beta}^R - \omega_\alpha - (\kappa_{\alpha+1,\beta} + \kappa_{\alpha+2,\beta})\omega_0$ (for $\beta = 0, 1, \ldots, |z_\alpha|, \ \alpha = 0, 3, \ldots, N_{\mathtt{E}} - 2$). Herein, $\underset{s}{\Delta} g_\alpha^D$ is the reaction free energy of the surface dissociation, and $\Delta\omega_\alpha$ the amount of freed (or occupied) adsorption sites due to the dissociation.

Insertion of (92), (95),(98) and (101) on the left hand side of (115) leads to the necessary constraint

$$\Delta g_{\alpha+1,\beta}^A + \Delta g_{\alpha+2,\beta}^A - \Delta g_\alpha^A - (\kappa_{\alpha+1,\beta} + \kappa_{\alpha+2,\beta}) \Delta g_0^A = \underset{s}{\Delta} g_{\alpha,\beta}^D - \Delta g_\alpha^D. \tag{116}$$

Note that this is an important constrain between adsorption energies and the dissociation energies.

6 Discussion and determination the model parameter

In this chapter we revise and discuss the model parameter. We start with a list of the appearing parameter:

- Electrolyte

  $n_\alpha^{\mathtt{E}}$ – Bulk particle densities, v_α^R – Partial molar volumes,

  T – Temperature, $\chi_{\mathtt{E}}$ – Dielectric susceptibility of the electrolyte,

  κ_α – Solvation number, Δg_α^D – Dissociation reaction Gibbs energy.

  $p^{\mathtt{E}}$ – Bulk pressure.

- Metal

  $n_M^{\mathtt{M}}$, $n_e^{\mathtt{M}}$ – Bulk particle densities, v_M^R – Partial molar volumes of the metal,

  T – Temperature, $\chi_{\mathtt{M}}$ – Dielectric susceptibility of the metal,

  $p^{\mathtt{M}}$ – Bulk pressure.

- Surface

  $\underset{s}{\mu_e^{\mathtt{M}}}$ – Surface chemical potential of the electrons, $a_\alpha^{\mathtt{R}}$ – Partial molar areas,

  $\kappa_{\alpha,\beta}$ – Solvation number, Δg_α^A – Adsorption energy,

  $\Delta g_{\alpha,0}^S$ – Solvation shell stripping energy, $\Delta g_{\alpha,\beta}^E$ – Reaction energy,

  $\underset{s}{\Delta g_{\alpha,\beta}^D}$ – Surface dissociation energy.

There are some parameter like temperature, pressure, susceptibilities and the bulk particle densities that are well known for most experimental setups. However, the other parameter either have to be calculated by atomistic theories or must be determined from measurements. In the next sections we discuss and suggest the magnitude of these parameter which will be used later on for simulations.

6.1 Solvation number

In the electrolyte we consider an agglomeration of solvent molecules around each ion[52] which we term solvation effect. Origin of this agglomeration is the microscopic electrostatic interaction of the ionic charge with the dipole of the solvent molecules [9]. Thus, each ion has a certain solvation number κ_α which indicates how many solvent molecules are confined to each ion of constituent A_α. Figure 4 provides a sketch of the solvation effect and a solvated ion.

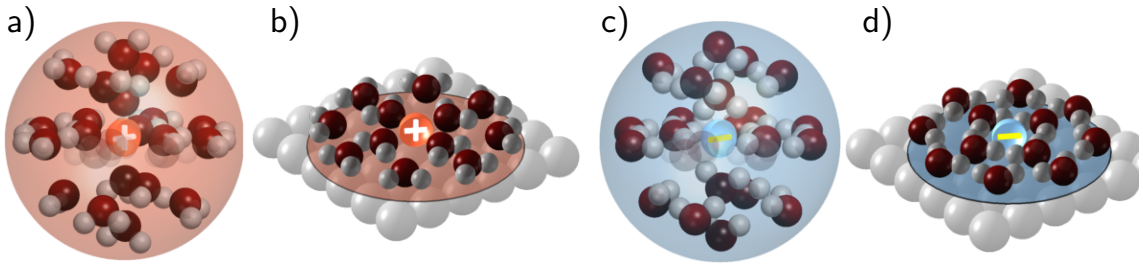

Figure 4: Model conception of solvated anions (a,b) and cations (c,d) in the volume (b,d) and on the surface (a,c).

The size of the solvation shell is controversially discussed in literature and investigated by various theoretical [59, 45, 17] and experimental methods [33, 32]. For aqueous electrolytes one finds values of $\kappa_\alpha = 1, \ldots, 50$ [33]. This broad range of values originates from the circumstance that solvation occurs in more than one shell around the central ion. While most investigations deal with first shell, which usually has values in the order of $3-8$ solvent molecules, the second shell is rather poor understood. It is assumed to capture many more solvent molecules and its presence as well as its importance is undoubted [33, 31].

Within our modeling procedure it seems thus reasonable to image the constituents A_α, $\alpha = 1, \ldots, N_{\mathrm{E}}$ as solvated ions with first and second solvation shell. Its value is assumed to be in the order of $\kappa_\alpha = 45$ for monovalent cations and anions.

The solvation effect of charged adsorbates at metal surfaces is likewise to be expected. We have assumed that the incoming ions do not change the solvation number during the elementary adsorption reaction (76). However, after the ions have reached the adsorbate state, they may either release parts of the original shell or a rearrangement of the shell takes place. This process is described by the solvation shell stripping reactions (77) with $\kappa_{\alpha,0} < \kappa_\alpha$. A further reduction of $\kappa_{\alpha,0}$ is due to the electron transfer reactions (78) with $\kappa_{\alpha,\beta+1} < \kappa_{\alpha,\beta} < \kappa_{\alpha,0}$. In this paper we simply estimate the solvation number of adsorbates by means of the horizontal first and second solvation shell, providing $\kappa_{\alpha,0} = 25$. Possibly a more solid data basis may be constituted by atomistic theories and simulations.

6.2 Molar volumes

In the metal the partial molar volume of metal ions v_M^R is determined either from the mass density of the metal, ρ_{M}^R, i.e. $v_M^R = m_M/\rho_{\mathrm{M}}^R$ or computed from its crystal structure. For silver with fcc crystal structure and lattice constant $\ell_M = 4.0853\,[\,\text{Å}\,]$ we compute

$$n_M = \frac{(8\frac{1}{8} + 6\frac{1}{2})}{N_{\mathrm{A}}\ell_M^3} = 97.0821\,[\,\mathrm{mol}/\ell\,] \tag{117}$$

and thus $v_M^R = 10.300\,[\,\mathrm{cm}^3/\mathrm{mol}\,]$.

In the electrolyte the setting is different. The solvation of ionic constituents has a strong impact on both the partial molar volume v_α^R of the electrolytic constituents. Therefore the electrolyte case needs more effort.

First of all, we determine the molar volume of the solvent A_0. It seems to be reasonable to assume that the molar volume of the solvent in the electrolyte is in the same range as the molar volume of the pure solvent. For example, water has a particle density $n_0^R = 55.408\,[\,\mathrm{mol}/\ell\,]$ and for the molar volume we obtain $v_0^R = 1/n_0^R = 18.048\,[\,\mathrm{cm}^3/\mathrm{mol}\,]$.

The solvated ions $\mathrm{A}_\alpha,\ \alpha = 1,\ldots,N$ are considered as an agglomeration of κ_α solvent molecules in a spherical cloud around the central ion, Figure 4. This picture suggests that the molar volume v_α^R of a solvated ion A_α is given by the volume $\hat{v}_\alpha^R$ of the central ion plus the volume of the surrounding solvent molecules $\hat{v}_0^R$,

$$v_\alpha^R = \hat{v}_\alpha^R + \kappa_\alpha \hat{v}_0^R\ . \tag{118}$$

In general the volume of a solvent molecule in the solvation shell is not equal to the volume of the unbound solvent molecule, but it should be in the same range. We estimate the magnitude of the molar volume of the solvated ion by assuming equality, and furthermore we assume that the central ion has the same molar volume as the solvent. Then we obtain the simple rule

$$v_\alpha^R \approx (1+\kappa_\alpha) v_0^R\ . \tag{119}$$

6.3 Molar areas

The molar area a_M^R of the metal ions is deduced from the considered crystal surface structure [54]. For silver one obtains for a (110) surface

$$a_M^R = \frac{(4\tfrac{1}{4} + 2\tfrac{1}{2})}{N_\mathsf{A}\sqrt{2}a^2} = 7.1233\cdot 10^8\,\left[\,\mathrm{cm}^2/\mathrm{mol}\,\right]\ . \tag{120}$$

We assume that each surface metal atom provides one adsorption site, i.e. $\omega_M = 1$.

Next we have to determine the molar areas a_α^R or the number of adsorption sites $\omega_\alpha = \frac{a_\alpha^R}{a_M^R}$ of all adsorbates. At first we estimate a_0^R of the adsorbed solvent molecules. Note that the metal is almost twice as densely packed as pure water, i.e. $v_0 \approx 2\ v_M^R$, and presumably a similar ratio is to be found on the surface. Thus we set

$$a_0^R = 2\ a_M^R\ . \tag{121}$$

The molar area of adsorbed and partially solvated ions (c.f. figure 4) are determined in an analogous manner as the partial molar volume, see (118). We assume that the molar area a_α^R consists of the area of the central ion, $\hat{a}_\alpha^R$, and the solvation shell, $\kappa_\alpha\ \hat{a}_0^R$, i.e.

$$a_\alpha^R = \hat{a}_\alpha^R + \kappa_\alpha \hat{a}_0^R\ . \tag{122}$$

Assuming further that the molar areas of the central ion and solvent molecules in the shell are of equal size to the unbound solvent molecule, ($\hat{a}_\alpha^R \approx a_0^R$, $\hat{a}_0^R \approx a_0^R$), we obtain

$$a_\alpha^R \approx (1+\kappa_\alpha) a_0^R\ . \tag{123}$$

Accordingly the molar areas of the reaction products of stripping reactions and electron transfer, respectively, are approximately given by

$$a_{\alpha,\beta}^R \approx (1+\kappa_{\alpha,\beta}) a_0^R\ . \tag{124}$$

6.4 Reference and adsorption Gibbs free energies

The reference free energy g_α^R of a constituent A_α covers, in the case of a solvated particle, contributions from the central ion and the surrounding solvation shell. Quite similar to the composition of the partial molar volume we decompose g_α^R as

$$g_\alpha^R = \tilde{g}_\alpha^R + \kappa_\alpha \, g_0^R \,, \qquad \alpha = 1, \dots, N_{\mathtt{E}} \tag{125}$$

where $\tilde{g}_\alpha^R$ is the Gibbs free energy of the central ion itself, and $\kappa_\alpha \, g_0^R$ the contribution of the solvation shell. Consequently we introduce a similar decomposition on the surface for the constituents $\underset{s}{A}_{\alpha,\beta}$, namely

$$\underset{s}{\psi}{}_{\alpha,\beta}^R = \underset{s}{\tilde{\psi}}{}_{\alpha,\beta}^R + \kappa_{\alpha,\beta} \underset{s}{\psi}{}_0^R \,, \qquad \beta = 0, 1, \dots, |z_\alpha|, \; \alpha = 1, \dots, N_S \tag{126}$$

where $\underset{s}{\tilde{\psi}}{}_{\alpha,\beta}^R$ is the reference free energy of the central ion on the surface.

This decomposition has some advantage in interpreting and estimating the adsorption energies. Consider, for example, the adsorption energy of a constituent $\underset{s}{A}_{\alpha,0}$, i.e. $\Delta g_{\alpha,0}^A = \underset{s}{\psi}{}_{\alpha,0}^R - g_\alpha^R - (\kappa_\alpha - \kappa_{\alpha,0}) g_0^R$. Insertion of the decomposition (125) and (126) leads to $\Delta g_{\alpha,0}^A = \Delta \tilde{g}_{\alpha,0}^A + \kappa_{\alpha,0} \Delta g_0^A$, with $\Delta \tilde{g}_{\alpha,0}^A = \underset{s}{\tilde{\psi}}{}_{\alpha,0}^R - \tilde{g}_0^R$ and $\Delta g_0^A = \underset{s}{\psi}{}_0^R - g_0^R$. One could now interpret $\Delta g_{\alpha,0}^A$ as adsorption energy of the central ion, $\Delta \tilde{g}_{\alpha,0}^A$, and of the solvation shell, $\kappa_{\alpha,0} \Delta \, g_0^A$. The adsorption energy of the central ion, $\Delta \tilde{g}_{\alpha,0}^A$, however, corresponds to the Gibbs free difference of a *single* particle and thus the adsorption energy difference are expectably in the range of ± 0.5eV.

With this decomposition we obtain for the adsorption energies in our model

$$\Delta g_\alpha^A = \Delta \tilde{g}_\alpha^A + \kappa_\alpha \Delta g_0^A \qquad \text{with} \quad \Delta \tilde{g}_\alpha^A = \underset{s}{\tilde{\psi}}{}_\alpha^R - \tilde{g}_\alpha^R, \tag{127}$$

$$\Delta g_{\alpha,0}^A = \Delta \tilde{g}_{\alpha,0}^A + \kappa_{\alpha,0} \Delta g_0^A \qquad \text{with} \quad \Delta \tilde{g}_{\alpha,0}^A = \underset{s}{\tilde{\psi}}{}_{\alpha,0}^R - \tilde{g}_\alpha^R, \tag{128}$$

$$\Delta g_{\alpha,\beta}^A = \Delta \tilde{g}_{\alpha,\beta}^A + \kappa_{\alpha,\beta} \Delta g_0^A \qquad \text{with} \quad \Delta \tilde{g}_{\alpha,\beta}^A = \underset{s}{\tilde{\psi}}{}_{\alpha,\beta}^R - \tilde{g}_\alpha^R - \beta \, \mathsf{sgn}(z_\alpha) \underset{s}{\mu}_e. \tag{129}$$

In Section 8.1 we provide explicit values for Δg_0^A and $\Delta \tilde{g}_{\alpha,\beta}^A$.

6.5 Self-ionization or autoprotolysis of the solvent

Since most considerable solvents dissociate slightly in ionic compounds, like water into protons (or hydronium) and hydroxide ions, we explicitly account for these species. For the solvent A_0 the ionic reaction products due to the self-ionization are denoted by A_1 and A_2. The autoprotolysis reaction of the solvent is thus

$$A_0 + (\kappa_1 + \kappa_2) A_0 \rightleftharpoons A_1 + A_2 \tag{130}$$

with dissociation reaction energy Δg_0^D. For water, the dissociation energy is $\Delta g_0^D = 1.034$eV, leading to a pH value of 7, i.e. $n_{\mathrm{H^+}}^{\mathtt{E}} = n_{\mathrm{OH^-}}^{\mathtt{E}} = 10^{-7} \, [\, \mathsf{mol}/\ell \,]$.

We also consider self-ionization to occur on the surface, where an adsorbed solvent species dissociates in two (partially) solvated ions,

$$\underset{s}{A_0} + (\kappa_{1,0} + \kappa_{2,0})\underset{s}{A_0} \rightleftharpoons \underset{s}{A_{1,0}} + \underset{s}{A_{2,0}}. \tag{131}$$

For water this corresponds to the dissociation of adsorbed $\mathrm{H_2O}$ into adsorbed $\mathrm{H^+}$ and $\mathrm{OH^-}$. Note that the corresponding surface reaction energy $\underset{s}{\Delta} g^D_{\mathrm{H_2O}} = \underset{s}{\psi}{}^R_{1,0} + \underset{s}{\psi}{}^R_{2,0} - \underset{s}{\psi}{}^R_0$ is not necessarily equal to the dissociation energy Δg^D_0 of the electrolyte phase. But it turns out that there is a necessary constraint, (116), between the adsorption energies $\Delta g^A_{\alpha,\beta}$, the surface dissociation energy $\underset{s}{\Delta} g^D_{\alpha,\beta}$, and the volume dissociation Δg^D, namely

$$\Delta \tilde{g}^A_{\alpha+1,\beta} + \Delta \tilde{g}^A_{\alpha+2,\beta} - \Delta \tilde{g}^A_{\alpha,\beta} = \underset{s}{\Delta} g^D_{\alpha,\beta} - \Delta g^D_\alpha. \tag{132}$$

Thus if one prescribes the reaction energies $\underset{s}{\Delta} g^D_{\alpha,\beta}$ and Δg^D_α one could determine an adsorption energy from (132).

Notice further that we automatically include a different *reaction pathway* for dissociation on the surface, namely

$$\underset{s}{A_0} + (\kappa_{1,1} + \kappa_{2,1})\underset{s}{A_0} \rightleftharpoons \underset{s}{A_{1,1}} + \underset{s}{A_{2,1}} \tag{133}$$

with reaction energy $\underset{s}{\Delta} g^D_{0,1}$. This could, for example, be the dissociation of adsorbed $\mathrm{H_2O}$ into adsorbed H and OH.

6.6 Bulk particle densities

The bulk particle densities $n^{\mathtt{E}}_\alpha,\ \alpha = 1, \dots, N_{\mathtt{E}}$ of the ionic species in the electrolyte are either determined by the amount of salt which is put into solution, if complete dissociation is ensured, or determined by the dissociation reaction energy Δg^D_α according to equation (114).

For a binary, monovalent salts which completely dissociate we thus prescribe $n^{\mathtt{E}}_A = n^{\mathtt{E}}_C = c\,[\,\mathrm{mol}/\ell\,]$. The determination of the bulk density of the (free) solute, $n^{\mathtt{E}}_0$, follows from the incompressibility constraint (80), i.e.

$$n^{\mathtt{E}}_0 = \frac{1}{v^R_0}\big(1 - \sum_{\alpha=1}^{N_{\mathtt{E}}} v^R_\alpha n^{\mathtt{E}}_\alpha\big). \tag{134}$$

6.7 Susceptibility

In general the electric susceptibility $\chi_{\mathtt{E}}$ of the electrolyte depends on its local composition. Particularly, this dependence could be of importance within the boundary layer where the influence of the susceptibility is maximal. However, to simplify our model we suppose a constant susceptibility because then the chemical potentials become independent of the electric field $\mathbf{E}$. In order to take the boundary layer into account we assume a smaller value of $\chi_{\mathtt{E}} = 25$ for an aqueous electrolyte than that of pure water. This is appropriate if the ions do not show a pronounced dipole character and is a common approximation in electrochemistry [10].

6.8 Surface chemical potential of the electrons

In the current model the surface chemical potential of the electrons $\underset{s}{\mu_e}$ is an unknown material parameter that depends on the surface structure. Its consistent incorporation in the general theory is the main scope of this quantity. However, for the example in Section 11 we use measured data of the work function as value for $\underset{s}{\mu_e}$.

7 Relationship to measurable quantities

In this section we bridge the gap of our theoretical model to experimental measurable properties. First we provide a relationship between $\underset{s}{\varphi}^{\mathtt{M}} - \varphi^{\mathtt{E}}$, the metal surface/electrolyte potential difference, and the measurable electrode potential E. Its introduction is intimately related to the used reference electrode. Next, a relation between the current I and the double layer charge Q is given, which incorporates adsorption and electron transfer reactions. Based on this relation the double layer capacity C is introduced. We show further how the reference potential $U^{\mathtt{R}}$ could be determined from a single experiment and introduce the potential of zero charge E^0. A brief discussion on the electronic surface chemical potential $\underset{s}{\mu_e}$ follows, which leads to the interpretation of $\underset{s}{\mu_e}$ as work function of the specific metal surface. Finally we provide relations of our model to measurable quantities.

7.1 Measurable cell potential E

As a first step to introduce the measurable electrode potential E we must supplement our metal/electrolyte interface by some reference electrode $\mathtt{R}$. The metal and the reference electrode are connected via some cables $\mathtt{C}_1$ and $\mathtt{C}_2$ to a voltmeter $\mathtt{V}$ which measures a voltage E between its two identical, metallic plates $\underset{s}{\mathtt{V}_1}$ and $\underset{s}{\mathtt{V}_2}$. As a reference electrode we consider a saturated calomel electrode (SCE), consisting of metallic mercury and solid calomel immersed in a saturated solution of potassium chloride. The reference electrode is coupled to the electrolyte $\mathtt{E}$ via some diaphragm.

The electrochemical cell, including measuring device and cables, may thus be written as

$$\underbrace{\underset{s}{\mathtt{V}_1} \,|\, \mathtt{C}_1 \,|\, \mathtt{M} \,|\, \mathtt{E} \,|\, \mathtt{R} \,|\, \mathtt{C}_2 \,|\, \underset{s}{\mathtt{V}_2}}_{E=\underset{s}{\varphi}_{\mathtt{V}_1} - \underset{s}{\varphi}_{\mathtt{V}_2}} \tag{135}$$

The measured cell potential E then corresponds to the surface potential difference between the two plates of the voltmeter, i.e.

$$E = \underset{s}{\varphi}_{\mathtt{V}_1} - \underset{s}{\varphi}_{\mathtt{V}_2}. \tag{136}$$

We denote the electrostatic potential of the bulk reference electrode $\mathtt{R}$ by $\varphi^{\mathtt{R}}$ and accordingly the bulk chemical potential of electrons as $\mu_e^{\mathtt{R}}$. Since the voltmeter plates and the cables are

metals, we have continuity of $\mu_e - e_0\varphi$ between $\underset{s}{\mathtt{V}_1}$ and the $\mathtt{M}|\mathtt{E}$ surface as well as between the $\mathtt{E}|\mathtt{R}$ surface and $\underset{s}{\mathtt{V}_2}$. Hence we obtain

$$E = \underset{s}{\varphi^{\mathtt{M}}} - \underset{s}{\varphi^{\mathtt{R}}} - \frac{1}{e_0}(\underset{s}{\mu_e^{\mathtt{M}}} - \underset{s}{\mu_e^{\mathtt{R}}}). \tag{137}$$

Note that equation (137) relates the measured cell potential E to the (surface) potential difference $\underset{s}{\varphi^{\mathtt{M}}} - \underset{s}{\varphi^{\mathtt{R}}}$ between the metal and the reference electrode. But we seek actually a relation between E and the metal/electrolyte potential drop, $\underset{s}{\varphi^{\mathtt{M}}} - \varphi^{\mathtt{E}}$.

The potential difference $\underset{s}{\varphi^{\mathtt{M}}} - \underset{s}{\varphi^{\mathtt{R}}}$ covers the potential drop between the metal and the electrolyte, $\underset{s}{\varphi^{\mathtt{M}}} - \varphi^{\mathtt{E}}$, as well as potential drop between the reference electrode and the electrolyte, $\underset{s}{\varphi^{\mathtt{R}}} - \varphi^{\mathtt{E}}$,

$$\underset{s}{\varphi^{\mathtt{M}}} - \underset{s}{\varphi^{\mathtt{R}}} = \underset{s}{\varphi^{\mathtt{M}}} - \varphi^{\mathtt{E}} - (\underset{s}{\varphi^{\mathtt{R}}} - \varphi^{\mathtt{E}}). \tag{138}$$

The question is now how a variation of $(\underset{s}{\varphi^{\mathtt{M}}} - \underset{s}{\varphi^{\mathtt{R}}}) \rightarrow (\underset{s}{\varphi^{\mathtt{M}}} - \underset{s}{\varphi^{\mathtt{R}}}) + \delta U$ distributes among the $\mathtt{M} \,|\, \mathtt{E}$ and $\mathtt{E} \,|\, \mathtt{R}$ interfaces. We emphasize that this question can only be addressed, without any *a priori* assumptions, by modeling the whole reference electrode/electrolyte interface in a similar manner as the metal/electrolyte interface.

However, it is a quite common assumption[29, 11] that the $\mathtt{E} \,|\, \mathtt{R}$ potential drop is constant, i.e.

$$\underset{s}{\varphi^{\mathtt{R}}} - \varphi^{\mathtt{E}} = U^{\mathtt{R},\mathtt{E}} = \text{const.} \tag{139}$$

This assumption is sometimes also called *ideally non-polarizable (reference) electrode* [11]. A variation $(\underset{s}{\varphi^{\mathtt{M}}} - \underset{s}{\varphi^{\mathtt{R}}}) \rightarrow (\underset{s}{\varphi^{\mathtt{M}}} - \underset{s}{\varphi^{\mathtt{R}}}) + \delta U$ thus affects only the $\mathtt{E} \,|\, \mathtt{R}$ potential drop and one obtains the relation

$$E = (\underset{s}{\varphi^{\mathtt{M}}} - \varphi^{\mathtt{E}}) + U^{\mathtt{R}} \qquad \text{with} \qquad U^{\mathtt{R}} = -\frac{1}{e_0}(\underset{s}{\mu_e^{\mathtt{M}}} - \underset{s}{\mu_e^{\mathtt{R}}}) - U^{\mathtt{R},\mathtt{E}}. \tag{140}$$

between the measurable cell potential E and the metal/electrolyte potential drop, $\underset{s}{\varphi^{\mathtt{M}}} - \varphi^{\mathtt{E}}$. The reference potential $U^{\mathtt{R}}$ is thus a constant with contributions from the reference electrode via $\underset{s}{\mu_e^{\mathtt{R}}}$, the constant part of the reference electrode/electrolyte potential drop $U^{\mathtt{R},\mathtt{E}}$, and the metal surface via $\underset{s}{\mu_e^{\mathtt{M}}}$.

We emphasize, however, that the assumption (139) is crucial and to be justified in an experimental setup. For example in a symmetric cell, where working and reference electrode (or counter electrode in a two-electrode setup) are identical, a variation of $(\underset{s}{\varphi^{\mathtt{M}}} - \underset{s}{\varphi^{\mathtt{R}}}) \rightarrow (\underset{s}{\varphi^{\mathtt{M}}} - \underset{s}{\varphi^{\mathtt{R}}}) + \delta U$ distributes equally among the $\mathtt{M} \,|\, \mathtt{E}$ and the $\mathtt{E} \,|\, \mathtt{R}$ interface, leading to $\underset{s}{\varphi^{\mathtt{R}}} - \varphi^{\mathtt{E}} = -(\underset{s}{\varphi^{\mathtt{M}}} - \varphi^{\mathtt{E}})$ [19]. Furthermore, $\underset{s}{\varphi^{\mathtt{R}}} - \varphi^{\mathtt{E}}$ could even be non-linear dependent on $\underset{s}{\varphi^{\mathtt{M}}} - \varphi^{\mathtt{E}}$, especially for large deviations from the potential of zero charge.

For the sake of this work we follow the classical assumption that $\underset{s}{\varphi^{\mathtt{R}}} - \varphi^{\mathtt{E}} = \text{const.}$ and rely thus on the relation (140).

7.2 Charge and capacity of the double layer

The double layer charge $Q\,[\,\mathrm{C/m^2}\,]$ is related to the electric current density $I\,[\,\mathrm{A/m^2}\,]$ which enters the metal electrode at the point $x_{\mathtt{M}}$ according to

$$I = \frac{dQ}{dt} \qquad \text{with} \qquad Q = \int_{x_{\mathtt{M}}}^{x_S} n^{\mathrm{F}}\,dx + \sum_{\alpha=e,M} z_\alpha e_0 \underset{s}{n}_\alpha - \sum_{\alpha=1}^{N_{\mathtt{E}}} \sum_{\beta=1}^{|z_\alpha|} e_0\,\mathrm{sgn}(z_\alpha)\beta \underset{s}{n}_{\alpha,\beta}. \quad (141)$$

A detailed derivation of the relation (141) based on non-equilibrium thermodynamics is given in Appendix C.

The charge Q consists of three parts: (i) the charge contained in the boundary layer of the metal side, (ii) the surface charge of metal ions and metal electrons and (iii) the charge which is produced by electron transfer reactions. Note that the latter part of the charge $(141)_2$ is usually absent in electrochemistry, for example see [29, 11, 49]. In case that part (iii) is included it gives rise to the so called Faradaic current.

Next we replace in $(141)_2$ the charge due to the metal constituents by the charge due to the electrolyte constituents. To this end we exploit the global electroneutrality condition, which is briefly sketched. We assume that the electric current which enters the electrolyte at $x_{\mathtt{E}}$ is equal to the electric current that leaves the metal at the point $x_{\mathtt{M}}$. Thus, if charge neutrality holds for a certain time t^* we also have charge neutrality for all times, i.e.

$$\int_{x_{\mathtt{M}}}^{x_{\mathtt{S}}} n^{\mathrm{F}}\,dx + \underset{s}{n}^{\mathrm{F}} + \int_{x_{\mathtt{S}}}^{x_{\mathtt{E}}} n^{\mathrm{F}}\,dx = 0\,. \quad (142)$$

This condition is termed global electroneutrality condition since it states that the whole metal/ electrolyte interface is uncharged.

By use of (142) we obtain a new representation of the double layer charge Q, viz.

$$Q = Q_{\mathsf{BL}} + \underset{s}{Q} \qquad \text{with} \quad Q_{\mathsf{BL}} = -\int_{x_{\mathtt{S}}}^{x_{\mathtt{E}}} n^{\mathrm{F}}\,dx \quad (143)$$

$$\text{and} \quad \underset{s}{Q} = -\Bigg(\sum_{\alpha=1}^{N_{\mathtt{E}}} z_\alpha e_0 \underset{s}{n}_\alpha + \sum_{\alpha=1}^{N_{\mathtt{E}}} \sum_{\beta=0}^{|z_\alpha|} z_\alpha e_0 \underset{s}{n}_{\alpha,\beta} \Bigg). \quad (144)$$

Here Q_{BL} represents the charge of the electrolytic boundary layer and $\underset{s}{Q}$ is the charge induced by the adsorbates and reaction products.

Notice that the pre-factor of $e_0 \underset{s}{n}_{\alpha,\beta}$ in (144) is z_α and not $z_{\alpha,\beta} = z_\alpha - \mathrm{sgn}(z_\alpha)\ \beta$, i.e. the charge number of constituent $\underset{s}{A}_{\alpha,\beta}$, c.f. the electron transfer reactions (78). This originates from the fact that the Faradaic current, i.e. the surface reaction of electrons, contributes to the charge Q as $-\sum_{\alpha=1}^{N_{\mathtt{E}}} \sum_{\beta=1}^{|z_\alpha|} e_0\,\mathrm{sgn}(z_\alpha)\beta \underset{s}{n}_{\alpha,\beta}$.

7.2.1 Charge representation of the metal/electrolyte interface model

Recall that the charge Q_{BL} of the electrolytic boundary layer is related to the gradients of the electric potentials by $Q_{\mathsf{BL}} = \varepsilon_0(1+\chi)(\partial_x\varphi\big|_{x^{\mathtt{E}}} - \partial_x\varphi\big|_S^{\mathtt{E}})$ with $\partial_x\varphi\big|_{x^{\mathtt{E}}} = 0$, see (111). We apply

equation (112) at $x = x_S$ to obtain

$$Q_{\mathrm{BL}} = \operatorname{sgn}(\underset{s}{\varphi} - \varphi^{\mathrm{E}}) \sqrt{2\varepsilon_0(1+\chi)\big(\hat{p}(\underset{s}{\varphi}^{\mathrm{M}} - \varphi^{\mathrm{E}}) - p^{\mathrm{E}}\big)} \tag{145}$$

This is a remarkable result since it states that the charge contribution of the electrolytic boundary layer to the double layer is exclusively determined by the local pressure p at $x = x_S$. Moreover we observe from (145) that the charge Q_{BL} can be determined without solving the coupled system of Poisson's equation and the momentum balance. However, we must solve the non-linear equation (105) to obtain p as a function of $\underset{s}{\varphi}^{\mathrm{M}} - \varphi^{\mathrm{E}}$ and thus $Q_{\mathrm{BL}} = \hat{Q}_{\mathrm{BL}}(\underset{s}{\varphi}^{\mathrm{M}} - \varphi^{\mathrm{E}})$.

The charge $\underset{s}{Q}$ due to the electrolyte adsorbates and their reaction products can be expressed in terms of the surface mole fractions $\underset{s}{y_\alpha}$ as

$$\underset{s}{Q} = -\frac{\sum_{\alpha=1}^{N_{\mathrm{E}}} z_\alpha e_0 \underset{s}{y_\alpha} + \sum_{\alpha=1}^{N_{\mathrm{E}}} \sum_{\beta=0}^{|z_\alpha|} z_\alpha e_0 \underset{s}{y_{\alpha,\beta}}}{a_V^R \underset{s}{y_V} + \sum_{\alpha=0}^{N_{\mathrm{E}}} a_\alpha^R \underset{s}{y_\alpha} + \sum_{\alpha=0}^{N_{\mathrm{E}}} \sum_{\beta=0}^{|z_\alpha|} a_{\alpha,\beta}^R \underset{s}{y_{\alpha,\beta}}} \,. \tag{146}$$

With the representations (92),(95),(98) and (101) for $\underset{s}{y_\alpha}$, $\underset{s}{y_{\alpha,\beta}}$ and $\underset{s}{y_V}$ we obtain an expression of $\underset{s}{Q}$ in terms of $(\underset{s}{\varphi}^{\mathrm{M}} - \varphi^{\mathrm{E}})$. Moreover, the relation (109) between surface charge and surface tension allows to rewrite (146) as

$$\underset{s}{Q} = -\hat{\gamma}'(\underset{s}{\varphi}^{\mathrm{M}} - \varphi^{\mathrm{E}}) \,, \tag{147}$$

with the abbreviation $\hat{\gamma}' = d\hat{\gamma}/d(\underset{s}{\varphi}^{\mathrm{M}} - \varphi^{\mathrm{E}})$. This result is important because it shows that the surface tension has an intrinsic impact on the surface charge.

Note that the representation (146) of $\underset{s}{Q}$ is a function of $\underset{s}{\varphi}^{\mathrm{M}} - \varphi^{\mathrm{E}}$ and of the surface tension γ. Similar to the volume we must solve the non-linear equation (102) to obtain γ as a function of $\underset{s}{\varphi}^{\mathrm{M}} - \varphi^{\mathrm{E}}$ and obtain consequently $\underset{s}{Q} = \hat{\underset{s}{Q}}(\underset{s}{\varphi}^{\mathrm{M}} - \varphi^{\mathrm{E}})$.

The double layer charge Q is thus also represented in terms of $\underset{s}{\varphi}^{\mathrm{M}} - \varphi^{\mathrm{E}}$, namely

$$\hat{Q}(\underset{s}{\varphi}^{\mathrm{M}} - \varphi^{\mathrm{E}}) = \hat{Q}_{\mathrm{BL}}(\underset{s}{\varphi}^{\mathrm{M}} - \varphi^{\mathrm{E}}) + \hat{\underset{s}{Q}}(\underset{s}{\varphi}^{\mathrm{M}} - \varphi^{\mathrm{E}}) \,. \tag{148}$$

7.2.2 Capacity representation of the metal/electrolyte interface model

The determination of the double layer capacity C relies on the general relation $I = \frac{dQ}{dt}$, and a variation of the measurable cell potential E, i.e.

$$I = \frac{dQ}{dt} = C \cdot \frac{dE}{dt} \quad \text{with} \quad C = \frac{dQ}{dE} = \frac{d\hat{Q}}{d(\underset{s}{\varphi}^{\mathrm{M}} - \varphi^{\mathrm{E}})}. \tag{149}$$

We emphasize that the representation $Q = \hat{Q}(\underset{s}{\varphi}^{\mathtt{M}} - \varphi^{\mathtt{E}})$ is only obtained if the electrochemical interface behaves quasi-static, i.e. remains in thermodynamic equilibrium. In [20] it is shown that this assumption is reasonable for slowly varying boundary conditions. Recall that $Q\,[\,\mathtt{C}/\mathrm{m}^2\,]$ covers contributions of the electrolytic boundary layer, adsorbed charged species on the surface as well as reaction products due to electron transfer. The decomposition (143), $Q = Q_{\mathtt{BL}} + \underset{s}{Q}$, into boundary layer and surface parts motivates a corresponding decomposition of the capacity into a volume and a surface capacity,

$$\hat{C} = \hat{C}_{\mathtt{BL}} + \underset{s}{\hat{C}} \quad \text{with} \quad \hat{C}_{\mathtt{BL}} = \frac{d\hat{Q}_{\mathtt{BL}}}{d(\underset{s}{\varphi}^{\mathtt{M}} - \varphi^{\mathtt{E}})} \qquad \text{and} \qquad \underset{s}{\hat{C}} = \frac{d\underset{s}{\hat{Q}}}{d(\underset{s}{\varphi}^{\mathtt{M}} - \varphi^{\mathtt{E}})} \,. \tag{150}$$

The function $\hat{C}_{\mathtt{BL}}$ is obtained from (145) as

$$\hat{C}_{\mathtt{BL}}(\underset{s}{\varphi} - \varphi^{\mathtt{E}}) = \operatorname{sgn}(\underset{s}{\varphi} - \varphi^{\mathtt{E}}) \sqrt{\frac{\varepsilon_0(1+\chi)}{2\big(\hat{p}(\underset{s}{\varphi}^{\mathtt{M}} - \varphi^{\mathtt{E}}) - p^{\mathtt{E}}\big)}}\; \hat{p}'(\underset{s}{\varphi}^{\mathtt{M}} - \varphi^{\mathtt{E}}) \,, \tag{151}$$

with the abbreviation $\hat{p}' = d\hat{p}/d(\varphi - \varphi^{\mathtt{E}})$. Note that due to (107) a relation between the derivative of the pressure and the free charge density exists,

$$p' = -n^{\mathrm{F}} \,. \tag{152}$$

The function $\underset{s}{C}$ is determined in an analogous manner. The relation (109) between the surface stress and the charge yields $\underset{s}{Q} = \hat{\gamma}'(\underset{s}{\varphi}^{\mathtt{M}} - \varphi^{\mathtt{E}})$. Thus we have

$$\underset{s}{\hat{C}} = -\hat{\gamma}''(\underset{s}{\varphi}^{\mathtt{M}} - \varphi^{\mathtt{E}}) \tag{153}$$

with the abbreviation $\hat{\gamma}'' = d^2\hat{\gamma}/d(\underset{s}{\varphi}^{\mathtt{M}} - \varphi^{\mathtt{E}})^2$. In the appendix B we provide an algebraic expression of the function $\underset{s}{\hat{C}}$.

7.3 Determination of the reference potential $U^{\mathtt{R}}$

We are interested in the investigation of a specific metal electrode, e.g. silver, with various surface orientations in contact to different electrolytes. For example, we will investigate Ag(110) in Section 9. For this reason it is necessary to determine the reference potential $U^{\mathtt{R}} = -\frac{1}{e_0}(\underset{s}{\mu_e^{\mathtt{M}}} - \mu_e^{\mathtt{R}}) - U^{\mathtt{R,E}}$. As discussed before, we consider $U^{\mathtt{R}}$ as a constant material parameters which depends on the metal surface and the used reference electrode. Note that $U^{\mathtt{R}}$ could in principle be computed from a model of the reference electrode/electrolyte interface. However, since we do not explicitly model the $\mathtt{E}|\mathtt{R}$ interface, we must determine $U^{\mathtt{R}}$ from a single measurement. It turns out that a non-adsorbing salt is sufficient for this purpose.

To this end we focus on a state where the measured potential E is identical to the reference potential U^{R}. The corresponding quantities of that state are indicated by *. For $E^* = U^{\mathrm{R}}$ the identity (140) implies that the surface potential $\underset{s}{\varphi}^*$ must be equal to the electrolyte potential φ^{E}, i.e.

$$E^* = U^{\mathrm{R}} \quad \Longleftrightarrow \quad \underset{s}{\varphi}^* = \varphi^{\mathrm{E}} \,. \tag{154}$$

According to relation (105) between the pressure and the electrostatic potential we have $\underset{s}{\varphi}^* = \varphi^{\mathrm{E}}$ if the pressure at the surface is equal to the pressure in the bulk electrolyte, i.e.

$$E^* = U^{\mathrm{R}} \quad \Longleftrightarrow \quad \hat{p}(\underset{s}{\varphi}^* - \varphi^{\mathrm{E}}) = p^{\mathrm{E}} \,. \tag{155}$$

From representation (145) of Q we conclude that the boundary layer charge must vanish,

$$E^* = U^{\mathrm{R}} \quad \Longleftrightarrow \quad \hat{Q}(\underset{s}{\varphi}^* - \varphi^{\mathrm{E}}) = 0 \,. \tag{156}$$

Hence, the measured value E^* is identical to the reference potential U^{R} **if** the boundary layer charge q vanishes.

In Appendix D we show that the reference potential U^{R} corresponds to the minimum of the boundary layer capacity C_{BL} if the partial molar volumes v_α^R and the charge numbers $|z_\alpha|$ of all ionic constituents $\alpha = 1, \ldots, N_E$ are equal. This can be achieved by assuming $v_\alpha^R = (1+\kappa_\alpha) v_0^{\mathrm{R}}$ with equal solvation numbers of all ionic species, i.e.

$$E^* = U^{\mathrm{R}},\ v_\alpha^R = (1+\kappa)\, v_0^R,\ |z_\alpha| = 1,\ \alpha = 1, \ldots, N_{\mathrm{E}} \quad \Longleftrightarrow \quad \min_U C_{\mathrm{BL}}(U) = U^{\mathrm{R}}. \tag{157}$$

However, we can only measure the total charge $Q = Q_{\mathrm{BL}} + \underset{s}{Q}$, but not the boundary layer charge Q_{BL} separately.

The trick to determine U^{R} from an independent measurement relies on an electrolyte which does not adsorb on the considered metal surface [54]. If there are no further ionic species in the electrolyte then the surface capacity does not contribute to the total capacity, i.e. $\underset{s}{C} \equiv 0$. In that case the reference potential corresponds to the potential where the capacity has a local minimum.

However, we allow self-ionization or autoprotolysis of the solvent which leads to additional ionic species in the electrolyte and on the surface which results in $\underset{s}{C} \neq 0$. In that case we have to assume that the surface capacity only shifts slightly the minimum of the total capacity.

For example a non-adsorbing electrolyte on a silver electrode is an aqueous solution with $\mathrm{KPF_6(H_2O)}$, where neither the anion $\mathrm{PF_6^-}$ nor the cation $\mathrm{K^+}$ adsorbs on silver surfaces [61, 62, 63]. We exploit this circumstance in Section 8.2 to determine U^{R} for (110), (100) and (111) surfaces of silver.

7.4 Potential of zero charge E^0 and applied potential U

For a non-adsorbing salt we exploited the circumstance $\hat{Q}(\underset{s}{\varphi}^* - \varphi^{\mathrm{E}}) = 0 \ \Leftrightarrow \ E^* = U^{\mathrm{R}}$ in order to determine U^{R} from a single experiment. Since $\underset{s}{Q} = 0$, the metal is uncharged

and E^* corresponds to the *potential of zero charge* of the metal surface $\underset{s}{M}$ in contact with a non-adsorbing electrolyte.

However, if the adsorption occurs, $E^* = U^{\mathrm{R}}$ is not the potential of zero charge anymore. The quantities of the state of zero charge are indicated by ^{0}. The condition of zero charge on the metal is in general

$$\int_{x_M}^{x^S} n^{\mathrm{F}} dx + e_0(z_M \underset{s}{n}_M - \underset{s}{n}_e) = 0 \quad \Longleftrightarrow \quad E^0 = (\underset{s}{\varphi}^0 - \varphi^{\mathrm{E}}) + U^{\mathrm{R}}. \tag{158}$$

If adsorption occurs, $\underset{s}{\varphi}^0 \neq \varphi^{\mathrm{E}}$ and thus $E^0 \neq U^{\mathrm{R}}$. However, we can determine $\underset{s}{\varphi}^0 - \varphi^{\mathrm{E}}$ from the condition $(158)_1$. Note that all model parameters, and especially the bulk salt concentrations n_α^B, are incorporated in the function $Q(\underset{s}{\varphi}^{\mathrm{M}} - \varphi^{\mathrm{E}})$. Hence the measured potential of zero charge, E^0, of an adsorbing electrolyte is dependent on the actual salt concentration, which was reported for various metals [61, 62, 63, 50, 36].

Our general relationship between the measured potential E and $\underset{s}{\varphi}^{\mathrm{M}} - \varphi^{\mathrm{E}}$ can be rewritten as

$$E = (\underset{s}{\varphi}^{\mathrm{M}} - \varphi^{\mathrm{E}}) + U^{\mathrm{R}} = (\underset{s}{\varphi} - \underset{s}{\varphi}^0) + E^0. \tag{159}$$

Experimentally, E^0 corresponds to the measured cell potential without any externally applied voltage, i.e. the cell potential after immersion of the metal into the electrolyte [40]. Applying a voltage U essentially means a deviation of E^0 by U, which gives

$$E = U + E^0. \tag{160}$$

We can thus identify the applied potential U as

$$U = (\underset{s}{\varphi} - \underset{s}{\varphi}^0) = (\underset{s}{\varphi}^{\mathrm{M}} - \varphi^{\mathrm{E}}) + (\underset{s}{\varphi}^0 - \varphi^E). \tag{161}$$

where $(\underset{s}{\varphi}^0 - \varphi^E)$ is constant and determined from $(158)_1$. Note, for a non-adsorbing salt we have $(\underset{s}{\varphi}^0 - \varphi^E) = 0$ and thus $U = (\underset{s}{\varphi}^{\mathrm{M}} - \varphi^{\mathrm{E}})$.

7.5 Measured Charge and Capacity

The crucial quantities that relate our electrochemical model to experimentally data is the double layer charge Q and the cell potential E. Recall the current/charge relation (149), i.e. $I = dQ/dE$, and consider $\tilde{Q}(E)$ as representation of the **measured** charge. The measured capacity $\tilde{C}(E)$ is then accordingly defined as

$$\tilde{C} = \frac{d\tilde{Q}}{dE}. \tag{162}$$

Our model lead to functions $\hat{Q}(E - U^{\mathrm{R}})$ and $\hat{C}(E - U^{\mathrm{R}})$ of the double layer charge and capacity. We emphasize that the functions $\tilde{Q}$ and $\hat{Q}$ (as well as $\tilde{C}$ and $\hat{C}$) are actually two representations of the same physical quantity, i.e.

$$Q = \tilde{Q}(E) = \hat{Q}(E - U^{\mathrm{R}}) \quad \text{and} \quad C = \tilde{C}(E) = \hat{C}(E - U^{\mathrm{R}}). \tag{163}$$

This allows for a comparison between **measured** and **computed** data of the electrochemical interfaces.

8 Examples: Silver in contact with various aqueous salt solutions

We consider aqueous solutions of $\mathrm{KPF_6}$, $\mathrm{KClO_4}$, $\mathrm{NaClO_4}$ and NaF in contact with various single crystal silver surfaces.

$\mathrm{KPF_6}$ is a *non-adsorbing* salt which is used to discuss several aspects of our model. Particularly it serves to determine the reference potential U^{R} and to validate our theory at experimental data for Ag(110)[61].

$\mathrm{KClO_4}$ and $\mathrm{NaClO_4}$ serve to compare our model to experimental data of different, independent research groups for Ag(100), Ag(110) and Ag(111).

NaF is studied for various concentrations. We compare our theory to measured capacity data for Ag(110)|NaF at various concentrations. After this validation step, the coupled system of Poisson and momentum equation,(83) and (84), is used to compute the structure of the space charge layer at three selected potentials.

8.1 Constituents and parameter

In the following we describe all constituents and the corresponding parameters.

The solvent is water, $A_0 = \mathrm{H_2O}$, which is subject to self-ionization and dissociates in solvated hydroxide ions, $A_1 = \mathrm{OH^-}$, and solvated protons[1], $A_2 = \mathrm{H^+}$. At room temperature $T = 298\,[\,\mathrm{K}\,]$ we have a pH value of 7, i.e. $n_1^{\mathrm{E}} = n_2^{\mathrm{E}} = 10^{-7}\,[\,\mathrm{mol}/\ell\,]$, which corresponds to a dissociation energy of $\Delta g^D_{\mathrm{H_2O}} = 1.043\mathrm{eV}$.

We consider $\mathrm{KPF_6}$, $\mathrm{KClO_4}$, $\mathrm{NaClO_4}$ and NaF salts which are assumed to dissociate completely to ionic species $A_3 \in \{\mathrm{PF_6^-}, \mathrm{ClO_4^-}, \mathrm{F^-}\}$ and $A_4 \in \{\mathrm{K^+}, \mathrm{Na^+}\}$. The salt concentration in the bulk is denoted by $c\ [\,\mathrm{mol}/\ell\,]$ and determines as $n_3^{\mathrm{E}} = n_4^{\mathrm{E}} = c$.

The susceptibility of the electrolyte is considered as $\chi_{\mathrm{E}} = 25$.

We compute the partial molar volume from the density of pure water as $v_0^R = 1.7973 \cdot 10^{-5}\ [\,\mathrm{m}^3/\mathrm{mol}\,]$. For the solvated ions we consider a solvation shell of $\kappa_\alpha = 45$ solvent molecules and compute the partial molar volume according to $v_\alpha^R = (1 + \kappa_\alpha) v_0^R$.

[1] Note that protons are considered as solvated protons. One might thus also think of $\mathrm{H_3O^+}$, or even $[\mathrm{H_2O}]_{\kappa_{\mathrm{H^+}}}\mathrm{H^+}$.

As metal we consider silver, $A_M = \mathrm{Ag}$ (lattice constant $\ell_{\mathrm{Ag}} = 4.0853$ Å, Fermi level $\mu_e^{\mathtt{M}} = 5.49\ [\,\mathrm{eV}\,]$) with $\underset{s}{A_M} = \{\mathrm{Ag}(110), \mathrm{Ag}(100), \mathrm{Ag}(111)\}$ surfaces. The of surface density of metal ions, $\underset{s}{n_M}$, is computed from the lattice constant of silver and the specific surface orientation: $n_M^{(110)} = 1.4038$, $n_M^{(100)} = 1.9853$, $n_M^{(111)} = 2.2925\ [\,10^{-9}\mathrm{mol/cm}^2\,]$. As surface chemical potential of the electrons $\underset{s}{\mu_e}$ we use the measured data of the work function [23, 21, 56], $\mu_e^{(110)} = 4.52$, $\mu_e^{(100)} = 4.64$, $\mu_e^{(111)} = 4.74\ [\,\mathrm{eV}\,]$. We assume that each surface metal atom provides one adsorption site, $\omega_M = 1$.

Water is assumed to adsorb on the surface as $\underset{s}{A_0} = \mathrm{H_2O}$ with an adsorption energy of $\Delta g_0^A = -0.08$ eV and a partial molar area of $a_0^R = 1.42 \cdot 10^8\,[\,\mathrm{mol/cm}^2\,]$. The adsorption energy of protons and hydroxide ions is computed from the reaction energy of the self-ionization on the surface, $\underset{s}{\Delta} g^D_{\mathrm{H_2O}}$ (c.f. Section 6.5). We assume that at the potential of zero charge the surface concentration of $\underset{s}{\mathrm{H}^+}$ is equal to the concentration of $\underset{s}{\mathrm{OH}^-}$ on the surface, i.e. $\underset{s}{\hat{y}}_{\mathrm{H}^+}(E^0) \overset{!}{=} \underset{s}{\hat{y}}_{\mathrm{OH}^-}(E^0)$. This leads to the constraint $\Delta\tilde{g}^A_{\underset{s}{\mathrm{H}^+}} = \Delta\tilde{g}^A_{\underset{s}{\mathrm{OH}^-}}$. Equation (116) determines the adsorption energy as $\Delta\tilde{g}^A_{\underset{s}{\mathrm{H}^+}} = \frac{1}{2}\big(\Delta g^A_{\mathrm{H_2O}} + \underset{s}{\Delta} g^D_{\mathrm{H_2O}} - \Delta g^D_{\mathrm{H_2O}}\big)$. Self-ionization on the surface is considered to be far more favorable than in the volume, i.e. $\underset{s}{\Delta} g^D_{\mathrm{H_2O}} \ll \Delta g^D_{\mathrm{H_2O}}$. We employ exemplarily $\underset{s}{\Delta} g^D_{\mathrm{H_2O}} = 0.05$eV, but provide also a parameter study in the following. We assume a surface solvation number of 25 for $\underset{s}{\mathrm{H}^+}$ and $\underset{s}{\mathrm{OH}^-}$.

Regarding the adsorption of the ionic salt species we distinguish between adsorbing, $\Delta\tilde{g}^A_{\alpha,\beta} > -1$eV, and non-adsorbing species, $\Delta\tilde{g}^A_{\alpha,\beta} \ll -1$eV. Non-adsorbing ions will not explicitly be considered since their surface concentration is practically zero. We assume that neither the alkali metal ions Na^+,K^+ nor the hexafluorophosphate ion PF_6^- adsorb on the metal surface (in the potential range of interest). Fluoride and perchlorate, however, are considered to adsorb as partially solvated ions $\underset{s}{A_{3,0}} \in \{\underset{s}{\mathrm{F}^-}, \underset{s}{\mathrm{ClO}_4^-}\}$. The respective solvation numbers and adsorption energies are discussed in the examples.

8.2 Reference potential

The reference potential $U^{\mathtt{R}}$ can be determined from a single potential of zero charge measurement of a non-adsorbing salt. It is experimentally known that neither K^+ nor PF_6^- adsorbs on silver and the potential of zero charge E^* is equal to the reference potential $U^{\mathtt{R}}$ for an aqueous KPF_6 solution (c.f. Section 8.2). The necessity of such a reference measurement originates from the fact that we do not explicitly model the reference electrode|electrolyte interface (c.f. Section 7.1).

Remember that the reference potential $U^{\mathtt{R}}$ depends on $\underset{s}{\mu_e^{\mathtt{M}}}$ according to $(140)_2$ and thus on the surface orientation. Consequently Valette [61, 62, 64, 65, 63] measures different zero charge potentials of the working electrode for the various silver surfaces. We can read off the measured

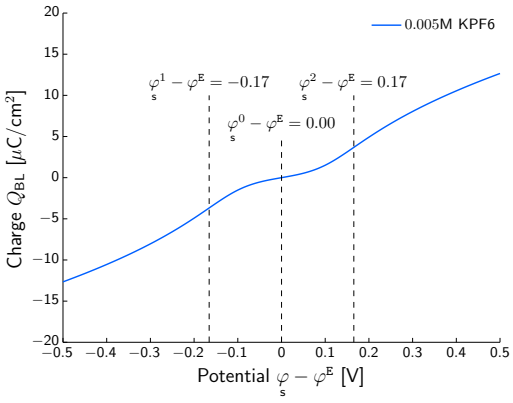

(a) Boundary layer charge Q_{BL}

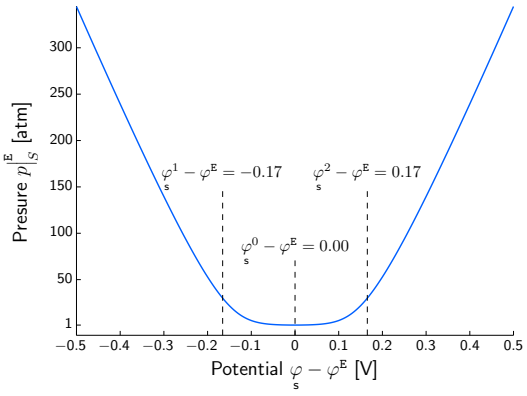

(b) Pressure at the interface $p|^{\mathrm{E}}_S$

Figure 5: Computed boundary layer charge Q_{BL} and pressure $p|^{\mathrm{E}}_S$ for a 0.005M KPF_6 solution as function of $\varphi_s - \varphi^{\mathrm{E}}$. The plots are obtained from equations (105) and (145), respectively. The dashed lines correspond to the potentials which are obtained from the turning point of $Q_{\mathrm{BL}}(U)$.

zero charge potential E^* for $A_M \in \{\mathrm{Ag}(110), \mathrm{Ag}(100), \mathrm{Ag}(111)\}$ vs SCE and obtain

$$U^{\mathrm{R}}_{\mathrm{Ag}(110)} = -0.97\,[\,\mathsf{V}\,]\ , \quad U^{\mathrm{R}}_{\mathrm{Ag}(100)} = -0.86\,[\,\mathsf{V}\,] \quad \text{and} \quad U^{\mathrm{R}}_{\mathrm{Ag}(111)} = -0.69\,[\,\mathsf{V}\,]\,. \tag{164}$$

9 Ag(110)|KPF_6 - general discussion of the model

The Ag(110)|KPF_6 interface serves as a first example to discuss the different aspects of our model. In the main part of the discussion we fix the bulk concentration of KPF_6 to 0.005M and rely on $\varphi_s - \varphi^{\mathrm{E}}$, the potential between the metal surface and the electrolyte, as scale of the electric potential. Finally we provide a computation of the capacity for salt concentrations of $(0.0025 - 0.1)$M with respect to the measured cell potential E.

First of all remember the decomposition (143) of the total charge Q in boundary layer and surface contributions, i.e. $Q = Q_{\mathrm{BL}} + Q_s$. We discuss the boundary layer and the surface contributions consecutively and validate our theory on the total capacity C.

9.1 Boundary layer charge and capacity

The boundary layer charge (see eq. (145))

$$Q_{\mathrm{BL}} = -\operatorname{sgn}(\varphi_s - \varphi^{\mathrm{E}})\sqrt{2\varepsilon_0(1+\chi)\big(p|^{\mathrm{E}}_S - p^{\mathrm{E}}\big)} \tag{165}$$

is determined by the pressure p at the interface, $p|^{\mathrm{E}}_S$. Equation (105) provides an implicit relation between $p|^{\mathrm{E}}_S$ and $\varphi^{\mathrm{M}}_s - \varphi^{\mathrm{E}}$ which can be used to determine $p|^{\mathrm{E}}_S = \hat{p}(\varphi^{\mathrm{M}}_s - \varphi^{\mathrm{E}})$.

Figure 5 displays the computed boundary layer charge Q_{BL} and the pressure $p|_S^{\mathrm{E}}$ at the metal surface for a 0.005M KPF_6 aqueous solution. The values $\underset{s}{\varphi}^0 - \varphi^{\mathrm{E}} = 0$ V, $\underset{s}{\varphi}^1 - \varphi^{\mathrm{E}} = -0.17$ V and $\underset{s}{\varphi}^2 - \varphi^{\mathrm{E}} = +0.17$ V correspond to the turning points of the boundary layer charge Q_{BL} and to local extrema of C_{BL} (see Figure 6). We find that the pressure increases if $\underset{s}{\varphi} - \varphi^{\mathrm{E}}$ is deflected from 0 V, in either positive or negative direction. Between 0 V and ± 0.17 V the pressure behaves non-linear, while beyond ± 0.17 V the pressure increases almost linearly. Origin of the increasing pressure is the Lorentz force $-n^{\mathrm{F}}\,\nabla\varphi$ (c.f. equation (84)) which tries to compress the electrolyte near the metal interface and whereby the pressure at the interface rises. The decrease of the boundary layer capacity beyond $\underset{s}{\varphi} - \varphi^{\mathrm{E}} = \pm 0.17$ V originates from the same effect.

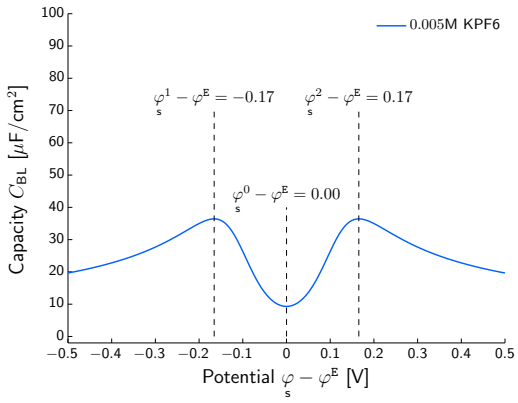

Figure 6: Computed boundary layer capacity C_{BL} as function of the electrolyte potential drop $\underset{s}{\varphi} - \varphi^{\mathrm{E}}$ for a 0.005M KPF_6 solution. The minimum of C_{BL} corresponds to the potential of zero charge, $\underset{s}{\varphi}^0 - \varphi^{\mathrm{E}} = 0$ V. C_{BL} has two maxima at $\underset{s}{\varphi}^{1,2} - \varphi^{\mathrm{E}} = \pm 0.17$ V.

If we were to ignore the pressure p in the whole derivation of Section 5.2.1 we would even obtain an unbounded capacity! This circumstance, i.e. the *failure* of the Poisson–Boltzmann approximation for $\underset{s}{\varphi} - \varphi^{\mathrm{E}} > \pm 0.1m$V, is well known in the literature, and several solutions were presented[7, 22, 2, 12]. However, tracing this failure back to the negligence of the material pressure p is quite unknown. V. Freise was the first who mentioned 1952[24] that the pressure p plays a crucial role in the theory of the diffuse double layer. But his work was not widely recognized and his capacity predictions were yet in the order of $(200 - 300)\mu\mathrm{F/cm}^2$. Common to all **extensions** of the classical Poisson–Boltzmann-theory is the representation of the charge Q_{BL} and the capacity C_{BL} as **single** equations $Q_{\mathrm{BL}}(\underset{s}{\varphi} - \varphi^{\mathrm{E}})$ and $C_{\mathrm{BL}}(\underset{s}{\varphi} - \varphi^{\mathrm{E}})$. But the general case is an (algebraic) equation **system**

$$C_{\mathrm{BL}} = C_{\mathrm{BL}}(\underset{s}{\varphi} - \varphi^{\mathrm{E}}, p|_S^{\mathrm{E}} - p^{\mathrm{E}}), \qquad g(\underset{s}{\varphi} - \varphi^{\mathrm{E}}, p|_S^{\mathrm{E}} - p^{\mathrm{E}}) = 0 \tag{166}$$

which determines the boundary layer capacity[2]. The equation $(166)_2$ indicates the constraint (105). The consistent modeling of this study incorporates

[2]Note, in our derivation we used the implicit function theorem to write $p|_S^{\mathrm{E}} = \hat{p}(\underset{s}{\varphi} - \varphi^{\mathrm{E}})$ in order to obtain the

- coupled electrostatics and mechanics: $\nabla p = -n^F(\varphi, p)\nabla\varphi$ and $\varepsilon_0(1+\chi_{\mathrm{E}})\partial_{xx}\varphi = n^{\mathrm{F}}(\varphi, p)$
- incompressibility: $\mu_\alpha \propto v_\alpha^R \cdot p$ (chemical potential linear in p) and $\sum_{\alpha=0}^{N_E} v_\alpha^R n_\alpha^R = 1$ (incompressibility constraint),
- and the solvation effect: $v_\alpha^R \neq v_0^R, \alpha = 1, \ldots, N_E$.

When all particles were to have the same partial molar volumes, $v_\alpha^R = v_0^R$, one obtains a decoupling of the Poisson- and the momentum equation (see the discussion in Section 5.2.1 and 5.3).

The solvation effect in the electrolyte essentially influences the height of the C_{BL} maxima via the partial molar volumes $v_\alpha^R = (1+\kappa_\alpha)\cdot v_0^R$. If solvation were neglected, i.e. $v_\alpha^R \approx v_0^R$, the capacity is highly overestimated. Figure 7 shows a parameter study of C_{BL} with respect to the solvation number $\kappa_\alpha = \kappa, \alpha = 1, \ldots, N_E$.

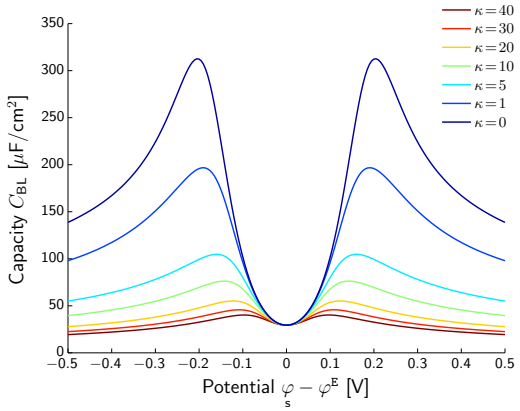

Figure 7: Parameter study of the boundary layer capacity C_{BL} with respect to the solvation number κ.

The specific metal surface has no impact to the boundary layer charge Q_{BL} and the capacity C_{BL}. From a physical point of view this is obvious since the free energy of the electrolyte phase is itself independent of the metal constituents. The metal surface determines only $\varphi_s - \varphi^{\mathrm{M}}$ for the electrolyte phase from the boundary condition $\varphi_s - \varphi^{\mathrm{M}} = (\mu_e^{\mathrm{M}} - \mu_e^{\mathrm{M}})/e_0$. Since Q_{BL} and C_{BL} are expressed in terms of $\varphi_s - \varphi^{\mathrm{E}}$, a different metal surface can only *shift* the potential scale, due to a different surface chemical potential $\mu_{e,s}$, but never changes the functions $\hat{Q}_{\mathrm{BL}}$ and $\hat{C}_{\mathrm{BL}}$. Note that this allows for an electrode independent survey of electrolytic solutions.

representation $C_{\mathrm{BL}} = C_{\mathrm{BL}}(\varphi_s - \varphi^{\mathrm{E}}, \hat{p}(\varphi_s - \varphi^{\mathrm{E}}) - p^{\mathrm{E}}) = \hat{C}_{\mathrm{BL}}(\varphi_s - \varphi^{\mathrm{E}})$, which was convenient in the further derivation. However, to actually **compute** C_{BL} one has to solve the coupled equation system (166).

9.2 Surface charge and capacity

Next we discuss the surface properties of the Ag(110)$|\mathrm{KPF}_6$ example. Due to the dissociation of water into protons and hydroxide ions we have **four** charged species in the electrolyte, namely K^+, PF_6^-, H^+ and OH^-. We assume that neither K^+ nor PF_6^- adsorbs on the metal surface, allow, however, for an adsorption of $\mathrm{H_2O}$, H^+ and OH^-. Regarding the adsorption of H^+ and OH^- we assume equal concentrations at the potential of zero charge (quite similar to an equal concentration of H^+ and OH^- in the bulk electrolyte).

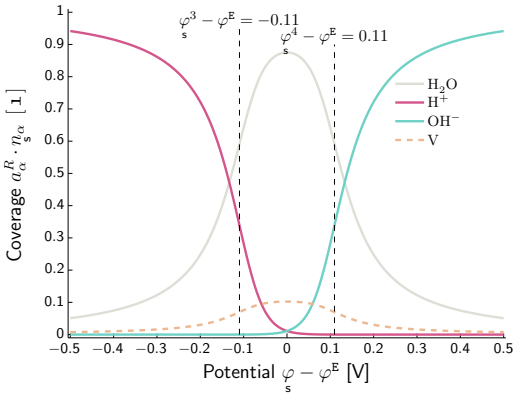

Figure 8: Coverage of the Ag(110) surface with respect to the potential $\underset{s}{\varphi} - \varphi^{\mathrm{E}}$.

Figure 8 shows the coverage $\underset{s}{n_\alpha}/\underset{s}{n_M^{\mathrm{R}}}$ of surface vacancies (V), adsorbed water ($\underset{s}{\mathrm{H_2O}}$), protons ($\underset{s}{\mathrm{H}^+}$) and hydroxide ions ($\underset{s}{\mathrm{OH}^-}$). Around the potential of zero charge, $\underset{s}{\varphi} - \varphi^{\mathrm{E}} \approx 0$, the surface is mainly covered with adsorbed water and surface vacancies. For $\underset{s}{\varphi} - \varphi^{\mathrm{E}} < 0$ the metal surface becomes negatively charged and thus attracts $\underset{s}{\mathrm{H}^+}$. For $\underset{s}{\varphi} - \underset{s}{\varphi}^{\mathrm{E}} > 0$ we have exactly the opposite situation and the coverage of $\underset{s}{\mathrm{OH}^-}$ increases. For both situation we observe a saturation due to the finite amount of adsorption sites on the surface.

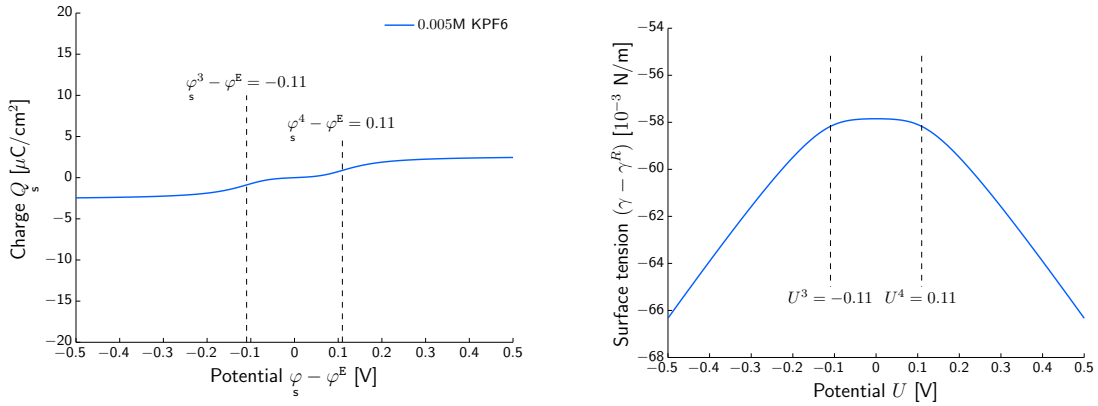

(a) Surface charge density Q_s

(b) Surface tension $\gamma - \gamma^R$

Figure 9: Computed Q_s as function of $\varphi_s - \varphi^E$, originating from the adsorption of protons (H^+) and hydroxide ions (OH^-). The potentials φ_s^3 and φ_s^4 correspond to the turning points of Q_s. According to equation (147) the surface tension γ also changes as a function of $\varphi_s - \varphi^E$.

The corresponding surface charge density Q_s is displayed in Figure 9a. According to equation (147), a variation of the surface charge also corresponds to a variation of the surface tension (Figure 9b). The turning points φ_s^3 and φ_s^4 of Q_s mark the transition from adsorption to saturation. It is quite remarkable that the surface gets indeed fully covered with H^+ or OH^-, even for the low bulk concentration of $n^E_{H^+} = n^E_{OH^-} = 10^{-7}\,[\,\text{mol}/\ell\,]$. But *the bulk* is actually an *infinite* reservoir of particles, and even if the concentration in *the bulk* is quite small, one could still have a transition of an *infinite* amount of particles from the bulk onto the surface.

The surface solvation effect plays a major role for the limits of the surface charge. Consider a Ag(110) surface with an elementary charge on each adsorption site. The surface charge would then be $\pm e_0 \cdot n_{M,s}^R \approx \pm 135 \mu\text{F}/\text{cm}^2$. But if each ion contains $\kappa_{\alpha,0}$ water molecules in its surface solvation shell, a *fully* covered surface corresponds to a surface charge of $\pm e_0 \cdot n_{M,s}^R/(1 + \omega_0\, \kappa_{\alpha,0}) \approx \pm 3.3 \mu\text{F}/\text{cm}^2$.

From a mathematical point of view the surface solvation effect, embedded in our surface thermodynamic theory (c.f. section 3), leads to an (algebraic) equation **system**

$$C_s = C_s(\varphi_s - \varphi^E, \gamma - \gamma_M^R), \qquad g_s(\varphi_s - \varphi^E, \gamma - \gamma_M^R) = 0 \tag{167}$$

for the surface capacity C_s. The equation $(166)_2$ indicates the constraint (102). Decoupling of $(167)_1$ and $(167)_2$ is achieved for $a_{\alpha,\beta}^R = a_0^R$, i.e. without solvation effect.

Adsorption energies of H^+ and OH^- have a major impact on the surface charge and capacity. The energies are calculated from the adsorption energy of water, $\Delta g_0^A = -0.08\text{eV}$, the dissociation energy in the electrolyte, $\Delta g^D_{H_2O} = 1.043\,[\,\text{eV}\,]$, and the surface dissociation energy $\Delta_s g^D_{H_2O}$. The central parameter which determines the width of the surface capacity,

i.e. $\underset{s}{\varphi}^4 - \underset{s}{\varphi}^3$, is actually $\underset{s}{\Delta} g^D_{\mathrm{H_2O}}$. If surface and volume dissociation energies are equal we observe a width beyond 1 V. It seems thus necessary that $\underset{s}{\Delta} g^D_{\mathrm{H_2O}} \ll \Delta g^D_{\mathrm{H_2O}}$ and we assumed $\underset{s}{\Delta} g^D_{\mathrm{H_2O}} = 0.10\,[\,\mathrm{eV}\,]$ for this example. Figure 10 shows a parameter study of the surface dissociation energy $\underset{s}{\Delta} g^D_{\mathrm{H_2O}}$. We emphasize that a broadly conceived parameter study will be published in a subsequent paper.

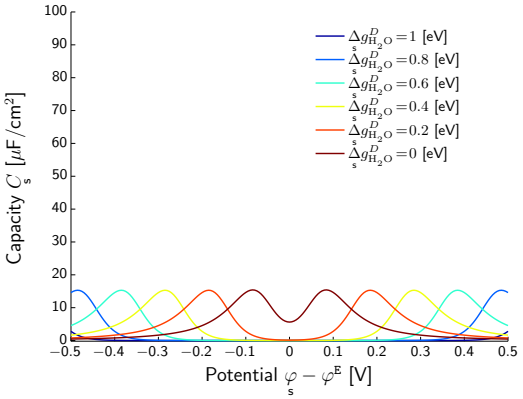

Figure 10: Parameter study of the dissociation energy $\underset{s}{\Delta} g^D_{\mathrm{H_2O}}$ from the surface reaction $\underset{s}{\mathrm{H_2O}} + (\underset{s}{\kappa}_{\mathrm{H^+}} + \underset{s}{\kappa}_{\mathrm{OH^-}})\underset{s}{\mathrm{H_2O}} \rightleftharpoons \underset{s}{\mathrm{H^+}} + \underset{s}{\mathrm{OH^-}}$ and its impact on the surface capacity $\underset{s}{C}$.

9.3 Total capacity and validation

Finally we provide computations of the total capacity $C = C_{\mathrm{BL}} + \underset{s}{C}$. In Figure 11 we display the capacity C as a function of the charge Q. The locations of the extrema correspond to $\big(Q^i, C^i\big) = \big(\hat{Q}(\underset{s}{\varphi}^i - \varphi^{\mathrm{E}}), \hat{C}(\underset{s}{\varphi}^i - \varphi^{\mathrm{E}})\big),\ i = 0, 1, 2$. The (implicit) (Q, C) plots are quite illustrative since they are independent of the actual electrostatic potential scale.

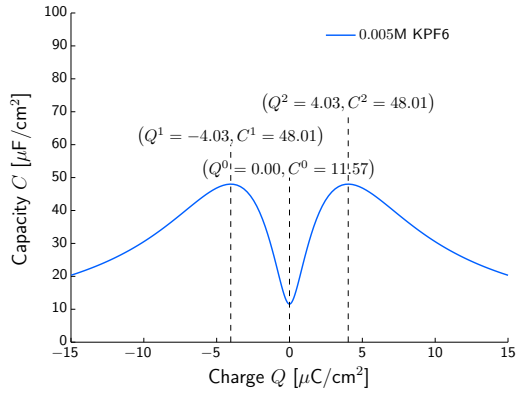

Figure 11: Implicit plot $\big(\hat{Q}(\underset{s}{\varphi} - \varphi^{\mathrm{E}}), \hat{C}(\underset{s}{\varphi} - \varphi^{\mathrm{E}})\big)$ for $\underset{s}{\varphi} - \varphi^{\mathrm{E}} \in [-0.5, 0.5]$ V.

For the comparison of our theory to experimental data we rely on the relation (140) between E and $\underset{s}{\varphi} - \varphi^{\mathrm{E}}$,

$$E = \underset{s}{\varphi} - \varphi^{\mathrm{E}} + U^{\mathrm{R}}_{\mathrm{Ag(110)}} \quad \text{with} \quad U^{\mathrm{R}}_{\mathrm{Ag(110)}} = -0.97\,[\,\mathrm{V}\,]\,, \tag{168}$$

Note that this relation between E and $\underset{s}{\varphi} - \varphi^{\mathrm{E}}$ corresponds to a **constant** space charge layer at the reference electrode|electrolyte interface.

In Figure 12a we display the computed capacity $\hat{C}(-E - U^{\mathrm{R}}_{\mathrm{Ag(110)}})$ with respect to E for various concentrations of $\mathrm{KPF_6}$. Figure 12b shows the measured capacity of G. Valette for Ag(110)|$\mathrm{KPF_6}$, Figure 3.a from [61].

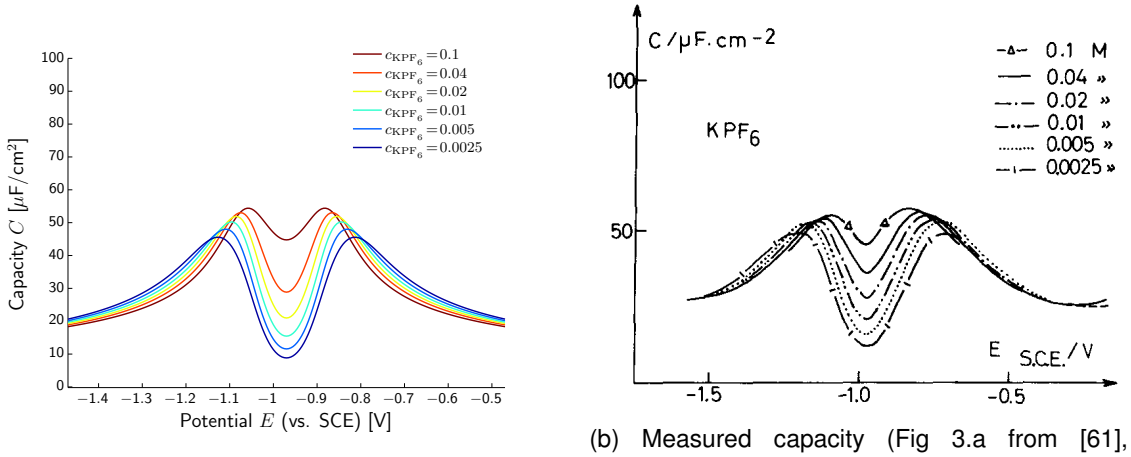

(a) Computed capacity

(b) Measured capacity (Fig 3.a from [61], reprinted with permission from Elsevier)

Figure 12: Comparison of the computed capacity (a) and the measured capacity (b) of the Ag(110)|$\mathrm{KPF_6}$ interface for concentrations of $(0.0025 - 0.1)$M.

Note that there is no parameter variation except the bulk concentration of $\mathrm{KPF_6}$, i.e. $n^{\mathrm{E}}_{\mathrm{K^+}} = n^{\mathrm{E}}_{\mathrm{PF_6^-}} = c_{\mathrm{KPF_6}}$. We obtain a broad qualitative and quantitative agreement of the whole capacity *spectrum*, i.e. with respect to the measured potential E **and** the salt concentration $c_{\mathrm{KPF_6}}$. This is, in the view of the very *simplistic* free energy models that we employed in Section 4, astonishing.

10 Ag(abc)|$\mathrm{Na_K}$ClO4 - comparison to multiple experimental data

In this example we briefly compare measured capacity data of Ag(110), Ag(100) and Ag(111) from different research groups to our new model. We rely exemplarily on the data of Schmickler/Beltramo for 0.05M $\mathrm{KClO_4}$ [54, 5, 6] and Valette[3] for 0.04M and 0.1M $\mathrm{NaClO_4}$ [62, 63, 61].

[3]Note that measured data for a 0.05M $\mathrm{NaClO_4}$ solution is not presented by Valette. To avoid a misunderstanding with respect to the concentration difference between the two examples we also display data for a 0.1M

It is assumed that ClO_4^- adsorbs on the surface, while K^+ and Na^+ do not adsorb. From this viewpoint the two solutions behave equally and can be directly compared.

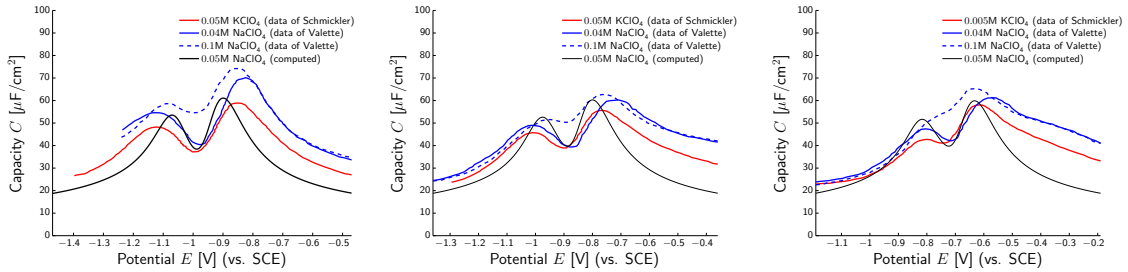

(a) Ag(110) (Data of [54] and [61]) (b) Ag(100) (Data of [54] and [62]) (c) Ag(111) (Data of [54] and [61])

Figure 13: Computed and measured capacity of aqueous 0.05M KClO_4 and $0.04/0.1\mathrm{M}\mathrm{NaClO}_4$ solutions of for various silver surfaces. All measurments were performed vs. SCE.

Figure 13 displays the measured data and computed capacity for Ag(110), Fig. 13a, Ag(110), Fig. 13c, and Ag(111), Fig. 13c.

It is well known in literature that the *shift* of the potential scale between the three surfaces originates from the different work functions[25, 60]. Within our derivation of the reference potential $U^{\mathrm{R}} = \frac{1}{e_0}(\underset{s}{\mu}{}_e^{\mathrm{M}} - \underset{s}{\mu}{}_e^{\mathrm{R}}) + U^{\mathrm{R,E}}$ this is naturally incorporated due to the dependency of $\underset{s}{\mu}{}_e^{\mathrm{M}}$ on the specific metal surface.

Even though the electrochemical systems are *equal* from a theoretical point of view, we observe quite large deviations between the experimental data. Several reasons contribute to this deviation: non-perfect metal surface (steps and defects), contaminations of electrolyte phase, variation of the diffusional potential $U^{\mathrm{R,E}}$, setup of the counter and reference electrode, and further issues. Since we do not explicitly account for such deviations within our model, it is sufficient for our purpose to observe that our computed capacity is within the measuring error between two experiments. However, we observe a systematic *broadening* of the capacity between the data of Valette, the data of Schmickler/Beltramo, and our computed capacity curves. One possible origin of this systematic deviation could be a violation of the assumption $\underset{s}{\varphi}{}^{\mathrm{R}} - \varphi^{\mathrm{E}} = \text{const.}$

We briefly describe the model parameters which were used to compute C in Figure 13. ClO_4^- is assumed to adsorb on the surface with an adsorption energy of $\Delta\tilde{g}^A_{\mathrm{ClO}_4^-} = -0.2\,[\,\mathrm{eV}\,]$. The solvation number of ClO_4^- on the surface is $\underset{s}{\kappa}_{\mathrm{ClO}_4^-} = 15$ and thus smaller than $\underset{s}{\kappa}_{\mathrm{OH}^-} = 25$. The reference potentials of each metal surface are employed according to (164). All other parameters are as described in Section 8.1. Note that the partial molar areas of all constituents remain equal for all three examples.

With these parameter we computed also the capacity spectrum for salt concentrations of $0.005-0.1$M NaClO_4. Figure 14 displays a comparison of our computed values to the measured data

NaClO_4 solution.

of Valette for a Ag(110) surface. We find a broad qualitative and quantitative agreement and re-emphasize that there is no other parameter variation than the bulk salt concentration c_{NaClO_4}.

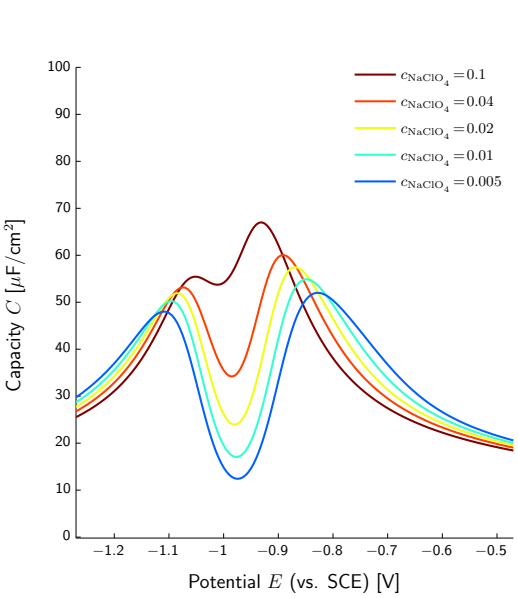

(a) Computed capacity

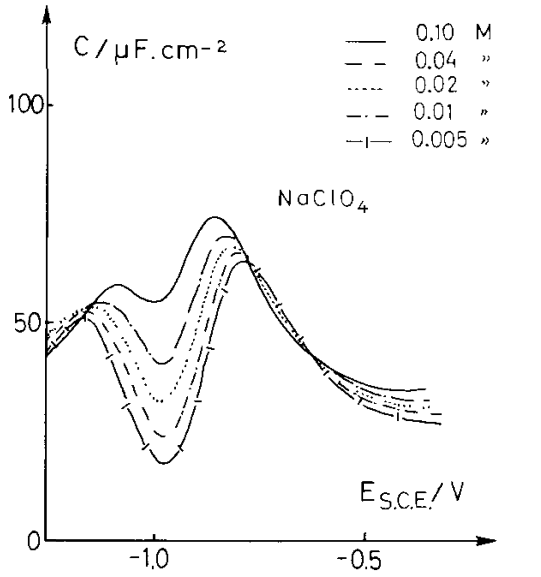

(b) Measured capacity (Fig 2.b from [61], reprinted with permission from Elsevier)

Figure 14: Comparison of the computed capacity (a) and the measured capacity (b) of the Ag(110)|NaClO_4 interface for concentrations of $(0.005 - 0.1)$M.

11 Ag(110)|NaF - structure of the double layer

As last example we consider an aqueous NaF solution in contact with Ag(110). After a brief discussion of the considered model parameter we provide computations of the capacity *spectrum* and validate our theory with the data of Valette. Then we use our metal/electrolyte/interface model to compute the structure of the space charge layer.

Note that this approach is physically rigorous since we use the same set of equations[4] to compute the capacity **and** the space charge layer.

11.1 Validation

The fluoride ion F^- is considered to adsorb on the metal surface. Two central parameter arise then in our model, the adsorption energy $\Delta\tilde{g}^A_{\mathrm{F}^-}$ and the surface solvation number $\underset{s}{\kappa}_{\mathrm{F}^-}$. All other parameters are kept equal to the examples before.

[4] Actually the equation system for the capacity is the first integral of the PDE system that determines the space charge layer structure.

In the volume, the solvation shell is considered as the whole *cloud* of solvent molecules which are *bound* to the central ion in either the first, second or even third solvation shell, without further distinction. The *first* shell which covers $4-8$ solvent molecules and is dependent on the actual chemical constituent[33]. However, the *second* shell covers far more solvent molecules is mainly determined by the charge of the central ion. This lead to the assumption that all monovalent ionic species have an equal solvation number in the electrolyte phase.

On the surface, however, this assumption might not hold. Since solvated ions strip off a part of their total solvation shell, the element specific *first* solvation shell can be more dominant on the surface. Hence we consider different solvation numbers for the adsorbates. In Section 10 we already assumed a solvation number of $\underset{s}{\kappa}_{\mathrm{ClO}_4^-} = 15$ for the adsorbed perchlorate ion. Fluoride is assumed to bind even less solvent molecules on the surface, and we employ $\underset{s}{\kappa}_{\mathrm{F}^-} = 8$. The adsorption energy for F^- is chosen as $\Delta\tilde{g}^A_{\mathrm{F}^-} = -0.16\,[\,\mathrm{eV}\,]$, whereby adsorption near the potential of zero charge occurs (see Figure 20 of the surface coverage).

We obtain then the capacity *spectrum* shown in Figure 15a for the Ag(110)|NaF interface. Note that similar to the examples before we vary only the bulk salt concentration of NaF, i.e. $n^{\mathrm{E}}_{\mathrm{F}^-} = n^{\mathrm{E}}_{\mathrm{Na}^+} = c_{\mathrm{NaF}}$. Figure 15b displays the measured data of Valette.

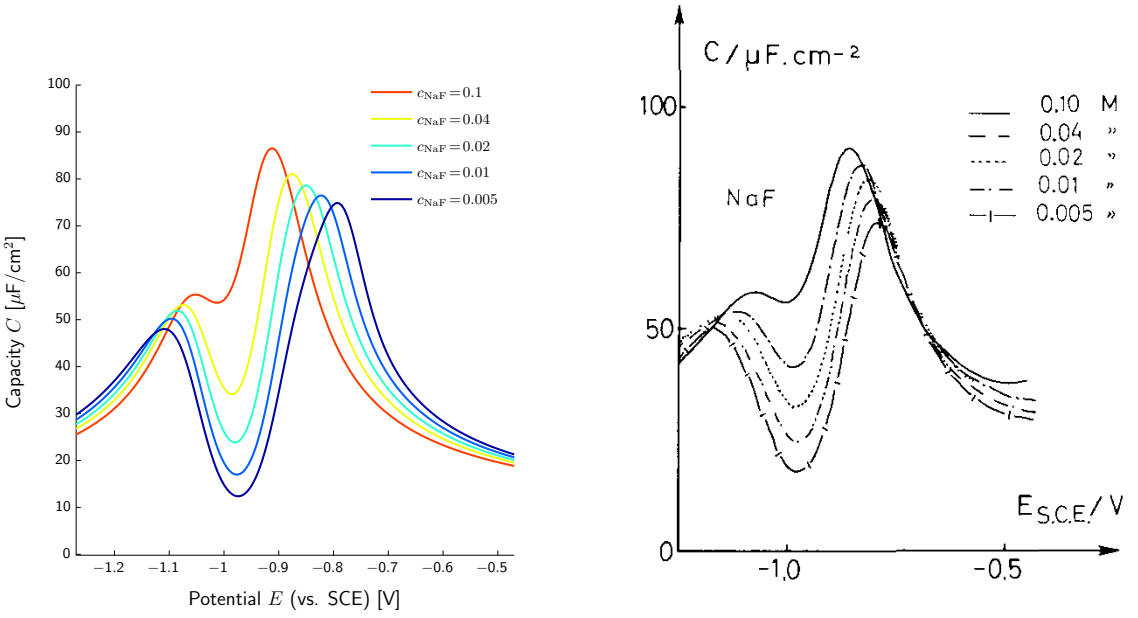

(a) Computed capacity

(b) Measured capacity (Fig 2.a from [61], reprinted with permission from Elsevier)

Figure 15: Comparison of the computed capacity (a) and the measured capacity (b) of the Ag(110)|NaF interface for concentrations of $(0.005-0.1)$M.

The overall agreement of the capacity *spectrum* is quite remarkable. Reconsider that we essentially employed an ideal, incompressible mixtures in the volume and a lattice based ideal mixture on the surface. Both models account entropically and mechanically for the solvation effect. However, the thermodynamic consistent coupling of mechanics and electrostatics in the volume and

on the surface gives obviously a broad accordance to measured data. Employing more sophisticated free energy models $\rho\psi^{\mathtt{M}}$, $\rho\psi^{\mathtt{E}}$ and $\underset{s}{\varphi}$ as well as a concentration dependent susceptibility $\chi^{\mathtt{E}}$ seems promising for modeling electrochemical interfaces in an even wider potential range and allows for more material specific surface effects, e.g. surface reconstruction[38].

However, for the sake of this work the comparison of Figure 15 is sufficient to validate our theory in the potential range $E = [-1.5, -0.5]$ V.

11.2 Structure of the double layer

After validating our theory and the considered parameters we use the metal/electrolyte/interface model to compute the *structure* of the space charge layer. By *structure* we mean the space dependent solutions of all molar densities $n_\alpha(x)$ in the metal and the electrolyte phase, the surface concentrations $\underset{s}{n_\alpha}$, and the electrostatic potential $\varphi(x)$. We employ $\varphi^{\mathtt{M}} = E$ as boundary condition and compute $\underset{s}{\varphi}$ and $\varphi^{\mathtt{E}}$ accordingly. We discuss the structure of the space charge layer exemplarily for three potential values, i.e. $E = \{-0.6, -0.9, -1.4\}$V vs (SCE) and a bulk salt concentration of $c_{\mathrm{NaF}} = 0.1\,[\,\mathrm{mol}/\ell\,]$.

Figure 16 displays the computed structure of the space charge layer for $E = -0.9$V, which corresponds to $\underset{s}{\varphi} - \varphi^{\mathtt{E}} = 0.07$V.

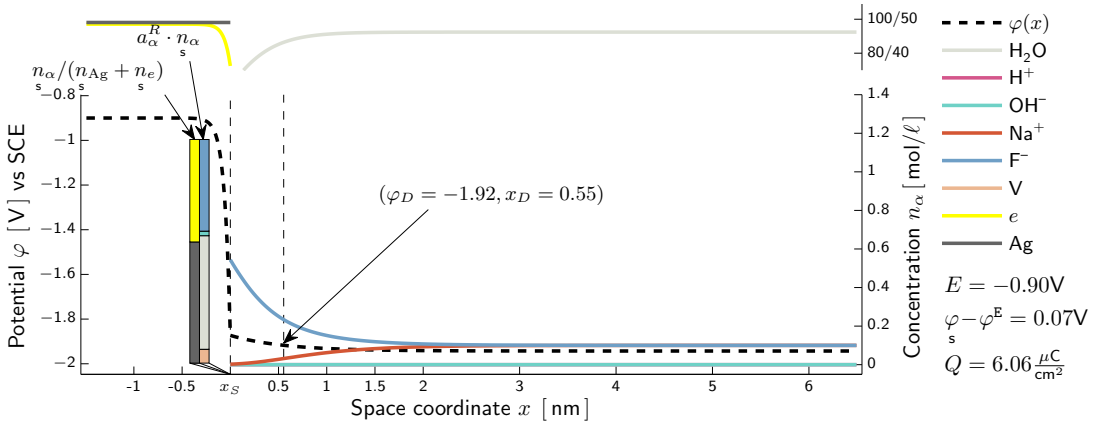

Figure 16: Structure of the Ag(110)|0.1M NaF (aq) interface at $E = -0.9$V.

The metal surface is positioned at $x_S = 0$, with the metal domain to its left and the electrolyte to its right. Scales are in absolute values as computed from our theory. The solid lines display the numerical solutions n_α for the electrolyte and the metal species, respectively. On the surface S, the right bar chart denotes the coverage $a_\alpha^R \cdot \underset{s}{n_\alpha}$ of adsorbates and surface vacancies. Note that $\sum_\alpha^{N_S} a_\alpha^R \underset{s}{n_\alpha} = 1$ according to (73). The left bar shows the ratio between surface electrons $\underset{s}{n_e}$ and surface metal ions $\underset{s}{n_M}$, i.e. $\underset{s}{n_e}/(\underset{s}{n_M} + \underset{s}{n_e})$ and $\underset{s}{n_M}/(\underset{s}{n_M} + \underset{s}{n_e})$. The black dashed line corresponds to the space dependent, continuous electrostatic potential φ.

We observe a space charge layer within the metal which originates from a decrease of the electron density n_e near the surface. Origin of this decease is the necessary condition $\varphi^{\mathtt{M}} - \underset{s}{\varphi} = -(\underset{s}{\mu_e} - \mu_e^{\mathtt{M}}) = -0.972\text{V}$. The space dependent profile of the electron density n_e is obtained from a solution of the Poisson equation (88) as $n_e(x) = \hat{n}_e(\varphi(x))$. The charge $Q_M = \int_{x_M}^{x_S} n^{\mathrm{F}} dx$, which is accordingly stored in the metallic boundary layer, is computed as

$$Q_M = \sqrt{2\varepsilon_0 \frac{\mu_e^{\mathtt{M}}}{v_M^R} \left(1 - \frac{\underset{s}{\mu_e}}{\mu_e^{\mathtt{M}}} - \frac{2}{5}\left(1 - \left(\frac{\underset{s}{\mu_e}}{\mu_e^{\mathtt{M}}} \right)^{\frac{5}{2}} \right) \right)} = 14.41 \left[\frac{\mu\text{C}}{\text{cm}^2} \right] . \tag{169}$$

Note that Q_M is constant because $\varphi^{\mathtt{M}} - \underset{s}{\varphi} = \text{const}$. Even though the space charge layer in the metal is rather thin, it stores quite an amount of charge in order to *generate* the potential drop $\varphi^{\mathtt{M}} - \underset{s}{\varphi} = -0.972\text{V}$.

The amount of electrons on the surface is then computed from the electroneutrality condition (142) as

$$\underset{s}{n_e} = \underset{s}{n_M} + (Q_M - Q)/e_0 \, . \tag{170}$$

At the potential of zero charge, E^0, the term Q vanishes per definition and the metallic boundary layer charge Q_M is balanced by the surface electrons in order to provide electroneutrality. However, for $E \neq E^0$ the surface electrons additionally balance the electrolytic and the adsorbate charge.

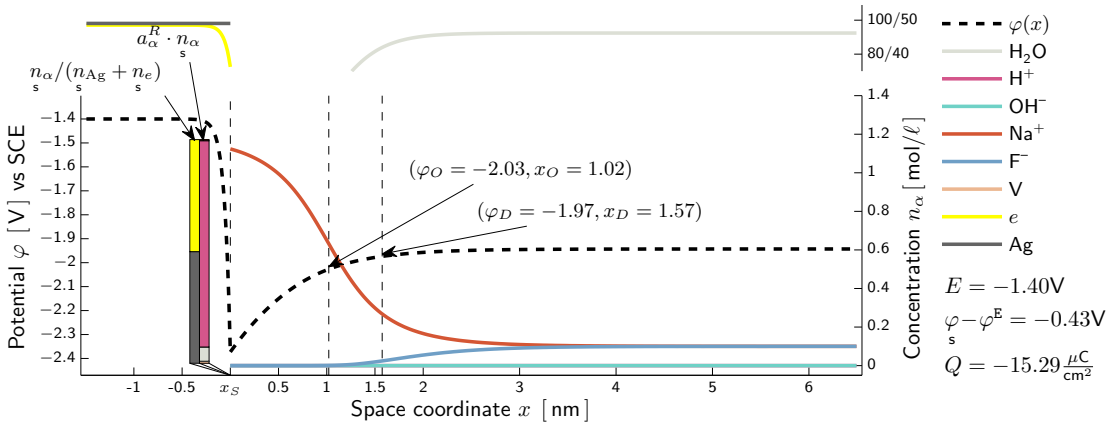

Figure 17: Structure of the Ag(110)|0.1M NaF (aq) interface at $E = -1.4\text{V}$.

In the electrolyte we observe a diffuse space charge layer, i.e. a Poisson–Boltzmann (PB) type behavior. One could characterize a PB-like behavior by the **absence** of a Stern layer, which we defined via the turning point of the free charge density n^{F}, i.e.

$$x_O = \begin{cases} x, & \text{if} \quad \exists\, x \in \mathbb{R} : \partial_{xx} n^{\mathrm{F}} = 0 \, , \; \partial_{xxx} n^{\mathrm{F}} \neq 0 \\ x_S, & \text{else} \end{cases} \tag{171}$$

Note that x_O is implicitly dependent on $\underset{s}{\varphi} - \varphi^{\mathrm{E}}$. Since in the PB-approximation n^{F} is strictly monotone, no turning point exists at all. For a 0.1M solution the potential range of the PB-approximation is $\underset{s}{\varphi} - \varphi^{\mathrm{E}} \approx \pm 80$mV and termed low potential regime.

However, beyond $\underset{s}{\varphi} - \varphi^{\mathrm{E}} \approx \pm 80$mV we observe the formation of a new layer (c.f. Figure 17), which is characterized by the region (x_S, x_O). Since *beyond* the turning point of n^{F}, i.e. $x > x_O$, the *diffuse* layer proceeds, we interpret the layer between the metal surface x_S and x_O as **Stern layer**[58]. The *point* x_O actually corresponds to the plane $x_O \times \mathbb{R}^2$, which we interpret as **outer Helmholtz-plane**. Consequently, we are able to define the outer Helmholtz- or Stern layer-potential: $\varphi_O = \varphi(x_O)$.

It is thus also possible to precisely define the different potential regimes, i.e.

$$\varphi_O = \underset{s}{\varphi} \ : \textbf{low potential} \qquad \text{and} \qquad \varphi_O \neq \underset{s}{\varphi} \ : \textbf{high potential}. \tag{172}$$

Note, in the low potential regime we have $x_O = x_S$ and thus no Stern layer (or outer Helmholtz plane) is present.

The diffuse layer is characterized by the domain (x_O, x_E). However, the Debye length $\lambda_D = \sqrt{\frac{\varepsilon_0(1+\chi_{\mathrm{E}})k_BT}{e_0^2\, c_{\mathrm{NaF}}}}$ is actually the proper length scale of the diffuse layer. Hence we define $x_D = x_O + \lambda_D$ and term $\varphi_D = \varphi(x_D)$ the diffuse layer potential.

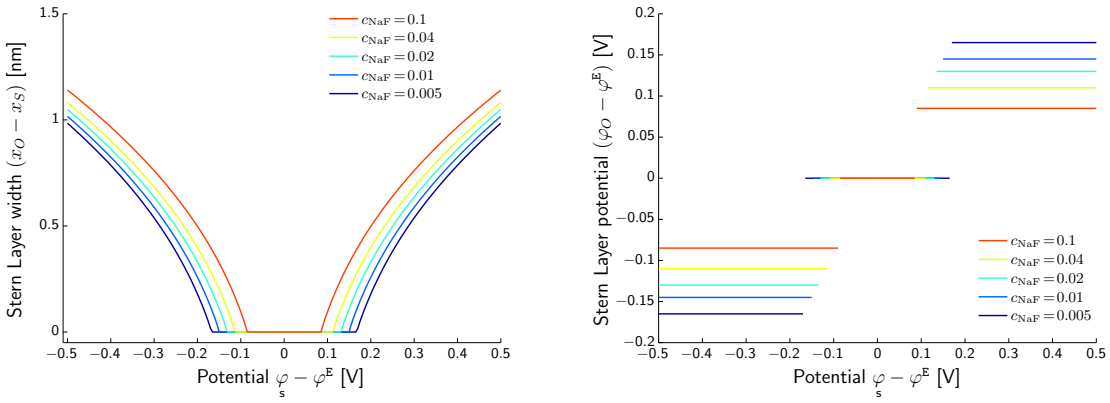

(a) Stern layer width

(b) Stern layer potential

Figure 18: Computed width of the Stern layer, $x_S - x_O$, as function of $\underset{s}{\varphi} - \varphi^{\mathrm{E}}$.

It is indeed quite remarkable that our model naturally predicts the formation of such a layer, however, with certain deviations from classical assumptions:

- In the classical view, the inner Helmholtz plane is assumed as fixed layer of *slightly* adsorbed, solvated ions closest to the metal surface. We observe indeed a local saturation of solvated ions, which also suggests the interpretation as Stern layer, however the width $(x_S - x_O)$ of this saturation layer is dependent on $\underset{s}{\varphi} - \varphi^{\mathrm{E}}$, see Figure 18a.

- Due to the perception of a fixed layer of (solvated) ions near the surface it is assumed that the outer Helmholtz-plane and the metal surface form a simple parallel plate capacitor of constant capacity[1, 31, 11]. Within our definition of the outer Helmholtz-plane we observe, however, that its capacity contribution

$$C_{\text{Stern}} = \frac{dQ_{\text{Stern}}}{dE} \quad \text{with} \quad Q_{\text{Stern}} = -\int_{x_S}^{x_O} n^{\text{F}} dx \tag{173}$$

  is not constant.

- For $\varphi_O = \underset{s}{\varphi}$ the diffuse layer capacity

$$C_{\text{diffuse}} = \frac{Q_{\text{diffuse}}}{dE} \quad \text{with} \quad Q_{\text{diffuse}} = -\int_{x_O}^{x_E} n^{\text{F}} dx \tag{174}$$

  contributes exclusively to the boundary layer capacity C_{BL}, since no Stern layer is formed (i.e. $x_O = x_S$). However, for $\varphi_O \neq \underset{s}{\varphi}$ the diffuse layer capacity vanishes since Q_{diffuse} becomes a constant, according to $\varphi_O - \varphi^{\text{E}} = \text{const}$ (c.f. Figure 18b). Consequently, the Stern layer capacity C_{Stern} becomes the single contribution to C_{BL} for $\underset{s}{\varphi} \neq \varphi_O$. This suggests the following decomposition

$$C_{\text{BL}} = \begin{cases} C_{\text{diffuse}}, & \text{for} \quad \varphi_O = \underset{s}{\varphi} \\ C_{\text{Stern}}, & \text{for} \quad \varphi_O \neq \underset{s}{\varphi} \end{cases} \tag{175}$$

- For $\varphi_O - \varphi^{\text{E}} > 0$, the Stern layer corresponds to the saturation layer of solvated cations, c.f. Figure 19, while for $\varphi_O - \varphi^{\text{E}} < 0$ solvated anions form the Stern layer, see Figure 17.

Note that our findings are independent of the actual metal surface (c.f. the discussion at the end of section 9.1). The Stern layer is exclusively determined by the properties of the electrolytic solution.

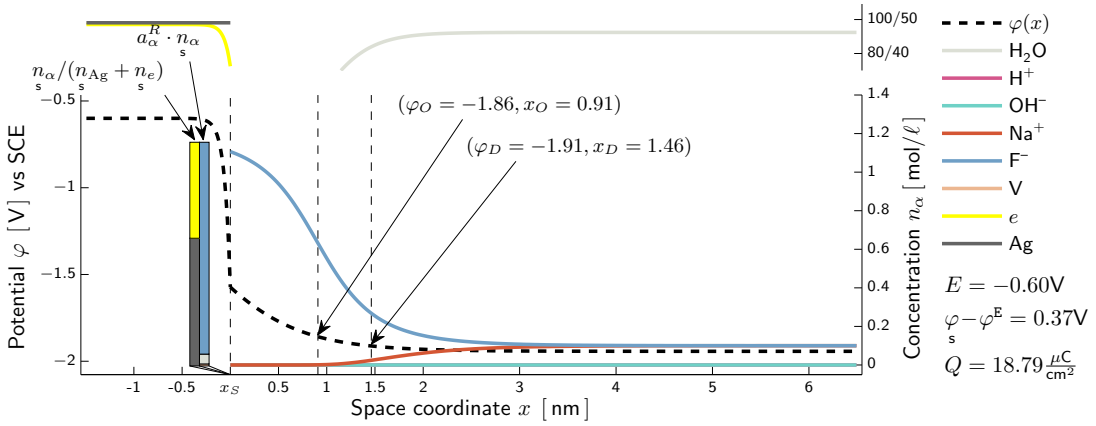

Figure 19: Structure of the Ag(110)|0.1M NaF (aq) interface at $E = -0.6$V.

In contrast, the *adsorption layer* on the metal is dependent on material specific parameters, i.e. the adsorption energies $\Delta\tilde{g}^A_\alpha$. Due to the adsorption of partially solvated ions on the metal surface, we interpret the mixture of adsorbates present on $x_S \times \mathbb{R}^2$ as **inner Helmholtz-plane**. Note that mathematically this layer has no actual width since the adsorbates are modeled as surface mole densities. Consequently, the electrostatic potential φ is continuous at x_S and no potential drop occurs at the inner Helmholtz-plane.

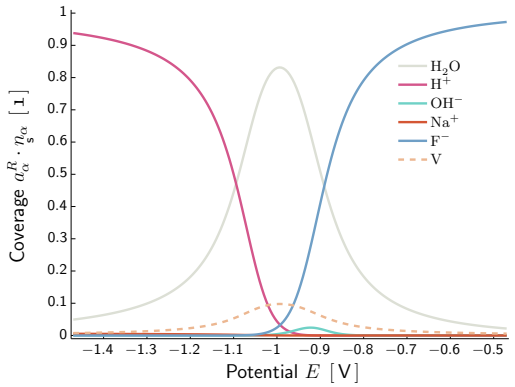

Figure 20: Coverage $a^R_\alpha \cdot \underset{s}{n_\alpha}$ of the metal surface with respect to E (vs SCE).

Figure 20 displays the computed coverage of the metal surface. For $\underset{s}{\varphi} - \varphi^{\mathrm{E}} > 0$ we observe an adsorption of F^- as well as an adsorption of OH^-. However, for $E > -0.9$V adsorbed OH^- is suppressed by F^-. Adsorbed OH^- as well as F^- was indeed found on silver surfaces[15, 34]. However, a detailed quantitative investigation is beyond this scope. We find that the increase of the right capacity maxima, c.f. Figure 15a, arises from the adsorption of F^-. Because the surface solvation shell number $\underset{s}{\kappa}_{\mathrm{F}^-}$ of F^- is smaller as $\underset{s}{\kappa}_{\mathrm{OH}^-}$. Additionally, the adsorption of F^- is favored compared to OH^-, i.e. $\Delta\tilde{g}^A_{\mathrm{F}^-} < \Delta\tilde{g}^A_{\mathrm{OH}^-}$. The non-linear interplay between these parameters actually increases the right capacity hump.

For $E < -1$V we observe an adsorption of solvated H^+. Within the considered potential range H^+ is not considered to react further. But surface electron transfer reactions $\mathrm{H}^+ + \mathrm{e}^- \rightleftharpoons \mathrm{H}$ as well as subsequent reactions $\mathrm{H} + \mathrm{H} \rightleftharpoons \mathrm{H}_2$ are indeed covered within our model. However, a broad investigation of the occuring parameters is part of a subsequent work.

Even though the concentration of H^+ in the electrolyte might seem rather negligible, its reservoir $\mu^{\mathrm{E}}_{\mathrm{H}^+}$ provides an *infinite* amount of H^+. Thus, the surface could indeed get fully covered with H^+ while its bulk concentration remains rather small. But we find also an increasing concentration of H^+ at the interface, which forms similar to Na^+ a saturation layer. Adsorbed protons on silver surfaces were found by Lipkowski and co-workes[43]. The adsorption of Na^+ is not to be expected in the potential range of interest. But adsorption as well as electron transfer reactions for cations are in principle incorporated in our theory.

12 Conclusion and Summary

In this study we derived a new model to describe the properties of the metal/electrolyte interface. It is based on continuum thermo-electrodynamics and employed here in a 1D equilibrium case. The model relies on mixture theories of the metal, the surface, and the electrolyte phase, which model several material specific effects such as solvation or incompressibility. We account for numerous chemical reactions, namely

- dissociation in the electrolyte as well as on the surface (especially the self-ionization of water),
- adsorption from the electrolyte and the metal,
- as well as electron transfer.

Then we derive the equilibrium representations of the mole densities in the volume and on the surface as function of the metal surface/electrolyte potential drop $\underset{s}{\varphi} - \varphi^{\mathrm{E}}$. We show how $\underset{s}{\varphi} - \varphi^{\mathrm{E}}$ is related to the measured cell potential E and derive functions for the charge Q and the capacity C of the metal/electrolyte interface. This allows for a comparison to experimental data, which shows a broad agreement with respect to cell potential as well as salt concentration.

We emphasize that we made no *a priori* assumptions on the structure of the metal/electrolyte interface, but rather *predict* the double layer based on our general mixture theories. This approach is justified by a validation of our model to measured capacity data. Since the same set of equations is used to compute the actual *structure* of the double layer, we provide (for the first time) a thermodynamically consistent picture of the metal/electrolyte interface in a broad potential range.

We are also able to reinterpret some classical conceptions of the double layer based on the results of our model. We find:

- a space charge layer in the metal that covers the constant charge Q_M and *generates* the potential drop $\varphi^{\mathrm{M}} - \underset{s}{\varphi}$,
- a potential dependent surface electron density, which balances the metallic boundary layer charge at the potential of zero charge,
- specifically adsorbed ions on the surface which are reinterpreted as inner Helmholtz plane,
- the formation of an ionic saturation layer near the surface, which is imagined as Stern layer,
- and the diffuse layer, which covers a constant charge Q_{diffuse} for $\varphi_O \neq \underset{s}{\varphi}$, i.e. in the high potential regime which implies $\varphi_O - \varphi^{\mathrm{E}} = \text{const}$.

12.1 Continuum thermodynamics versus microscopic model

The continuum approach ignores the atomistic structure of the material at hand and covers material specific phenomena in the explicit free energy function. In contrast, atomistic models like molecular dynamics (MD) or density functional theory (DFT) resolve the microscopic structure of the material.

Then at least two natural questions appear: Are the regimes where continuum thermodynamics and microscopic models can be applied disjunct? How is continuum thermodynamics related to the corresponding microscopic model in those regimes where both can be applied? The answer to these questions is not obvious at all. Clearly the microscopic oscillations of neighboring atoms are not reflected by continuum models. But nevertheless both models might be capable to embody correctly the envelopes or the mean values of these oscillations. For example, let us consider a metal in the vicinity of its surface to vacuum. We compare the predictions of the electronic charge distribution of the atomistic Lang-Kohn model [42] with the predictions of the continuum Thomas-Fermi model [57, 37]. Both models are used to calculate the surface energy of metals. To this end both models must first calculate the electronic charge distribution, which they do with a different degree of accuracy. In the metal far away from the surface the electronic charge is roughly equal to the charge density of the metal ions. Near to the surface the electron density decreases and tends to zero a little bit outside the metal. From a macroscopic point of view the electronic charge distribution is approximately the same in both models. However, the Lang-Kohn model show more fine details like the Friedel oscillations around the mean value of the electronic density. The mean value, however, is well predicted by the Thomas-Fermi model as well. Particularly both models show a boundary layer on the metal side of the surface and(!) a nonzero electron density within a thin boundary layer outside the metal.

Which type of model approach is to be used relies also on the type of experiment which is used to investigate the metal/electrolyte interface. Measurements of currents and capacities vs potentials were extended in the last decades by scanning tunneling microscopes (STM), X-ray photoelectron spectroscopy (XPS) and additional imaging techniques with the scope of a visual representation of the electrode/electrolyte interface. Quite crude, one could say that imaging techniques like STM and XPS go hand in hand with microscopic methods, like MD or DFT, while the measurements of currents and capacities have their counterparts in continuum non-equilibrium thermodynamics.

12.2 A remark on surface thermodynamics

In our model the *electronic cloud* in front of the metal surface is taken into account, but not explicitly resolved. The current model includes theses electrons as surface constituents characterized by a surface electron density. This gives an example for a common strategy of continuum thermodynamics. Some properties of a material that one does not resolve on the scale of interest are described by an object that is called a *singular surface*, S. The notion *singular* indicates that bulk fields may become discontinuous across S, however, S may carry an own mixture in terms of surface densities. The fundamental setting of surface thermodynamics is quite similar to continuum thermodynamics of the volume. It deals with surface balance equations, there

is a local surface entropy inequality and corresponding to the volume there is a surface free energy function which is the central quantity of the constitutive model for surfaces. The consistent coupling of surface thermodynamics to electrodynamics was quite recently well developed [30, 4, 47]. Continuum surface thermodynamics has many applications. Among them we find the modeling of different phases of the same substance as well as the modeling of thin elastic membranes, e.g. the hull of rubber balloons.

Its application to metal surfaces, however, describing adsorbates as well as surface electrons within one theory, is quite rare.

12.3 Outlook

Our model should be considered as fundamental framework of the metal/electrolyte interface. The model is easy to be adopted to other metal surfaces, different solvents and salts, as well as mixtures of electrolytes. It allows for numerous further investigations of the double layer structure, providing a systematic insight of its complex structure. Additionally, the extension of our model to the non-equilibrium situation is straight forward. Our model provides a thermodynamically consistent extension of the classical Poisson–Nernst–Planck model, which ensures that in equilibrium its results are in broad agreement to experimental data. Furthermore, model based investigations of cyclic voltammetry as well as impedance spectroscopy provide a substantial benefit to modern electrochemistry, with a whole new level of accuracy.

A Free energy densities

The free energy densities for the volume and the surface, respectively, of Section 4 must be derived from phenomenological or microscopic approaches.

A.1 Free energy - electrolyte

At first we derive the free energy density (38) of the electrolyte. The free energy consists of three contributions: (i) reference free energy, (ii) free energy due to the liquid pressure and (iii) free energy due to the entropy of mixing. Further energetic contributions are not considered here, meaning in thermodynamic terminology, the electrolyte is modeled as a simple mixture [47, 16].

Recall the general constitutive relations for the pressure and the entropy density from Section 2.4,

$$p = -\rho\hat{\psi} + \sum_{\alpha=0}^{N} n_\alpha \mu_\alpha \qquad \text{and} \qquad \rho\eta = -\frac{\partial \rho\hat{\psi}}{\partial T} \,. \tag{176}$$

For our purpose we have to transform the constitutive relations (176) in a more proper representation. For this reason we consider the free energy density in terms of the mole fractions y_α and the total mass density ρ,

$$\rho\psi = \rho\hat{\psi}(T, n_0, \ldots, n_N) = \rho\check{\psi}(T, \rho, y_0, \ldots, y_{N-1}) \,. \tag{177}$$

In the new variables the constitutive relations (176) may be rewritten as

$$p = \rho^2 \frac{\partial \check{\psi}}{\partial \rho} \qquad \text{and} \qquad \rho\eta = -\frac{\partial \rho \check{\psi}}{\partial T} \,. \tag{178}$$

The mechanical contribution to the free energy are derived from a simple linear elastic relation for a homogenous mixture of the volume V under the pressure p,

$$p = p^R + K_E \left(\frac{V_{p^R}}{V} - 1 \right) \,. \tag{179}$$

Here V_{p^R} is the volume of the mixture under the reference pressure p^R and K_E is the bulk modulus of the mixture. For the volume V_{p^R} a linear relation to the number of particles $\mathcal{N}_\alpha, \alpha = 0, 1, \ldots, N$ is assumed, *i.e.*

$$V_{p^R} = \sum_{\alpha=0}^{N} v_\alpha^R \mathcal{N}_\alpha, \tag{180}$$

where v_α^R denotes the partial molar volume of constituent α at temperature T and reference pressure p^R. We assume that the molar volumes v_α^R are constant. Insertion of the reference volume in (179) yields

$$p = p^R + K_E \left(n\, H - 1 \right) \qquad \text{with} \qquad H = \sum_{\alpha=0}^{N} v_\alpha^R y_\alpha \,. \tag{181}$$

Finally the mechanical contribution $\rho\psi^{\text{mech}}$ to the free energy density (38) follows from (181), (178) and by integration. The integration constant is chosen such that the mechanical free energy vanishes if the pressure p is equal to p^R.

The entropic contribution to the free energy density. In a simple mixture the entropy of mixing is represented by

$$S^{\text{mix}} = -k_B \sum_{\alpha=0}^{N} \mathcal{N}_\alpha \ln \left(\frac{\mathcal{N}_\alpha}{\mathcal{N}} \right) \,. \tag{182}$$

It is important to recall that the particle number $\mathcal{N}_\alpha$ of constituent $\alpha > 0$ indicates the numbers of solvated constituents, and $\mathcal{N}_0$ represents exclusively that part of the solvent that is not tied within any solvation shell.

In a homogenous mixture the mixing entropy density $\rho\eta^{\text{mix}}$ is given by $S^{\text{mix}} = V \rho\eta^{\text{mix}}$. Thus we have

$$\rho\eta^{\text{mix}} = -k_B n \sum_{\alpha=0}^{N} y_\alpha \ln(y_\alpha) \,. \tag{183}$$

Insertion of (183) into the constitutive relation $(178)_2$ and integration yields to the entropic contribution $\rho\psi^{\text{mix}}$ of the free energy density (38).

A.2 Free energy - metal surface

The modeling of the surface free energy (55) is based on the general constitutive relations for the surface tension and and the surface entropy density,

$$\gamma = \underset{s}{\hat{\psi}} - \sum_{\alpha=0}^{N_s} \underset{s}{n_\alpha} \underset{s}{\mu_\alpha} \quad \text{and} \quad \underset{s}{\eta} = -\frac{\partial \underset{s}{\psi}}{\partial T} \,. \tag{184}$$

To extract the electronic contribution we write $\underset{s}{\psi} = \underset{s}{\psi_e}(T, \underset{s}{n_e}) + \underset{s}{\hat{\psi}_r}(T, \underset{s}{n_0}, \underset{s}{n_1}, \ldots, \underset{s}{n_{N_S-1}})$. In analogy to the electrolyte we exchange variables and obtain

$$\underset{s}{\psi} = \underset{s}{\psi_e}(T, \underset{s}{n_e}) + \underset{s}{\check{\psi}_r}(T, \underset{s}{y_0}, \ldots, \underset{s}{y_{N_S-2}}, \underset{s}{n_M}) \,. \tag{185}$$

After a short calculation we obtain from (184) new representations of the surface tension γ and the surface entropy density $\underset{s}{\eta}$ in the new variables

$$\gamma = -\underset{s}{n_M^2} \frac{\partial \frac{1}{\underset{s}{n_M}} \underset{s}{\check{\psi}_r}}{\partial \underset{s}{n_M}} \qquad \text{and} \qquad \underset{s}{\eta} = -\frac{\partial \underset{s}{\check{\psi}}}{\partial T}. \tag{186}$$

Note, the electron density cancels out in γ because we have assumed in Section 5.2.3 that the surface chemical potential $\underset{s}{\mu_e}$ is a constant.

The mechanical contribution of the free energy density is derived from the simple relation between surface tension and the surface mole density of the metal ions,

$$\gamma = \gamma^R + \underset{s}{K} \left(a_M^R \underset{s}{n_M} - 1 \right) \,. \tag{187}$$

The surface tension decreases if the surface metal lattice is elongated, i.e. if $\underset{s}{n_M}$ decreases.

Insertion of the constitutive relation (187) into $(186)_1$ yields the mechanical part of the free energy density.

The entropic contribution follows from the mixing entropy S^{mix} on the surface which is given by Boltzmann's formula,

$$S^{\text{mix}} = k_B \ln(W). \tag{188}$$

Herein W represents the number of realizations of a thermodynamic state on the surface to be defined as follows.

The surface of the metal lattice is formed by $\underset{s}{\mathcal{N}_M}$ metal ions which provide $\omega_M \underset{s}{\mathcal{N}_M}$ adsorption sites, where $\omega_M \geq 1$ is a constant. The surface electrons do not require adsorption sites. Thus the adsorption sites are at the disposal of the adsorbates from the electrolyte and of the further interfacial constituents which arise on S. We assume that each of these interfacial constituents with number $\underset{s}{\mathcal{N}_\alpha}$ needs ω_α adsorption sites and thus covers $\omega_\alpha \underset{s}{\mathcal{N}_\alpha}$ adsorption sites. In general

not all adsorption sites are occupied. The empty sites are called vacancies and we calculate their number by

$$\underset{s}{\mathcal{N}}_V = \omega_M \underset{s}{\mathcal{N}}_M - \sum_{\alpha=0}^{N_S-2} \omega_\alpha \underset{s}{\mathcal{N}}_\alpha. \tag{189}$$

We define the thermodynamic state on the surface by the sequence of occupation numbers $(\underset{s}{\mathcal{N}}_1, \underset{s}{\mathcal{N}}_2, ..., \underset{s}{\mathcal{N}}_{N_S-2}, \underset{s}{\mathcal{N}}_V)$ on $\omega_M \underset{s}{\mathcal{N}}_M$ sites. Thus it has

$$W = \frac{(\omega_M \underset{s}{\mathcal{N}}_M)!}{\underset{s}{\mathcal{N}}_1! \cdot \underset{s}{\mathcal{N}}_2! \cdots \underset{s}{\mathcal{N}}_V!} \tag{190}$$

realizations. To calculate $S^{\text{mix}} = k_B \ln W$ we assume that exclusively large numbers are involved so that we may apply Stirling's formula. Furthermore we introduce the surface number densities and the mixing entropy density according to $N_\alpha = \underset{s}{n}_\alpha A$ and $S^{\text{mix}} = \underset{s}{\eta}^{\text{mix}} A$, where A denotes the surface area. Insertion of the surface entropy density into (186) and integration gives the mixing entropy contribution of the surface free energy density (57).

B Representation of the surface capacity

Here we provide a semi-explicit representation of the surface capacity $\underset{s}{C}$. First of all note that the surface charge $\underset{s}{Q}$ has the representation

$$\underset{s}{Q} = -\frac{\sum_{\alpha=1}^{N_{\mathrm{E}}} z_\alpha e_0 \underset{s}{y}_\alpha + \sum_{\alpha=1}^{N_{\mathrm{E}}} \sum_{\beta=0}^{|z_\alpha|} z_\alpha e_0 \underset{s}{y}_{\alpha,\beta}}{a_V^R \underset{s}{y}_V + \sum_{\alpha=0}^{N_{\mathrm{E}}} a_\alpha^R \underset{s}{y}_\alpha + \sum_{\alpha=0}^{N_{\mathrm{E}}} \sum_{\beta=0}^{|z_\alpha|} a_{\alpha,\beta}^R \underset{s}{y}_{\alpha,\beta}} \,. \tag{191}$$

With the representations (92),(95),(98) and (101) for $\underset{s}{y}_\alpha$, $\underset{s}{y}_{\alpha,\beta}$ and $\underset{s}{y}_V$ we obtain an expression of $\underset{s}{Q}$ in terms of $(\underset{s}{\varphi} - \varphi^{\mathrm{E}})$ and $(\gamma - \gamma^R)$, i.e. $\underset{s}{Q} = \underset{s}{\hat{Q}}(\underset{s}{\varphi} - \varphi^{\mathrm{E}}, \gamma - \gamma^R)$. The surface charge is thus a function of $\underset{s}{\varphi}$ **and** the surface tension γ. The surface fractions $\underset{s}{y}_{\alpha,\beta}$ obey the constraint (102), i.e.

$$\underset{s}{y}_V(\gamma - \gamma^R) + \sum_{\alpha=0}^{N_{\mathrm{E}}} \underset{s}{y}_\alpha(\underset{s}{\varphi} - \varphi^{\mathrm{E}}, \gamma - \gamma^R) + \sum_{\alpha=0}^{N_{\mathrm{E}}} \sum_{\beta=0}^{|z_\alpha|} \underset{s}{y}_{\alpha,\beta}(\underset{s}{\varphi} - \varphi^{\mathrm{E}}, \gamma - \gamma^R) - 1 = 0 \,, \tag{192}$$

which is an implicit relationship between $\underset{s}{\varphi} - \varphi^{\mathrm{E}}$ and $\gamma - \gamma^{\mathrm{R}}$. Hence, we may use the implicit function theorem to deduce a solution $\gamma = \hat{\gamma}(\underset{s}{\varphi} - \varphi^{\mathrm{E}})$ from equation (192), which satisfies $d\hat{\gamma}/d(\underset{s}{\varphi} - \varphi^{\mathrm{E}}) = \underset{s}{Q}$ (c.f. equation (147)). The surface capacity $\underset{s}{C}$ is thus

$$\underset{s}{\hat{C}} = \frac{d\underset{s}{\hat{Q}}}{d\underset{s}{\varphi} - \varphi^{\mathrm{E}})} = \Big(\frac{\partial \underset{s}{Q}}{\partial(\underset{s}{\varphi} - \varphi^{\mathrm{E}})} + \underset{s}{Q} \cdot \frac{\partial \underset{s}{Q}}{\partial(\gamma - \gamma^R)}\Big). \tag{193}$$

With the (dimensionless) abbreviations

$$\underset{s}{f_1} := \sum_{\alpha=1}^{N_{\mathtt{E}}} z_\alpha \underset{s}{y_\alpha} + e_0 \sum_{\alpha=1}^{N_{\mathtt{E}}} \sum_{\beta=0}^{|z_\alpha|} z_\alpha \underset{s}{y_{\alpha,\beta}} \tag{194}$$

$$\underset{s}{f_2} := \underset{s}{y_V} + \omega_0 \underset{s}{y_0} + \sum_{\alpha=1}^{N_{\mathtt{E}}} \omega_\alpha \underset{s}{y_\alpha} + \sum_{\alpha=1}^{N_{\mathtt{E}}} \sum_{\beta=0}^{|z_\alpha|} \omega_{\alpha,\beta} \underset{s}{y_{\alpha,\beta}} \tag{195}$$

$$\underset{s}{f_3} = \sum_{\alpha=1}^{N_{\mathtt{E}}} z_\alpha^2 \underset{s}{y_\alpha} + \sum_{\alpha=1}^{N_{\mathtt{E}}} \sum_{\beta=0}^{|z_\alpha|} z_\alpha^2 \underset{s}{y_{\alpha,\beta}} \tag{196}$$

$$\underset{s}{f_4} = e_0 \sum_{\alpha=1}^{N_{\mathtt{E}}} z_\alpha \, \omega_\alpha \, \underset{s}{y_\alpha} + e_0 \sum_{\alpha=1}^{N_{\mathtt{E}}} \sum_{\beta=0}^{|z_\alpha|} z_\alpha \, \omega_{\alpha,\beta} \, \underset{s}{y_{\alpha,\beta}} \tag{197}$$

$$\underset{s}{f_5} = \underset{s}{y_V} + \omega_0 \underset{s}{y_0} + \sum_{\alpha=1}^{N_{\mathtt{E}}} \omega_\alpha \underset{s}{y_\alpha} + \sum_{\alpha=1}^{N_{\mathtt{E}}} \sum_{\beta=0}^{|z_\alpha|} \omega_{\alpha,\beta}^2 \underset{s}{y_{\alpha,\beta}} \tag{198}$$

we obtain for the surface capacity the expression

$$\underset{s}{\hat{C}} = -\frac{e_0^2}{k_B T a_V^R} \left(\frac{\underset{s}{f_1} \cdot \underset{s}{f_4} - \underset{s}{f_3} \cdot \underset{s}{f_2}}{(\underset{s}{f_2})^2} + \frac{\underset{s}{f_1}}{\underset{s}{f_2}} \frac{\underset{s}{f_4} \cdot \underset{s}{f_2} - \underset{s}{f_1} \cdot \underset{s}{f_5}}{(\underset{s}{f_2})^2} \right). \tag{199}$$

Note that the term $\frac{e_0^2}{k_B T a_V^R}$ indeed has units $\frac{\mathtt{F}}{\mathtt{m}^2}$ and that all functions $\underset{s}{f_k}, k = 1, \ldots, 5$, are dependent on $\underset{s}{\varphi} - \varphi^{\mathtt{E}}$ **and** $\gamma - \gamma^R$.

C Current-charge relation

In this section we derive the relation (141) between the current and the electric charge. The derivation is based on non-equilibrium thermodynamics. The necessary theory can be find in the textbooks [47, 16], or in our previous publication [20].

We have still the one-dimensional setting of Section 2.1. However, to avoid confusion concerning the surface normal, in this appendix we use the three-dimensional versions of the formulas. First of all we introduce at the points $x_{\mathtt{M}}$, $x_{\mathtt{S}}$ and $x_{\mathtt{E}}$ parallel surfaces, viz. $A_{\mathtt{M}} := \{x_{\mathtt{M}}\} \times \mathbb{R}^2$, $S := \{x_{\mathtt{S}}\} \times \mathbb{R}^2$ and $A_{\mathtt{E}} := \{x_{\mathtt{E}}\} \times \mathbb{R}^2$. The corresponding surface normals $\boldsymbol{\nu}$ are identical and point into the positive x direction, i.e. $\boldsymbol{\nu} = (1, 0, 0)$. We assume that the surface speeds of $A_{\mathtt{M}}$,$A_{\mathtt{E}}$ and S are zero, whereby the following balance equations assume a simpler form.

The electric current I $[\mathrm{A}/\mathrm{m}^2]$ flowing into the metal through the area $A_{\mathtt{M}}$ is given by

$$I = \left(\tfrac{z_e e_0}{m_e} \boldsymbol{j}_e \cdot \boldsymbol{\nu} + \tfrac{z_M e_0}{m_M} \boldsymbol{j}_M \cdot \boldsymbol{\nu} \right)|_{A_{\mathtt{M}}} . \tag{200}$$

Herein $\boldsymbol{j}_{e,M}$ $[\mathrm{kg}/\mathrm{sm}^2]$ are the mass flux densities of electrons and metal ions, respectively. The following objective is the representation of the right hand side of (200) by time derivatives. To

this end we introduce the particle balance equations for electrons and metal ions,

$$\frac{d}{dt}\int_{x_{\mathtt{M}}}^{x_{\mathtt{S}}} m_\alpha n_\alpha \, dx = (\boldsymbol{j}_\alpha \cdot \boldsymbol{\nu})|_{A_{\mathtt{M}}} - (\boldsymbol{j}_\alpha \cdot \boldsymbol{\nu})|_S \, , \qquad \alpha = e, M \, . \tag{201}$$

Next we introduce the corresponding surface balance equations, which are used to determine the fluxes in (200),

$$\frac{d}{dt}(m_e \underset{s}{n}_e) = r_e + (\boldsymbol{j}_e \cdot \boldsymbol{\nu})|_S \qquad \text{and} \qquad \frac{d}{dt}(m_M \underset{s}{n}_M) = (\boldsymbol{j}_M \cdot \boldsymbol{\nu})|_S \tag{202}$$

Herein denotes r_e the production density of electrons due to electron transfer reactions on the surface S. The metal ions do not participate in chemical reaction, i.e. we have $r_M = 0$. Inserting the balance equations (201) and (202) into (200) yields

$$(\boldsymbol{j}^{\mathrm{F}} \cdot \boldsymbol{\nu})|_{A_{\mathtt{M}}} = \frac{d}{dt}\Big(\int_{x_{\mathtt{M}}}^{x_{\mathtt{S}}} n^{\mathrm{F}} \, dx + \sum_{\alpha=e,M} z_\alpha e_0 \underset{s}{n}_\alpha \Big) - \tfrac{z_e e_0}{m_e} r_e \, . \tag{203}$$

The electrons are exclusively involved in the electron transfer reactions (78). For this reason we may write

$$r_e = -\sum_{\alpha=1}^{N_{\mathtt{E}}} \sum_{\beta=1}^{|z_\alpha|} \mathrm{sgn}(z_\alpha) m_e R_{\alpha,\beta} \, , \tag{204}$$

where $R_{\alpha,\beta}$ denote the reaction rate of the electron transfer reaction (α, β) that produces the surface constituent $A_{\alpha,\beta}$. Its balance equation can now be used to eliminate the production density r_e. The balance equation has a simple form because $A_{\alpha,\beta}$ only lives on the surface S,

$$\frac{d}{dt}(m_{\alpha,\beta} \underset{s}{n}_{\alpha,\beta}) = r_{\alpha,\beta} \, , \qquad \beta = 1, \dots, |z_\alpha| \, , \alpha = 1, \dots, N_{\mathtt{E}} \, . \tag{205}$$

Recall that the constituent $A_{\alpha,\beta}$ is involved in two electron transfer reactions. Hence the production density $r_{\alpha,\beta}$ is represented by

$$r_{\alpha,\beta} = m_{\alpha,\beta}(R_{\alpha,\beta} - R_{\alpha,\beta+1}) \, , \tag{206}$$

where we fix $R_{\alpha,|z_\alpha|+1} = 0$. By means of (205) we may replace the reaction rates in (204) by time derivatives appearing in (205). At first we obtain

$$r_e = -m_e \sum_{\alpha=1}^{N_{\mathtt{E}}} \sum_{\beta=1}^{|z_\alpha|} \mathrm{sgn}(z_\alpha) \Big(\frac{r_{\alpha,\beta}}{m_{\alpha,\beta}} + \frac{r_{\alpha,\beta+1}}{m_{\alpha,\beta+1}} + \cdots + \frac{r_{\alpha,|z_\alpha|}}{m_{\alpha,|z_\alpha|}} \Big) \, . \tag{207}$$

Rearrangement of the sums and inserting the surface balance equations yields

$$r_e = -m_e \frac{d}{dt}\Big(\sum_{\alpha=1}^{N_{\mathtt{E}}} \sum_{\beta=1}^{|z_\alpha|} \mathrm{sgn}(z_\alpha) \beta \underset{s}{n}_{\alpha,\beta} \Big) \, . \tag{208}$$

Finally we substitute the production density r_e in (203) by the representation (208). The result is

$$I = \frac{\partial}{\partial t}\Big(\int_{x_{\mathtt{M}}}^{x_{\mathtt{S}}} n^{\mathrm{F}} \, dx + \sum_{\alpha=e,M} z_\alpha e_0 \underset{s}{n}_\alpha + \sum_{\alpha=1}^{N_{\mathtt{E}}} \sum_{\beta=1}^{|z_\alpha|} z_e e_0 \, \mathrm{sgn}(z_\alpha) \beta \underset{s}{n}_{\alpha,\beta} \Big) \, . \tag{209}$$

D Reference Potential

In Section (7.3) we discuss how to determine of the reference potential U^{R} from a capacity-potential plot. To this end we use the proposition: If

$$v_\alpha^R = (1+\kappa)\, v_0^R \quad \text{and} \quad |z_\alpha| = 1,\ \alpha = 1, \dots, N_{\mathrm{E}} \tag{210}$$

then we have the equivalence

$$E^* = U^{\mathrm{R}} \quad \Longleftrightarrow \quad \frac{dC_{\mathrm{BL}}}{d(\underset{s}{\varphi} - \varphi^{\mathrm{E}})}\bigg|_{\underset{s}{\varphi}=\varphi^{\mathrm{E}}} = 0\,. \tag{211}$$

Its proof starts from a useful relation between the charge and the capacity which follows from the equations (145) and (151),

$$CQ = k_0 P'\,. \tag{212}$$

We abbreviate $C = C_{\mathrm{BL}}$, $Q = Q_{\mathrm{BL}}$ and $P = p - p^{\mathrm{E}}$, and k_0 is a constant. The abbreviation P' denotes the derivative of the pressure P with respect to the potential difference $\underset{s}{\varphi} - \varphi^{\mathrm{E}}$.

The twofold derivative of (212) yields

$$C''Q + 3C'C = kP'''\,. \tag{213}$$

We conclude that $Q|_{\underset{s}{\varphi}=\varphi^{\mathrm{E}}} = 0$ implies $C'|_{\underset{s}{\varphi}=\varphi^{\mathrm{E}}} = 0$ iff the pressure satisfies $P'''|_{\underset{s}{\varphi}=\varphi^{\mathrm{E}}} = 0$.

Next we calculate the derivatives of the pressure P. To this end we use the representations (107) and (82) for the pressure and the electric charge density,

$$P'''|_{\underset{s}{\varphi}=\varphi^E} = -\Big(\frac{e_0}{k_BT}\Big)^2\Big(\sum_{\alpha=0}^{N_{\mathrm{E}}} z_\alpha^3 e_0 n_\alpha^{\mathrm{E}}\Big) + \frac{e_0}{(k_BT)^2}\Big(\sum_{\alpha=0}^{N_{\mathrm{E}}} z_\alpha^2 e_0 n_\alpha^{\mathrm{E}}\Big)\Big(\sum_{\gamma=0}^{N_{\mathrm{E}}} z_\gamma e_0 v_\gamma^R n_\gamma^{\mathrm{E}}\Big) \tag{214}$$

Assuming that the conditions (210) hold, then $P'''|_{\underset{s}{\varphi}=\varphi^E} = 0$ due to the electro neutrality condition (36).

Until now we only showed that the capacity C_{BL} has an extremum at U_R. To proof that C_{BL} has a local minimum at U^{R} we have to show that C_B'' is positive at U^{R}. We differentiate the equation (213),

$$C'''Q + C''C + 3C''C + 3C'C' = kP''''\,. \tag{215}$$

We conclude that C'' is positive at U^{R} iff P'''' is positive at U^{R}. A simple but cumbersome calculation yields:

$$\begin{aligned} P''''|_{\underset{s}{\varphi}=\varphi^E} =& \frac{1}{(k_BT)^3}\Big(\sum_{\alpha=0}^{N_{\mathrm{E}}} z_\alpha^4 e_0^4 n_\alpha^{\mathrm{E}}\Big) - \frac{3}{(k_BT)^3}\Big(\sum_{\alpha=0}^{N_{\mathrm{E}}} z_\alpha^2 e_0^2 n_\alpha^{\mathrm{E}}\Big)\Big(\sum_{\beta=0}^{N_{\mathrm{E}}} z_\beta^2 e_0^2 \upsilon_\alpha n_\alpha^{\mathrm{E}}\Big) \\ &+ \frac{3}{(k_BT)^3}\Big(\sum_{\alpha=0}^{N_{\mathrm{E}}} z_\alpha^2 e_0^2 n_\alpha^{\mathrm{E}}\Big)^2\Big(\sum_{\beta=0}^{N_{\mathrm{E}}} v_\beta^2 n_\beta^{\mathrm{E}}\Big). \end{aligned} \tag{216}$$

We observe that the second and the third term are quadratic in the number densities n_α^{E} of the ions. Thus in a dilute solution, i.e. $n_\alpha \ll 1\mathrm{mol}/\ell$, the second and third term are small in comparison to the first term. Therefore in a dilute solution P'''' is positive at U^{R} and thus C_{BL} has a local minimum at U^{R}, at least in a dilute solution.

References

[1] A. Bonnefont, F. Argoul, M. Bazant. Analysis of diffuse-layer effects on time-dependent interfacial kinetics. *J. Electroanal. Chem.*, 500(1-2):52–61, 2001.

[2] A. Ajdari, M. Z. Bazant, and M. S. Kilic. Steric effects in the dynamics of electrolytes at large applied voltages. I. Double-layer charging. *Phys. Rev. E*, 75:021502, Feb 2007.

[3] A. Ajdari, M. Z. Bazant, and M. S. Kilic. Steric effects in the dynamics of electrolytes at large applied voltages. II. Modified Poisson-Nernst-Planck equations. *Phys. Rev. E*, 75(2):021503, Feb 2007.

[4] D. Bedeaux. Nonequilibrium thermodynamics and statistical physics of surfaces. In P. Ilya and S. A. Rice, editors, *Advances in Chemical Physics*, volume 64, pages 47–109. John Wiley Sons, Inc., 1986.

[5] G. Beltramo, M. Giesen, and H. Ibach. Anomalous helmholtz-capacitance on stepped surfaces of silver and gold. *Electrochimica Acta*, 54(18):4305 – 4311, 2009.

[6] G. Beltramo and E. Santos. Characterisation of chloride and bromide specific adsorption process on silver single crystal surfaces by impedance spectroscopy: Part i. an extended model to obtain the charge density from impedance spectra applied to ag(111) at low concentrations of halides. *Journal of Electroanalytical Chemistry*, 556(0):127 – 136, 2003.

[7] J. Bikerman. Structure and capacity of electrical double layer. *Philosophical Magazine*, 33(220):384–397, 1942.

[8] J. Bikerman. XXXIX. structure and capacity of electrical double layer. *Philosophical Magazine Series 7*, 33(220):384–397, 1942.

[9] J. Bockris and A. Reddy. *Modern Electrochemistry 1: Ionics*. Kluwer Academic Publishers, 2002.

[10] J. O. Bockris, M. A. V. Devanathan, and K. Muller. On the structure of charged interfaces. *Proceedings of the Royal Society of London. Series A. Mathematical and Physical Sciences*, 274(1356):55–79, 1963.

[11] J. O. Bockris and A. K. N. Reddy. *Modern Electrochemistry 2nd Edition*, volume Fundamentals of Electrodics. Plenum Press, 1998.

[12] I. Borukhov, D. Andelman, and H. Orland. Steric effects in electrolytes: A modified poisson-boltzmann equation. *Phys. Rev. Lett.*, 79(3):435–438, July 1997.

[13] D. Bothe and W. Dreyer. Continuum thermodynamics of chemically reacting fluid mixtures. *Acta Mech.*, 226:1757–1805, 2015.

[14] D. L. Chapman. Li. a contribution to the theory of electrocapillarity. *Philosophical Magazine Series 6*, 25(148):475–481, 1913.

[15] M. Danckwerts. *Elektrochemische in-situ SHG-Untersuchungen zur Struktur kristalliner Elektrodenoberflächen unter Adsorptions- und Reaktionsbedingungen*. PhD thesis, FU Berlin, FHI (Ertl Group), 2003.

[16] S. R. deGroot and P. Mazur. *Non-equilibrium Thermodynamics*. Dover Publications, 1984.

[17] R. Dogonadze and A. Kornyshev. Polar solvent structure in the theory of ionic solvation. *Journal of the Chemical Society*, 1974.

[18] W. Dreyer, C. Guhlke, and M. Landstorfer. A mixture theory of electrolytes containing solvation effects. *Electrochemistry Communications*, 43(0):75 – 78, 2014.

[19] W. Dreyer, C. Guhlke, and R. Müller. Overcoming the shortcomings of the Nernst–Planck model. *Phys. Chem. Chem. Phys.*, 15:7075–7086, 2013.

[20] W. Dreyer, C. Guhlke, and R. Müller. Modeling of electrochemical double layers in thermodynamic non-equilibrium. *Phys. Chem. Chem. Phys.*, 2015.

[21] A. W. Dweydari and C. H. B. Mee. Work function measurements on (100) and (110) surfaces of silver. *physica status solidi (a)*, 27(1):223–230, 1975.

[22] M. Eigen and E. Wicke. The thermodynamics of electrolytes at higher concentration. *J. Phys. Chem.*, 58(9):702–714, 1954.

[23] H. E. Farnsworth and R. P. Winch. Photoelectric work functions of (100) and (111) faces of silver single crystals and their contact potential difference. *Phys. Rev.*, 58:812–819, 1940.

[24] V. Freise. Zur Theorie der diffusen Doppelschicht. *Zeitschrift für Elektrochemie, Berichte der Bunsengesellschaft für physikalische Chemie*, 56(8):822–827, 1952.

[25] A. Frumkin, B. Damaskin, N. Grigoryev, and I. Bagotskaya. Potentials of zero charge, interaction of metals with water and adsorption of organic substances ii. potentials of zero charge and work function. *Electrochimica Acta*, 19(2):75 – 81, 1974.

[26] A. N. Frumkin. Wasserstoffüberspannung und Struktur der Doppelschicht. *Z. Phys. Chem. A*, 164:121–133, 1933.

[27] C. L. Gardner, W. Nonner, and R. S. Eisenberg. Electrodiffusion model simulation of ionic channels: 1d simulations. *Journal of Computational Electronics*, 3(25-31), 2004.

[28] G. Gouy. Sur la constitution de la charge électrique à la surface d'un électrolyte. *Journal de Physique Théorique et Appliquée*, 9(4):457–468, 1910.

[29] D. C. Grahame. The electrical double layer and the theory of electrocapillarity. *Chem. Rev.*, 41(3):441–501, 1947.

[30] C. Guhlke. *Theorie der elektrochemischen Grenzfläche*. PhD thesis, TU-Berlin, 2015.

[31] C. Hamann and W. Vielstich. *Elektrochemie*. John Wiley & Sons Australia, Limited, 2005.

[32] H. G. Hertz. Structure of the solvation shell of dissolved particles. *Angewandte Chemie International Edition in English*, 9(2):124–138, 1970.

[33] J. F. Hinton and E. S. Amis. Solvation numbers of ions. *Chemical Reviews*, 71(6):627–674, 1971.

[34] S. L. Horswell, A. L. N. Pinheiro, E. R. Savinova, M. Danckwerts, B. Pettinger, M.-S. Zei, , and G. Ertl. A comparative study of hydroxide adsorption on the (111), (110), and (100) faces of silver with cyclic voltammetry, ex situ electron diffraction, and in situ second harmonic generation. *Langmuir*, 20(25):10970–10981, 2004.

[35] I. Prigogine, R. Defay. *Chemical Thermodynamics*. Longmans, 1954.

[36] Z. Kerner, T. Pajkossy, L. A. Kibler, and D. M. Kolb. The double layer capacity of pt(100) in aqueous perchlorate solutions. *Electrochemistry Communications*, 4(10):787 – 789, 2002.

[37] A. Kiejna and K. Wojciechowski. *Metal Surface Electron Physics*. Elsevier Science, 1996.

[38] D. Kolb. Reconstruction phenomena at metal-electrolyte interfaces. *Progress in Surface Science*, 51(2):109 – 173, 1996.

[39] D. Kolb. An atomistic view of electrochemistry. *Surface Science*, 500(1–3):722 – 740, 2002.

[40] D. M. Kolb. Elektrochemische Oberflächenphysik. *Angewandte Chemie*, 113(7):1198–1220, 2001.

[41] M. Landstorfer and T. Jacob. Mathematical modeling of intercalation batteries at the cell level and beyond. *Chem. Soc. Rev.*, 42:3234–3252, 2013.

[42] N. D. Lang and W. Kohn. Theory of metal surfaces: Charge density and surface energy. *Phys. Rev. B*, 1:4555–4568, Jun 1970.

[43] J. Lipkowski and P. Ross. *Electrocatalysis*. Frontiers in Electrochemistry. Wiley, 1998.

[44] G. Lippmann. Beziehungen zwischen den capillaren und elektrischen Erscheinungen. *Annalen der Physik*, 225(8):546–561, 1873.

[45] Y. Marcus. The solvation number of ions obtained from their entropies of solvation. *Journal of Solution Chemistry*, 15(4):291–306, 1986.

[46] J. Meixner and H. G. Reik. *Thermodynamik der irreversiblen Prozesse*, volume 3, pages 413–523. Springer, Berlin, 1959.

[47] I. Müller. *Thermodynamics, Interaction of Mechanics and Mathematics Series*. Pitman Advanced Publishing Program, Boston, 1985.

[48] W. Nernst. Die elektromotorische Wirksamkeit der Ionen. *Z. Phys. Chem.*, IV:129–181, 1889.

[49] J. Newman and K. Thomas-Alyea. *Electrochemical Systems*. Wiley, 2004.

[50] T. Pajkossy and D. Kolb. Double layer capacitance of pt(111) single crystal electrodes. *Electrochimica Acta*, 46(2021):3063 – 3071, 2001.

[51] M. Planck. Über die Erregung von Electricität und Wärme in Electrolyten. *Ann. Phys.*, 275(2):161–186, 1890.

[52] P.W. Atkins, J.D. Paula. *Physical Chemistry*. Oxford University Press, 2006.

[53] I. Rubinstein. *Electro-Diffusion of Ions*. Society for Industrial and Applied Mathematics, 1990.

[54] W. Schmickler and E. Santos. *Interfacial electrochemistry*. Springer, 2010.

[55] Z. Schuss, B. Nadler, and R. S. Eisenberg. Derivation of poisson and nernst-planck equations in a bath and channel from a molecular model. *Phys. Rev. E*, 64(3):036116, Aug 2001.

[56] H. L. Skriver and N. M. Rosengaard. Surface energy and work function of elemental metals. *Phys. Rev. B*, 46:7157–7168, 1992.

[57] A. Sommerfeld and H. Bethe. *Elektronentheorie der Metalle*. Springer, 1967.

[58] O. Stern. Zur Theorie der elektrolytischen Doppelschicht. *Z. Elektrochem. angew. phys. Chem.*, 30(21-22):508–516, 1924.

[59] W. Still, A. Tempczyk, R. Hawley, and T. Hendrickson. Semianalytical treatment of solvation for molecular mechanics and dynamics. *Journal of the American Chemical Society*, 112(16):6127–6129, Aug. 1990.

[60] S. Trasatti. Work function, electronegativity, and electrochemical behaviour of metals: Ii. potentials of zero charge and "electrochemical" work functions. *Journal of Electroanalytical Chemistry and Interfacial Electrochemistry*, 33(2):351 – 378, 1971.

[61] G. Valette. Double layer on silver single-crystal electrodes in contact with electrolytes having anions which present a slight specific adsorption: Part I. the (110) face. *J. Electroanal. Chem.*, 122:285–297, 1981.

[62] G. Valette. Double layer on silver single crystal electrodes in contact with electrolytes having anions which are slightly specifically adsorbed: Part II. the (100) face. *J. Electroanal. Chem.*, 138(1):37–54, 1982.

[63] G. Valette. Double layer on silver single crystal electrodes in contact with electrolytes having anions which are slightly specifically adsorbed: Part III. the (111) face. *J. Electroanal. Chem.*, 269(1):191–203, 1989.

[64] G. Valette and R. Parsons. Adsorption on well-defined solid surfaces: Bromide adsorption on a (110) face of silver. *J. Electroanal. Chem.*, 191(2):377–386, 1985.

[65] G. Valette and R. Parsons. Adsorption on well-defined solid surfaces chloride adsorption on a (110) face of silver. *Journal of Electroanalytical Chemistry and Interfacial Electrochemistry*, 204(204):291 – 297, 1986.